universität wien

# MASTERARBEIT / MASTER'S THESIS

Titel der Masterarbeit / Title of the Master's Thesis

„Construction of mutant ϕCh1-ΔORF44, its characterization and first steps in the generation of mutant ϕCh1-ΔORF56"


verfasst von / submitted by

Yan Christian Jérôme Gillen, BSc


angestrebter akademischer Grad / in partial fulfilment of the requirements for the degree of

Master of Science (MSc)

Wien, 2017 / Vienna 2017

| | |
|---|---|
| Studienkennzahl lt. Studienblatt / degree programme code as it appears on the student record sheet: | A 066 830 |
| Studienrichtung lt. Studienblatt / degree programme as it appears on the student record sheet: | Master Molecular Microbiology, Microbial Ecology and Immunobiology |
| Betreut von / Supervisor: | Ao. Univ.- Prof. Dipl.- Biol. Dr. Angela Witte |

# Acknowledgments

First and foremost I would like to thank my supervisor Ao. Univ.- Prof. Dipl.- Biol. Dr. Angela Witte for having given me the opportunity to perform my graduate work in her laboratory. The fact that she was always willing to help, even with regard to the most trivial issues I had encountered, made working in her laboratory a valuable and fun experience. A very warm thank you to her as well for having presented opportunities that have had a major impact regarding the choice of my professional career.

I would also like to express my gratitude towards my laboratory colleagues and friends Martin Kaufmann and Michael Tschurtschenthaler for their support and friendship during the times spent in- and outside of the lab.

I want to thank all the bachelor students for their help and for teaching me the virtue of patience. A special thank you goes out to bachelor student Nadja Brait for her valuable contributions leading to the creation of strain *N. magadii* L11-ΔORF44, representing a major achievement of this thesis.

I also would like to acknowledge Prof. Udo Bläsi and Prof. Isabella Moll as well as their respective groups for providing help when needed.

Last but not least, I would like to thank my family and friends. A very heartfelt sign of gratitude goes out to my parents Pascale and Jean Gillen-Rob for their continuous support all throughout my life leading up to this special occasion. A warm thank you as well to my aunt Christiane Rob for her support all throughout my academic path.

A final shout-out goes out to all of my friends in Vienna and Luxembourg for their friendship and support during the period leading to this moment.

To my grandfather

Jean-Louis Rob

# Table of contents

# 1. Introduction

## 1.1. *Archaea*

### 1.1.1. The three domains of life – A classification of the living

The classification of all living organisms into three distinct domains of life is a principal dogma in all of natural sciences, but that has not always been the case. Up until the 19th century, life itself was organized in two distinct kingdoms: '*Animalia*', representing all animals in Earth's ecosystem as well as '*Plantae*', the kingdom representing all of plant life (Linnaeus, 1735). This so-called binomial nomenclature represented the classification of life according to Carl Linnaeus (later: Carl von Linné) who first postulated this idea in his publication entitled '*Systema Naturae'*. Alongside this binomial nomenclature, Linnaeus adapted a supplementary system allowing for an organization of individual life forms into 'genus' as well as 'species'. This classification proved itself as being quite robust until the advent of modern science, bringing along the discovery of unicellular organisms not fitting Linnaeus' binomial nomenclature method of classification. A first major adaptation in the classification of life occurred in 1866 with the subdivision of life into three kingdoms through Ernst Haeckel: '*Animalia*', '*Plantae*' and an additional kingdom called '*Protista*'. '*Protista*' regrouped all of the unicellular organisms that, according to Haeckel himself, were neither plants nor animals (Haeckel, 1866).

A further instauration in the classification of life was achieved by Robert Harding Whittaker in 1969 through his so-called five-kingdom taxonomic classification implying five distinct kingdoms: Animalia, Plantae, Fungi, Protista and Monera ("unicellular organisms with prokaryotic cell organization" – bacteria today) (Whittaker, 1969). This method of classification co-existed alongside Edouard Chatton's classification system associated with the distinction of eukaryotic and prokaryotic life forms (Chatton, 1938).

In 1977, a major breakthrough in the classification of life was achieved by Carl Richard Woese's and George Edward Fox's discoveries through their work with 16S (18S) ribosomal RNA. Their groundbreaking results were based on the premise that there is a molecule of "appropriately broad distribution" and that it is "a component of all self-replicating systems": 16S (18S) rRNA. Through 16S rRNA analysis they were able to identify a third "urkingdom" next to *eubacteria* and *urkaryotes*: the *archaebacteria* (Woese and Fox, 1977). Woese's contributions to the establishment of modern taxonomy did not end there; in 1990 he established a new taxonomic rank above the primary kingdoms: the

domain (Woese, 1990). This discovery led to the creation of the three highest categories of classification, namely the three domains of life *Archaea*, *Bacteria* and *Eucarya*.

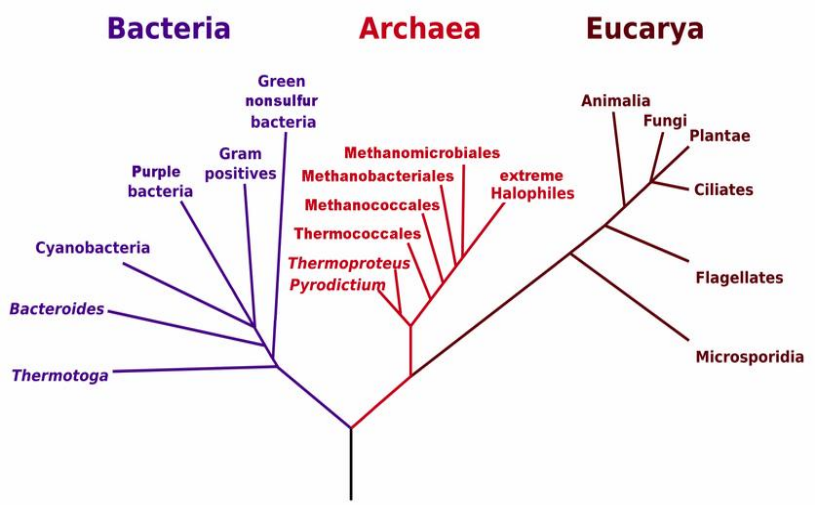


Adapted from Woese, 1990

**Figure 1: Carl Woese's model for a phylogenetic tree of life based on 16S (18S) ribosomal RNA sequences**

An illustration of the phylogenetic tree of life according to Carl Woese, based on 16S (18S) rRNA sequence analysis. Woese's results led him to the establishment of three different domains of life: *Bacteria*, *Archaea* and *Eucarya*. His tree of life also illustrates the close relationship between *Eucarya* and *Archaea:* Both have a common ancestor.

(Woese, 1990)

### 1.1.2. Archaeal diversity – The main phyla

The current classification of *Archaea* makes a distinction between two main phyla: the *Euryarchaeota* and the *Chrenarchaeota* (Woese, 1990). The phylum *Euryarchaeota* is a rather diverse phylum regrouping anoxically growing methanogens producing methane, *halobacteria* which thrive in high salt environments as well as thermophilic aerobic and anaerobic *Archaea* (Woese, 1990).

The phylum *Chrenarchaeota* regroups thermophilic as well as hyperthermophilic *Archaea*. The best characterized species of *Chrenarchaeota* is *Sulfolobus solfataricus* thriving at temperatures of up to 80°C and a pH as low as 2 (Brock *et al*., 1972). Hyperthermophilic *Archaea* may thrive at temperatures of up to 110°C.

Three additional, minor phyla have also been described, namely *Korarchaeota*, *Thaumarchaeota* and *Nanoarchaeota* (Brochier-Armanet *et al*., 2008; Huber *et al*., 2002; Barns *et al*., 1996). These phyla have more of a historic value as up to this date, not many approved published species belong to any of these three phyla; *Korarchaeota*, *Thaumarchaeota* and *Nanoarchaeota* are preliminarily made up of molecular

sequences derived from environmental probes (Brochier-Armanet *et al*., 2008; Huber *et al*., 2002; Barns *et al*., 1996).

### 1.1.3. Unique characteristics of *Archaea* - Archaeal membrane, cell wall and S-layer

Compared to the other two kingdoms *Bacteria* and *Eucarya*, whose membrane lipids are composed of ester-linked unbranched fatty acids (Figure 2 a), the membrane lipids of *Archaea* are composed of ether-linked branched isoprenoid chains (Figure 2 c) (Jarrell *et al*., 2011; Albers and Meyer, 2011). Ether-linked membrane lipids portray an advantage for *Archaea* that thrive in extreme environments as ether-linked lipids present a much higher resistance towards hydrolysis than ester-linked lipids (Van de Vossenberg *et al*., 1998). Other membrane lipids found in archaeal membranes are the so-called tetraether lipids that associate in a very firm lipid monolayer spanning the whole of the membrane (Figure 2 b) (Matsumi et al., 2011; Albers and Meyer, 2011). This organization represents another advantage for thermophilic *Archaea* living in environments characterized by very high temperatures; the organization of tetraether lipids in a solid monolayer helps in resisting membrane lipid denaturation through extreme heat while at the same time assuring sufficient membrane fluidity required for growth (Jarrell *et al*., 2011; Van de Vossenberg *et al*., 1998; Matsumi *et al*., 2011).

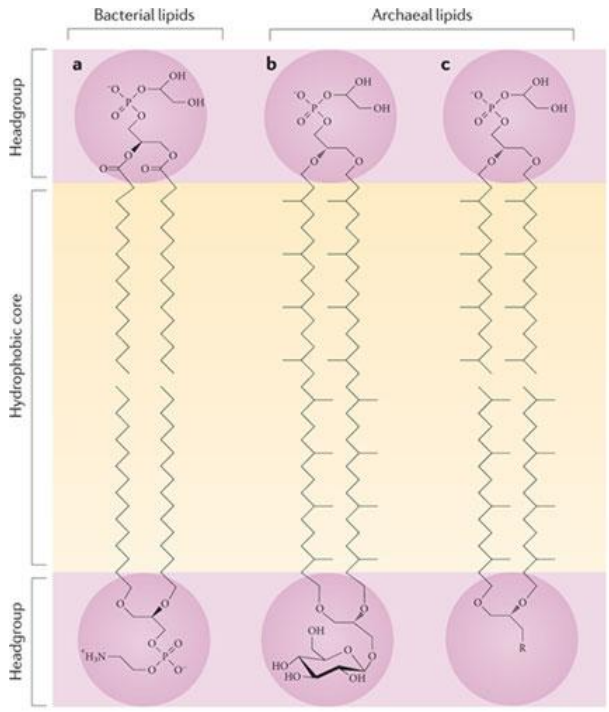


Albers and Meyer, 2011

**Figure 2: An illustration of membrane lipid structure in *Bacteria*, *Eucarya* and *Archaea* lipid bilayers.**

**a** In *Bacteria* and *Eucarya* the hydrophobic fatty acid core region is linked to a hydrophilic, glycerol-3-phosphate backbone via ester bonds. **b** Archaeal tetraether lipids forming the archaeal monolayer membrane, important for thriving in high-temperature environments. Tetraether lipids are composed of two hydrophilic headgroups that are ether-linked to a hydrophobic 40 C isoprene chain. **c** Archaeal diether lipids composed of 20 C isoprenoid chains ether-linked to a glycerol-1-phosphate backbone. (Adapted from Albers and Meyer, 2011)

The cell wall of most methanogenic *Archaea* is composed of pseudopeptidoglycan (pseudomurein) whereas bacterial cell walls are composed of peptidoglycan (Albers and Meyer, 2011). Both peptidoglycan as well as pseudopeptidoglycan serve the purpose of conferring structural integrity to the cell and counteracting osmotic pressure from the cell's cytoplasm.

One of the most commonly found cell surface proteins making up the cell wall in *Archaea* is the protective surface layer (S-layer), mostly anchored to the cytoplasmic membrane (Albers and Meyer, 2011). Composed of (glyco)proteins, the archaeal S-layer's main functions are maintaining cell integrity through the generation of a rigid cell wall as well as maintaining the osmotic equilibrium and chemical protection (Kandler *et al*., 1998). Many additional functions are attributed to the S-layer, depending on the species in which it is found. Different types of archaeal S-layers are illustrated in Figure 3.

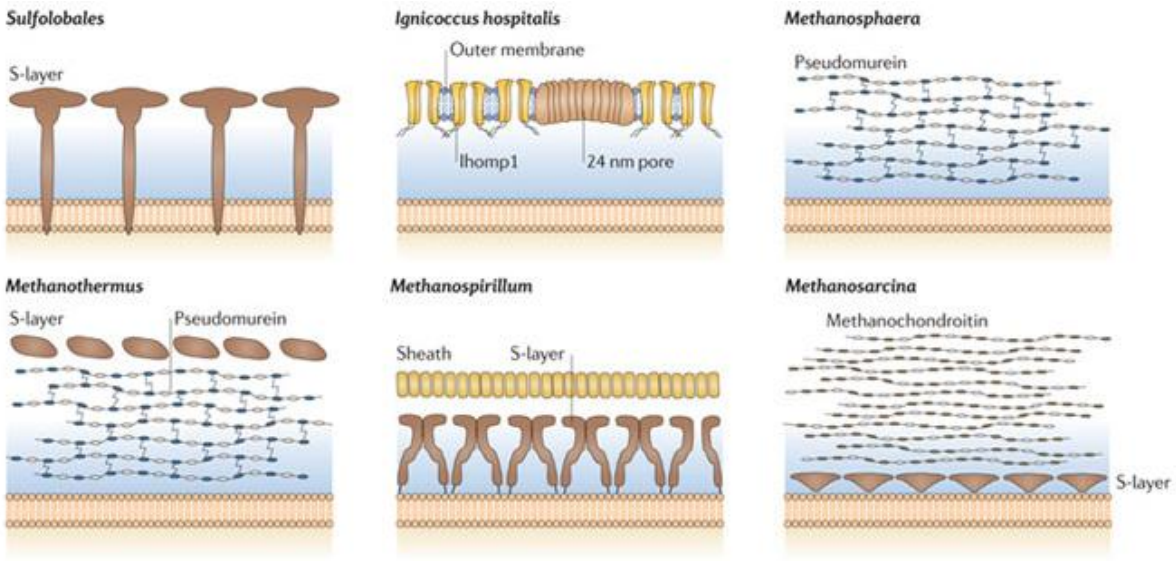


Adapted from Albers and Meyer, 2011

**Figure 3: Different types of archaeal cell walls with their respective S-layer**

The S-layer of representatives of the order of Sulfolobales is composed exclusively of 2 proteins making up the cell wall. The S-layer is anchored in the cytoplasmic membrane via the smaller component protein. The cell walls of other *Archaea* are composed of several polymers, among them pseudomurein and methanochondroitin, two polysaccharides. *Igniococcus hospitalis* and *Methanosphaera* do not possess an S-layer. Additionally, *Igniococcus hospitalis* is the only representative in the domain of the *Archaea* having an outer membrane, resembling the one observed in gram-negative bacteria. (Adapted from Albers and Meyer, 2011).

### 1.1.4. Halophilic and haloalkaliphilic *Archaea*

#### 1.1.4.1. General characteristics

One of the most proficient characteristics of *Archaea* is the fact that an unusually high proportion of archaeal species is capable of thriving in extreme environments such as environments with high or low pH and/or temperatures. Here, emphasis will be put on archaeal species adapted to survive at high salt concentrations (halophiles) and high salt concentrations alongside high pH (haloalkaliphiles).

Halophilic *Archaea* may be subdivided into two categories: moderate halophiles and extreme halophiles. Moderate halophiles need environments containing 0.5-2.5 M NaCl in order to thrive properly (Andrei *et al.*, 2012). Extreme halophilic *Archaea* however need higher sodium chloride concentrations in their environment ranging from 2.5-5.2 M NaCl for prosperous growth (Andrei *et al.*, 2012). High-salt environments that are home to extreme halophilic *Archaea* are for instance found in the Dead Sea. Here,

evaporation rates are higher than precipitation rates, thus leading to a hypersaline environment. Haloalkaliphilic *Archaea* are obligate alkaliphile organisms and are found in so-called hypersaline alkaline habitats (Grant and Larsen, 1989). The most prominent example for such a hypersaline alkaline habitat is Lake Magadi in Kenya, Africa. Here, salt concentrations reach beyond 300 g/L whereas pH levels may exceed 11 (Oren, 2002; Ma *et al*., 2010). As mentioned before, species capable of surviving in such harsh conditions are mostly found in the domain of the *Archaea* within the family of the *Halobacteriaceae*, members of the phylum *Euryarchaeota*.

Many times a reddish-purple coloration may be observed in the waters of hypersaline soda lakes which results from bacterioruberin (a 50 C carotenoid pigment) and its derivatives in the membrane of the members of *Halobacteriaceae* thriving in such environments (*Shahmohammadi et al*., 1998). Bacterioruberin exhibits a very important role in assuring the survival of *Halobacteriaceae* in hypersaline alkaline habitats: Such habitats are additionally influenced by intense sunlight, leading to water evaporation and eventually the formation of the habitat itself. Bacterioruberin exhibits UV-protecting characteristics, thereby protecting *Halobacteriaceae* species from UV irradiation and thus from DNA damage (Shahmohammadi *et al*., 1998).

#### 1.1.4.2. Adaptation to high extracellular salt concentrations

As mentioned above, halophilic and haloalkaliphilic *Archaea* are capable of coping with moderate to high extracellular salt concentrations. This adaptation is achieved via the use of the so-called "salt-in" approach, a prevailing strategy among members of the *Halobacteriales* in which sodium is effectively pumped out of the cell's cytoplasm via the use of $Na^+/H^+$ antiporter membrane proteins (Oren A., 1999). At the same time, potassium chloride accumulates in the cell to a concentration at least as high as the surrounding extracellular sodium chloride concentrations (Fendrihan *et al*., 2006). In turn, this high intracellular KCl/salt concentration requires an adaptation of halo(alkali)philic enzymes as well as proteins in general to such high intracellular potassium chloride concentrations (Oren A., 1999; Fendrihan *et al*., 2006). Another method of adaptation to high extracellular salt concentrations is the "compatible solute" strategy where $Na^+$ ions are pumped out of the cell and the extracellular salt concentration is compensated via the synthesis of organic compatible solutes comprising "zwitter-ions" such as *e.g.* glycerol (Oren A., 1999). This strategy however is not relevant for members of the *Halobacteriales*.

#### 1.1.4.3. Haloalkaliphilic *Archaea* – Additional adaptation to high pH

Alongside high extracellular salt concentrations, haloalkaliphilic *Archaea* have to handle high pH as well. High extracellular salt concentrations as well as a high pH of up to 11 and an additional very low $Mg^{2+}$ concentration of less than 10 mM are required here (Kamekura *et al*., 1997). Environments exhibiting these characteristics permanently are generally found in so-called soda deserts or soda lakes of which Lake Magadi in Kenya is one of the most prominent examples. Such soda lakes are almost exclusively inhabited by haloalkaliphilic *Archaea* and mainly characterized by the accumulation of $Na_2CO_3$ which forms through the universal evaporation as well as general high concentrations of sodium chloride (Horikoshi K., 1999; Extremophiles Handbook, Horikoshi K., 2011). Adaptation to high pH levels is mandatory for haloalkaliphilic *Archaea* as their intracellular enzymes have a functional optimum at neutral pH. Aerobic haloalkaliphilic *Archaea* are using $Na^+/H^+$ antiporter membrane proteins linked to $H^+$-coupled respiration in order to maintain a near-neutral intracellular pH for optimal enzyme activity; the electrochemical gradient established by $Na^+$- and $H^+$ ions is used here for energy transduction (Van de Vossenberg *et al*., 1999; Horikoshi K., 1999).

### 1.1.5. The haloalkaliphilic archaeon *Natrialba magadii*

#### 1.1.5.1. Discovery and characteristics

The haloalkaliphilic archaeon *Natrialba magadii* is a member of the *Halobacteriaceae* family and has first been isolated by Tindall *et al*. in 1984 from the waters of Lake Magadi, Kenya (Tindall *et al*., 1984). At the time of discovery, *N. magadii* was classified into a new genus – *Natronobacterium*, the species name being *Natronobacterium magadii* (Tindall *et al*., 1984). Later 16S rRNA sequence comparison of *Natronobacterium magadii* with three other species of the genus *Natronobacterium* however led to the re-classification of *Natronobacterium magadii* into the genus *Natrialba* with the full species name now being *Natrialba magadii* (Kamekura *et al*., 1997).

As mentioned before, Lake Magadi is characterized by a salt concentration of up to 300 g/L with a pH potentially exceeding 11, thus making it a soda lake (Oren A., 2002; Ma *et al*., 2010). These harsh environmental conditions imply that aside from *N. magadii*, Lake Magadi is exclusively inhabited by *Alcolapia grahami*, a species of fish from the *Cichlidae* family (Seegers *et al*., 1999).

In order to grow optimally in laboratory conditions, *N. magadii* requires a rich medium containing 3.5-4 M of sodium chloride; NaCl concentrations below 1.5 M result in cell lysis through excessive osmotic pressure. Additionally, a pH optimum of 9.5-11 is required alongside a temperature optimum of 37°C-42°C. Sodium carbonate ($Na_2CO_3$) as well as a low $Mg^{2+}$ ion concentration are required for optimal growth. *N. magadii* is a strictly aerobically and chemoorganotrophically growing organism: Its carbon- and energy source are peptides and amino acids that need to be supplied in the rich medium and are proteolitically degraded. In its natural habitat, amino acids are supplied mainly through bird droppings as Lake Magadi is a popular breeding ground for *e.g.* flamingos.

In terms of morphology, *N. magadii* cells are rod-shaped, roughly 5 µm in length (Tindall *et al*., 1984) and motile through the presence of polar flagella. The cells incorporate carotenoid pigments, showcased by a reddish colour of cultures and colonies which is especially visible under stress conditions (*e.g.* growth in mineral medium).

The *N. magadii* generation time under laboratory conditions is roughly 9 hours (compared to 20 minutes for *E. coli*) which is due to the fact that it thrives in a harsh environment and especially because of the fact that *N. magadii* is a polyploid organism containing up to 50 copies of chromosomal DNA per cell, all of which need to be replicated in order to be transferred to the daughter cells upon division.

### 1.1.5.2. Main laboratory strains used – *N. magadii* L11 and *N. magadii* L13

Two main strains are being used in the laboratory: The lysogenic wild-type strain *N. magadii* L11 harboring the virus ϕCh1 integrated into its genome as a provirus and the strain *N. magadii* L13 cured from the virus ϕCh1 through repeated passaging. The presence of the virus ϕCh1 in *N. magadii* has first been proven by Witte *et al*. in 1997 through the observation that a culture of *N. magadii* spontaneously started lysis as it reached the stationary phase of growth: The supernatant resulting from the lysed culture contained ϕCh1 virus particles, thus making ϕCh1 a lysogenic virus (Witte *et al*., 1997). To this day, *N. magadii* is the only known host of ϕCh1. As mentioned before, *N. magadii* L13 represents the cured strain where ϕCh1 has been gotten rid of via repeated passaging of an *N. magadii* L11 culture. Electron micrographs of both strains as well as typical growth behavior of both *N. magadii* L11 and *N. magadii* L13 can be seen in Figure 4 A and B. The cured strain *N. magadii* L13 may however still be re-infected by ϕCh1 and represents thus a useful indicator strain for studying ϕCh1 (Witte *et al*., 1997).

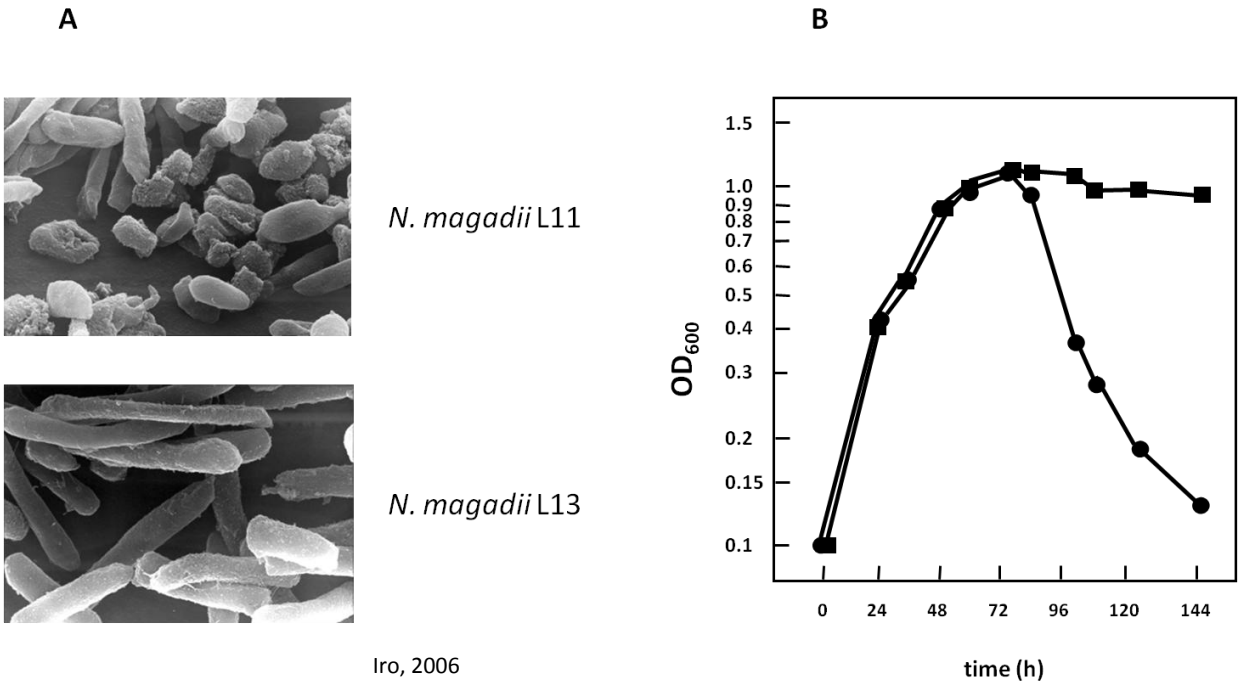


**Figure 4: Electron micrographs of *N. magadii* L11, *N. magadii* L13 and growth kinetics of both strains**

**A** Visualization of the morphology differences between *N. magadii* L11 and *N. magadii* L13; mostly lysed cells can be seen for *N. magadii* L11, due to the infection by the lysogenic virus ϕCh1. **B** Graph showcasing growth kinetics of both strains: *N. magadii* L11 is represented by circles and *N. magadii* L13 is represented by squares. Exponential growth behaviour is almost identical for both strains but virus-induced lysis occurs after roughly three days in the case of *N. magadii* L11 whereas no lysis can be observed for the cured strain *N. magadii* L13.

### 1.1.5.3. Genetic manipulations of *N. magadii*

Genetic manipulations of *N. magadii* represent a considerable challenge for a number of reasons. As mentioned before, up to 50 genome copies may be present per cell which contributes to the rather long generation time of about 9 hours. Alongside the long generation time, the lack of high-end genetic manipulation tools for use in haloalkaliphilc *Archaea* represents a major challenge. Taking into account these facts, it would take a tremendous amount of time to perform genetic manipulations exclusively in *N. magadii* which is why most of the preliminary genetic manipulations are performed in *E. coli* with its comparatively short generation time of 20-30 minutes before performing the actual manipulations in *N. magadii*.

#### 1.1.5.3.1. Transformation of *N. magadii*

The fact that research in halo(alkali)philic *Archaea* is a rather slowly progressing discipline resulted in the fact that the first successful transformation of a halophilic archaeon was performed as recently as in 1987 by Cline and Doolittle where a polyethylene glycol-based method of transformation using spheroplasts was adopted in order to successfully transform ϕH DNA into *Halobacterium salinarum* (Cline and Doolittle, 1987). The same year, Charlebois *et al*. managed to adapt the polyethylene glycol-based method of transformation to work in *Haloferax volcanii* (Charlebois *et al*., 1987). It has been shown though that the method established by Charlebois *et al*. does not work for *N. magadii* as the S-layer could not be removed using EDTA (Mayrhofer-Iro *et al*., 2013). Subsequent adaptation of the polyethylene glycol-based transformation method, involving consecutive incubation of *N. magadii* cells in bacitracin (inhibiting glycosylation of the S-layer) and proteinase K in order to yield competent *N. magadii* spheroplasts, resulted in the generation of viable cells capable of taking up DNA (Mayrhofer-Iro *et al*., 2013). Although a lower transformation efficiency was recorded, it represents a first reliable method of transformation of DNA fragments into the haloalkaliphilic archaeon *N. magadii* (Mayrhofer-Iro *et al*., 2013).

#### 1.1.5.3.2. Available selection markers and shuttle vectors

As of this date, two distinct shuttle vectors are available for transformations in *N. magadii* as well as *E. coli*: pRo-5 and pNB102.

Shuttle vector pRo-5 is based upon the *E. coli* vector pKSII+ containing the point-mutated *gyrB* gene from the halophilic archaeon *Haloferax alicantei* conferring resistance to the antibiotic novobiocin, as no selection marker for haloalkaliphilc *Archaea* existed before (Mayrhofer-Iro *et al*., 2013). Alongside the *gyrB*/novobiocin resistance marker, pRo-5 also contains a supplementary *bla* resistance marker, conferring an additional ampicillin resistance for selection in *E. coli* (Mayrhofer-Iro *et al*., 2013). Furthermore, it contains parts of ϕCh1 ORF53 and ORF54 that are necessary for a minimal origin of replication in order to achieve autonomous replication in *N. magadii*. pRo-5 yielded the highest transformation efficiency from all the tested constructs pRo-1 to pRo-11, each one containing different parts of ORF53/ORF54 (Mayrhofer-Iro *et al*., 2013). Novobiocin is a DNA gyrase inhibitor inhibiting the B subunit of DNA gyrase by blocking the ATP-binding site (Holmes *et al*., 1991).

Shuttle vector pNB102 results from the haloarchaeal plasmid pNB101 in which the *E. coli* replicon ColE1 has been introduced as well as two selection markers conferring resistance to both ampicillin as well as mevinolin, thus making it another shuttle vector suitable for use in both *E. coli* and *N. magadii* (Zhou et al., 2004). Mevinolin is a HMG-CoA inhibitor, thereby blocking synthesis of archaeal isoprenoid lipids (Lam and Doolittle, 1992).

## 1.2. Haloarchaeal viruses

Haloarchaeal viruses comprise viruses capable of infecting halo(alkali)philic *Archaea* and often occur in the natural habitats of said *Archaea*. Although around 20 haloarchaeal viruses have been identified so far, the best studied ones so far are ϕH infecting *Halobacterium salinarum* and ϕCh1 infecting the haloalkaliphilic archaeon *N. magadii*. ϕH has first been discovered and characterized in 1974 by Torsvik and Dundas whereas ϕCh1 has been discovered and characterized by Witte *et al*. in 1997. Additional representatives of haloarchaeal viruses are viruses HF1 and HF2 which were the first reported lytic viruses; additionally they have a broad host range such as *Halobacterium*, *Haloarcula*, *Haloferax*, *Halorubrum* and *Natrialba* (Dyall-Smith *et al*., 2003).

ϕH infecting *H. salinarum* represents the best studied haloarchaeal virus to date and is, among the known haloarchaeal viruses, the closest relative of the *N. magadii*-infecting virus ϕCh1. Although ϕH and ϕCh1 are temperate viruses exhibiting a head-tail morphology and a high sequence similarity, the main difference between both viruses is that the genome of ϕH (59 kbp) persists as a covalently closed DNA molecule (plasmid) in the cytoplasm of *H. salinarum* whereas the genome of ϕCh1 (58 kbp) is integrated into the chromosome of *N. magadii* where it persists as prophage (Klein *et al*., 2002; Schnabel *et al*., 1984; Witte *et al*., 1997).

### 1.2.1. ϕCh1 – A haloalkaliphilic virus

#### 1.2.1.1. Discovery and general characteristics

The discovery of virus ϕCh1 infecting the haloalkaliphilic archaeon *N. magadii* resulted through the preliminary observation by Witte *et al*. that a culture of wild-type *N. magadii* spontaneously started lysis as it reached the stationary phase of growth; the culture supernatant contained ϕCh1 virus particles which were subsequently isolated (Witte *et al*., 1997). ϕCh1 is a temperate virus, member of the family of the *Myoviridae* as well as so far the only haloalkaliphilic virus isolated (Witte *et al*., 1997). Phylogenetically, its closest relative is the halophilic virus ϕH infecting *H. salinarum* with a sequence identity to ϕH of 97% (Torsvik and Dundas, 1974). However, although a high sequence identity has been recorded between ϕH and ϕCh1, their method of persistance in the host cell differs fundamentally: ϕH persists inside *H. salinarum* as a so-called eipsomal prophage whereas the genome of ϕCh1 is integrated into the host chromosome where it persists as an integrated prophage (Schnabel *et al*., 1984; Witte *et al*., 1997). As mentioned above, ϕCh1 may infect *N. magadii*, yielding the wild-type strain *N. magadii* L11 carrying ϕCh1 integrated into the host chromosome as provirus (Witte *et al*., 1997). The same strain can be cured of the virus through repeated passaging of an *N. magadii* L11 culture; the cured strain is labeled *N. magadii* L13 and serves as an indicator strain for studying infection through ϕCh1 (Witte *et al*., 1997). In terms of morphology, ϕCh1 closely resembles other *Myoviridae* species capable of infecting species of *Haloarchaea* (Torsvik and Dundas, 1974). Figure 5 illustrates the general morphological characteristics of virus ϕCh1. Analog to its host *N. magadii*, ϕCh1 needs high environmental salt concentrations of at least 2 M NaCl in order to maintain its infectivity as well as a pH in the vicinity of the one required for the

survival of its host *N. magadii* (Witte *et al*., 1997). ϕCh1 being a temperate virus, it possesses a lysogenic as well as a lytic life cycle.

An additional, rather unusual characteristic of ϕCh1 is the fact that the mature viral particle also contains several different RNA species that are between 80 and 700 nucleotides in length and it has been shown that the virion-associated RNA is host encoded (Witte *et al*., 1997).

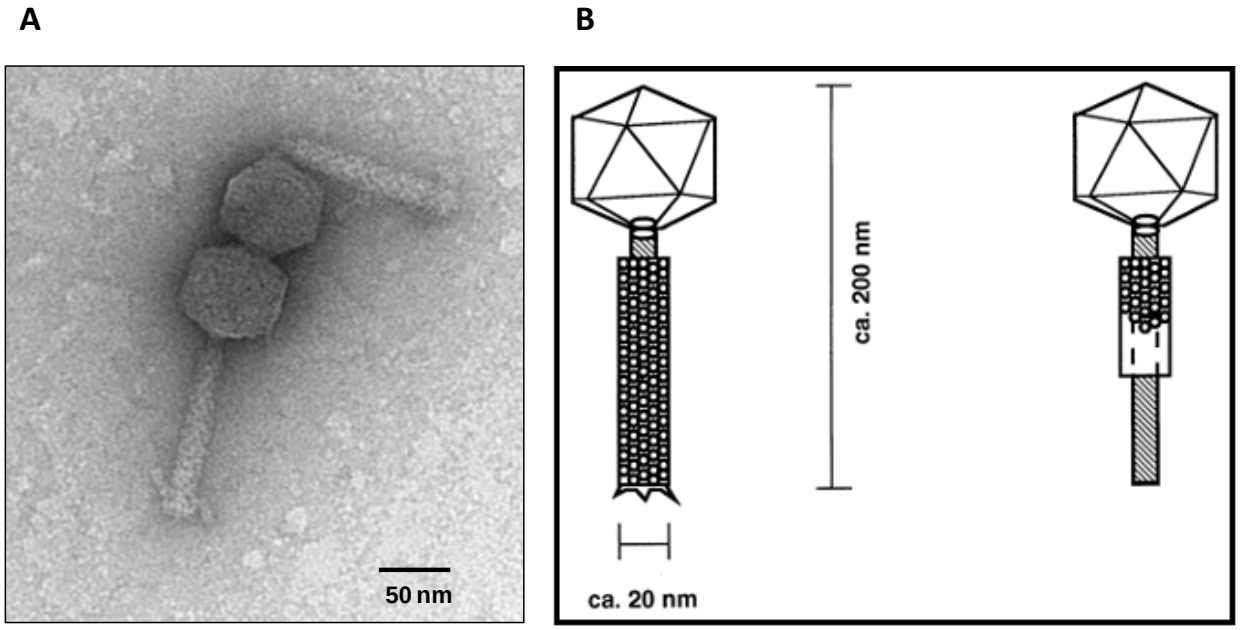


Adapted from Witte *et al*., 1997

**Figure 5: General morphological characteristics of the haloalkaliphilic virus ϕCh1**

**A** Electron micrograph of isolated ϕCh1 viral particles, negatively stained using phosphotungstate. The *Myoviridae*-typical head-tail morphology is clearly discernable. **B** Schematic representation of a ϕCh1 virus particle alongside its dimensions. The icosahedral head encapsulating the viral genome as well as the virus' contractible tail and tail fibers are visualized. The second icon represents an illustration of the conformational changes involving the virus' contractible tail upon infection of *N. magadii*. (Witte *et al*., 1997)

### 1.2.1.2. ϕCh1 – Morphological aspects

ϕCh1 exhibits a classic head-tail morphology with the size of a mature viral particle being roughly 200 nm in length by 20 nm in width. The viral head comprising the viral genome of 58.498 bp measures roughly 70 nm in diameter and exhibits an icosahedral structure, whereas the virus' contractible tail measures approximately 130 nm (Witte *et al*., 1997; Klein *et al*., 2002). One of the best studied morphological aspects of ϕCh1 is the so-called major capsid protein E encoded by the open-reading frame 11 (ORF11) which represents a late gene; protein E is associated with the host cell wall after transcription and translation (Klein *et al*., 2000). The release of progeny virus particles can only be achieved upon proteolytic cleavage of membrane-attached protein E (Klein *et al*., 2000). Other proteins constituting the viral particle have also been identified through SDS-PAGE analysis and have subsequently been subdivided in two distinct categories: Four major proteins A, E, H and I as well as five minor proteins B, C, D, F and G (Witte *et al*., 1997).

### 1.2.1.3. Genome organization

ϕCh1 genome was first completely sequenced in 2002 by Klein *et al*., leading to the identification of 98 different open-reading frames spanning a genome size of a total of 58.498 bp (Klein *et al*., 2002). Klein *et al*. proposed a so-called "headful" mechanism of DNA packaging in the viral capsid as the genome of ϕCh1 is terminally redundant as well as circularly permuted, a characteristic found e.g. in the closely related virus ϕH (Klein *et al*., 2002).

Subsequent comparative analysis of amino acid sequences deduced from the identified ORFs with protein databases revealed that out of the 98 ORFs identified, 48 ORFs have matches to other known sequences; 31 are similar to "*conserved hypothetical proteins of unknown function*" whereas 17 were "*similar to proteins with a known function*" (Klein *et al*., 2002). A schematic overview of the ϕCh1 genome with an illustration of the 98 identified open-reading frames as well as putative and verified functions of the respective gene products is laid out in Figure 6.

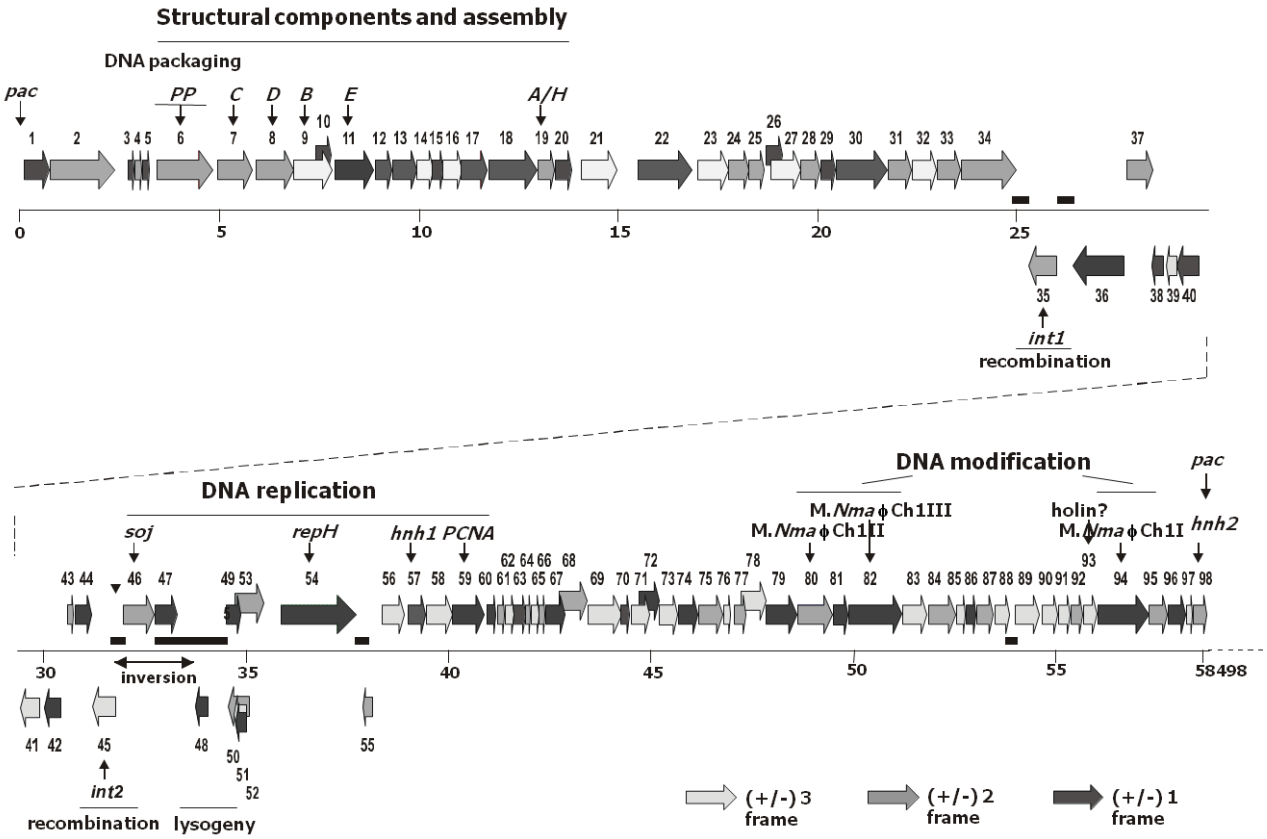


**Figure 6: The linear 58498 bp genome of ϕCh1 with the 98 identified open-reading frames**

The identified ORFs are represented by the arrows; putative as well as verified functions of the respective gene products are indicated. The greyscale of the arrows indicates the frame of the ORFs: light grey – third frame, mid grey – second frame, dark grey – first frame. The linear genome is subdivided into 3 functional genetic modules: the 5‘ end regroups ORFs for structural components as well as assembly, the middle part (with the invertible region) regroups ORFs involved in DNA replication and the 3‘ end regroups ORFs responsible for DNA modifications. Most of the ORFs involved in DNA modifications still have unknown functions, except for the identification of three distinct ϕCh1 methyltransferases: M.*Nma*ϕCh1II, M.*Nma*ϕCh1III and the main, ORF94-encoded methyltransferase M.*Nma*ϕCh1I (Klein *et al*., 2002).

The genome of ϕCh1 is characterized by an organization in what is called functional genetic modules: Such an organization is characteristic among many bacteriophages with a double-stranded genome.

Most of the ORFs encoding proteins that are similar to the ones with a known function share sequence similarities with the *H. salinarum*-infecting virus ϕH (Klein *et al*., 2002). The identification of all these analogies confirms the close similarity of both ϕH and ϕCh1 given the disparity of the habitats in which both their hosts thrive. However, the characterization of the ORFs whose gene products have not yet been attributed a function still is an ongoing process.

### 1.2.1.4. Lysogenic state versus lytic state – A model of regulation

#### 1.2.1.4.1. The lysogenic region of ϕCh1

As mentioned above, ϕCh1 is a temperate virus whose genome is integrated into the host chromosome, capable of switching between lytic as well as lysogenic state depending on the growth state of its host *N. magadii*, such a mechanism of control being essential for all temperate viruses. During the early exponential growth phase, ϕCh1 persists in the host genome as provirus and upon occurrence of the stationary growth phase newly synthesized viral particles are released through lysis of the host cells (Witte *et al*., 1997). For many bacteriophages, gene regulation is under the governance of transcriptional repressors (*e.g.* bacteriophage λ; Ptashne M., 1967/2004). The mechanism of regulation coordinating transition from lysogenic to lytic life cycle involves binding of sequence-specific DNA-binding proteins allowing for selective gene expression depending on the stage of the viral life cycle; such proteins are typical for bacteriophages and mostly belong to the helix-turn-helix family (Pabo and Sauer, 1984). In the case of ϕCh1, one such repressor is represented by ORF48 (*rep*) which shows a homology to the ϕH repressor that is responsible for the blocking of early lytic gene transcription in ϕH (Klein *et al*., 2002; Stolt and Zillig, 1994). Subsequent investigations conducted by Iro *et al*. have shown that the ORF48 gene product gp48 actually contains a helix-turn-helix DNA-binding domain among other characteristics which, taken together, led to the identification of ORF48 together with ORF49 as a so-called repressor-operator system making up the lysogenic region of ϕCh1 (Iro *et al*., 2007). Evidence gathered by Iro *et al*. suggests that ORF49 probably has an involvement in the activation of the lytic life cycle (Iro *et al*., 2007).

#### 1.2.1.4.2. Influence of ORF43/44 on ORF48 and ORF49

Previous work conducted by Gropp *et al*. led to the observation that several fragments from the immunity-conferring plasmid pϕHL conferred immunity to *H. salinarum* against ϕH infection when cloned individually, though different immunity-conferring efficiencies were recorded between cloning the individual fragments compared to cloning the entire pϕHL construct (Gropp *et al*., 1992). Subsequently, Stolt and Zillig identified two distinct transcripts of the immunity-conferring construct pϕHL (T9 and T10) that acted particularly co-operatively with the ϕH repressor (Stolt and Zillig, 1993). Since the ϕH repressor is homologous to ϕCh1 ORF48 (*rep*) and since these two transcripts exhibited high sequence

similarities to ϕCh1 ORF43 (90%) and ORF44 (94%), both ORF43 and ORF44 seemed good candidates for having a function relative to gene regulation in ϕCh1 (Klein *et al*., 2002; Iro *et al*., 2007).

ORF43 and ORF44 have overlapping start- and stop codons as well promoter sequences exclusively present upstream of ORF43 ($p_{43}$), suggesting that ORF43 and ORF44 are co-transcribed as well as co-translated together, thus forming an operon (Klein *et al*., 2002). Among other results, Iro *et al*. have shown that, in the halophilic model organism *H. volcanii*, gp43 as well as gp43/44 have an enhancing effect on ORF49 transcription via direct or indirect binding to 5' repeats in the ORF48 (*rep*) sequence (Iro *et al*., 2007). Gp44 alone however completely abolishes the enhancing effect, thus making it a putative repressor molecule (Iro *et al*., 2007). Constitutive expression of ORF48, which is potentially controlled by gp43/44 binding, represses ORF49 expression with ORF49 probably being involved in the activation of the ϕCh1 lytic life (Iro *et al*., 2007).

Taking into account the fact that the aforementioned experiments have been performed in the halophilic model organism *H. volcanii* in a virus-free background, advances in the field of ORF43/44 characterization have been made in 2015 by Christoph Hofbauer as he performed analogous experiments in the virus-cured strain *N. magadii* L13, yielding comparable results: Cloning ORF43 and ORF43/44 under the control of the constitutive promoter $p_{43}$ in the cured strain *N. magadii* L13 showed no difference in reporter gene expression when compared to the wild-type (Hofbauer C., 2015). However, transformation of ORF44 under the control of $p_{43}$ in *N. magadii* L13 revealed a 48 hour delay in reporter gene expression and subsequent densitometry analysis revealed a 48-hour repressing activity of gp44 when it comes to reporter gene expression (Hofbauer C., 2015). Most importantly, transformation of ORF44 alone resulted in the expression of a truncated reporter protein; the truncation of the reporter protein may be the result of a putative RNase function exhibited by gp44 (Hofbauer C., 2015; Iro M., 2006).

Taken together, these preliminary results suggest a putative, direct or indirect regulating activity of gp43/44 on ORF49 with a putative repressor activity of gp44 and thus a potential regulating effect on the progression from the lysogenic towards the lytic life cycle of ϕCh1.

### 1.2.1.5. ϕCh1 ORF43/44 – A putative VapBC toxin-antitoxin system

#### 1.2.1.5.1. ORF43/44 – Indications for a potential VapBC TA system

A prevailing hypothesis relative to a potential ORF43/44 function is the analogy to the so-called VapBC toxin-antitoxin system. The enhancing effect of ORF43 as well as ORF43/44 on ORF49 transcription alongside the repressor effect of ORF44 as well as the fact that the ORF44 gene product gp44 exhibits a PIN-like domain in its sequence led to the establishment of said hypothesis (Iro et al., 2007; Iro M., 2006). Experiments conducted by Michaela Iro in *H. volcanii* have shown that ϕCh1 gp44 is capable of degrading ORF48 mRNA as well as mRNA originating from transcription of the intergenic region between ORF48 and ORF49 (Iro M., 2006). These results are in accordance with the fact that gp44 has a predicted PIN-like domain, thus making gp44 capable of exhibiting a nuclease function.

Type II VapBC (**V**irulence **a**ssociated **p**rotein) toxin-antitoxin systems are so-called PIN-domain TA systems and represent the largest family of bacterial toxin-antitoxin systems (Arcus *et al*., 2011; Robson *et al*., 2009). VapBC TA systems build an operon where the VapC part contains a PIN domain exhibiting a ribonuclease function whereas VapB is the stable antitoxin (inhibitor) containing a transcription factor domain (Arcus *et al*., 2011). *vapBC* transcription is autoregulated via promoter binding and the method of VapC toxin activation is unknown although it is believed to result from proteolytic degradation of the stable VapB part (Arcus *et al*., 2011). Function-wise, not much is known about type II VapBC toxin-antitoxin systems; the general consensus is that toxin-antitoxin systems have their origin in the horizontal gene pool (Arcus *et al*., 2011). The fact that TA systems are capable of invading plasmids as well as genomes by behaving as so-called "selfish elements" led to the hypothesis that such systems may have been taken over by the host organisms to exhibit functions that generally benefit the host (Arcus *et al*., 2011). Figure 7 represents a schematical illustration of a classical VapBC toxin-antitoxin system.

Through analogy with the *H. influenza* hypothesis established by Daines *et al*., it is conceivable that gp44, through its nuclease/RNase activity, may cause growth retardation in the ϕCh1 host *N. magadii* via the degradation of mRNA translatable into growth-promoting proteins (Daines *et al*., 2007). Through this mode of action, the host would remain longer in the exponential growth phase and ϕCh1/*N. magadii* might adapt to existing stress situations.

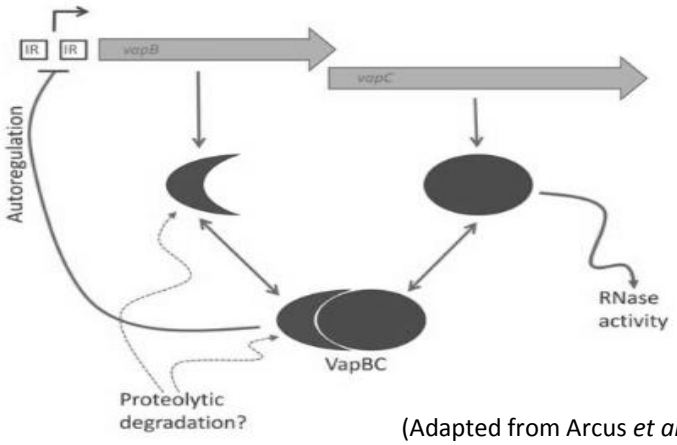


(Adapted from Arcus *et al.*, 2011)

**Figure 7: Illustration of a typical *vapBC* toxin-antitoxin system**

The start-and-stop codons of the two genes encoding for the stable antitoxin (*vapB*) and for the RNase (*vapC*) overlap, thus forming an operon together. The *vapBC* operon encodes proteins forming a tight complex together which binds to inverted repeats (IR) in the promoter region of the *vapBC* operon. This binding method results in the autoregulation of *vapBC* operon transcription. The method of VapC toxin activation is unknown although it is believed to result from the proteolytic degradation of the stable inhibitor VapB (Arcus *et al.*, 2011).

### 1.2.1.5.2. The PIN-domain

PIN-domain proteins are widespread throughout all three domains of life (Arcus *et al.*, 2011). The nomenclature derives from the fact that sequence similarities to the N-terminal part of the so-called PilT protein (a component of type IV pili) have been identified (Arcus *et al.*, 2011). PIN-domains are small protein domains, composed of around 130 amino acids characterized by the presence of three to four conserved acidic residues (Arcus *et al.*, 2011). These acidic residues form the active site of the PIN-domain where either $Mg^{2+}$- or $Mn^{2+}$ ions bind: PIN-domains are thereby capable of cleaving single-stranded RNA in an ion-dependent manner (Arcus *et al.*, 2011).

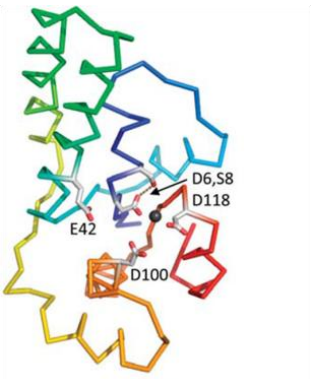


**Figure 8: Schematic representation of a PIN-domain**

Three to four conserved acidic residues make up the active site of a PIN-domain. The $Mn^{2+}$ ion needed in order to catalyze the PIN-domain nuclease activity is highlighted as a black circle: It directly binds to the active site.

(Arcus *et al.*, 2011)

# 2. Materials and Methods

## 2.1. Materials

### 2.1.1. Bacterial and archaeal strains used

*Escherichia coli*

| Strain | Genotype | Source |
|---|---|---|
| XL1 - Blue | *recA1 endA1 gyrA96 thi-1 hsdR17 supE44 relA1 lac [F′ proAB lacI$^q$ ZΔ M15* Tn*10 (Tet$^r$)].* | Novagen |
| Rosetta(DE3)pLysS | F$^-$ *ompT hsdS$_B$*(*R$_B^-$ m$_B^-$*) *gal dcm lacY1* (DE3) pRARE6 (Cm$^R$) | Novagen |

*Natrialba magadii*

| Strain | Genotype | Source |
|---|---|---|
| *N. magadii* L11 | Wild-type strain, contains ϕCh1 integrated as provirus | Witte *et al*., 1997 |
| *N. magadii* L13 | Cured strain, does not contain ϕCh1 anymore | Witte *et al*., 1997 |
| *N. magadii* L11-pRo-5-ORF56 | Wild-type strain containing an additional copy of ϕCh1 ORF56 | Master's thesis Léa Schöner, 2013 |
| *N. magadii* L11-ΔORF44-R | ϕCh1 ORF44 deletion mutant containing a novobiocin resistance cassette in reverse orientation | This thesis |

### 2.1.2. Media

**Lysogeny broth (LB) medium for growth of *E. coli***

| | |
|---|---|
| Peptone | 10 g |
| Yeast extract | 5 g |
| Sodium chloride | 5 g |

dd$H_2O$ ad 1L, pH 7, autoclave; 15 g/L agar for LB/Agar plates

**Rich medium (NVM$^+$) for haloalkaliphilic *Archaea***

| | | |
|---|---|---|
| Casamino acids (Casein hydrolysate) | 8.8 | g |
| Yeast extract | 11.7 | g |
| Sodium citrate tribasic dihydrate (Tri-Na citrate) | 0.8 | g |
| Potassium chloride (KCl) | 2.35 | g |
| Sodium chloride (NaCl) | 235 | g |

pH 9 - 9.5, dd$H_2O$ ad 935 mL, autoclave
10 g/L agar for NVM/Agar plates, 5 g/L agar for soft agar, autoclave

After autoclaving, complement medium (ad 1L total medium) by adding:

| | |
|---|---|
| 0.57 M sodium carbonate ($Na_2CO_3$, dissolved in sterile dd$H_2O$), | 63 mL |
| 1 M magnesium sulfate ($MgSO_4$, autoclaved), | 1 mL |
| 20 mM iron(II) sulfate ($FeSO_4$, dissolved in sterile dd$H_2O$), | 1 mL |

Note:
NVM$^-$: Uncomplemented medium
NVM$^+$: Complemented medium

### 2.1.3. Antibiotics and other additives used

| Compound | Stock concentration | Final concentration | Preparation |
|---|---|---|---|
| Ampicillin | 20 mg/mL | 100 µg/mL | Dissolved in dd$H_2O$, sterile filtered, storage at 4°C |
| Tetracycline | 10 mg/mL | 10 µg/mL | Dissolve in half the volume dd$H_2O$, add half the volume 96% EtOH, light protection, storage at -20°C |
| Novobiocin | 3 mg/mL | 3 µg/mL | Dissolved in dd$H_2O$, sterile filtered, light protection, storage at -20°C |
| Mevinolin | 10 mg/mL | 7.5 µg/mL | Stock solution prepared from commercially available tablets*, light protection, storage at -20°C |
| Bacitracin | 7 mg/mL | 70 µg/mL | Dissolved in sterile dd$H_2O$, sterile filtered, light protection, storage at 4°C |
| IPTG | 1 M | 0.5 – 1 mM | Dissolved in dd$H_2O$, sterile filtered, storage at -20°C |
| X-Gal | 10 mg/mL | 20 µg/mL | Dissolved in N-N-dimethylformamide, storage at -20°C |

* 120 mg active compound (6 tablets of Lovastatin Hexal® 20mg) are dissolved in 12 mL of 96% EtOH, let stir for 20 minutes, centrifuge (5000 x g, 15 minutes, 4°C), collect supernatant (= 10 mg/mL).

### 2.1.4. Plasmids used

| Construct | Characterization | Source |
|---|---|---|
| pBlueScript II KS(+) | mcs, *bla*, ColE1 ori, *lacZα* | Stratagene |
| pUC19 | *bla*, pMB1 ori, mcs, *lac*Za | Yanish - Perron *et al*., 1985 |
| pRo-5 | *bla*, gyrB (Nov$^R$), ColE1 ori, ϕCh1 ori | Mayrhofer – Iro *et al*., 2013 |
| pRSET - A | *bla*, pUC ori, T7 promoter, N-terminal 6x His-tag | Invitrogen |
| pRo-5-ORF56 | pRo-5 containing ϕCh1 ORF56 | Schöner, 2013 |
| pKSII-ORF56-1-4 | pBlueScript II KS(+) containing up- and downstream region of ϕCh1 ORF56 | Haider, 2015 |
| pUC19-Nov$^R$ "reverse" | pUC19 containing the novobiocin resistance cassette in reverse orientation | Wurzer, 2015 |
| pUC19-Nov$^R$ "forward" | pUC19 containing the novobiocin resistance cassette in forward orientation | Wurzer, 2015 |
| pKSII-Δ56-Nov$^R$-R | pBlueScript II KS(+)containing up- and downstream regions of ϕCh1 ORF56, flanking a novobiocin resistance cassette in reverse orientation | This thesis |
| pKSII-Δ56-Nov$^R$-F | pBlueScript II KS(+)containing up- and downstream regions of ϕCh1 ORF56, flanking a novobiocin resistance cassette in forward orientation | This thesis |
| pKSII-ΔORF44-1-4 | pBlueScript II KS(+) containing the up- and downstream regions of ϕCh1 ORF44 | Tschurtschenthaler, 2015 |
| pKSII-ΔORF44-1-4-Nov$^R$-F | pBlueScript II KS(+) containing up- and downstream regions of ϕCh1 ORF44, flanking a novobiocin resistance cassette in forward orientation | Brait, 2016 |
| pKSII-ΔORF44-1-4-Nov$^R$-R | pBlueScript II KS(+) containing up- and downstream regions of ϕCh1 ORF44, flanking a novobiocin resistance cassette in reverse orientation | Tschurtschenthaler, 2015 |
| pRSET-34 | pRSET-A containing ϕCh1 ORF34 | Witte, 2016 |
| pRSET-Mtase | pRSET-A containing ϕCh1 ORF94 | Witte, 2014 |

### 2.1.5. Kits used

| Kit | Usage | Manufacturer | Product N° |
|---|---|---|---|
| GeneJET Plasmid Miniprep Kit | Isolation/Purification of plasmid DNA in *E. coli* | Thermo Scientific | K0503 |
| GeneJET Plasmid Midiprep Kit | Isolation/Purification of plasmid DNA in *E. coli* | Thermo Scientific | K0489 |
| Wizard® Plus SV Minipreps DNA Purification System | Isolation/Purification of plasmid DNA in *E. coli* | Promega | A1460 |
| QIAquick® Gel Extraction Kit | Purification of gel-extracted DNA fragments | QIAGEN | 28706 |
| GeneJET PCR Purification Kit | Purification of PCR products | Thermo Scientific | K0701 |
| SuperSignal® West Pico Chemiluminescent Substrate | Chemiluminescence substrate for HRP visualization on immunoblots (Western Blot) | Thermo Scientific | 34080 |
| Chemiluminescent Nucleic Acid Detection Module | Detection of biotin-labeled nucleic acids (Southern Blot) | Thermo Scientific | 89880 |

### 2.1.6. Enzymes used

| Enzyme | Manufacturer | Product N° | Details |
|---|---|---|---|
| **Restriction enzymes** | Thermo Scientific | **/** | Used for DNA restriction |
| | New England Biolabs | **/** | High fidelity restriction enzymes for southern blotting applications |
| **DNA polymerases** | | | |
| *GoTaq* DNA polymerase/*GoTaq* Green Mastermix | Promega | M3001/M7123 | Used for analytic test PCRs; no proofreading activity |
| *Pfu*-DNA polymerase | Promega | M7741 | Used for cloning; 3' – 5' proofreading activity |
| **DNA modifying enzymes** | | | |
| T4 DNA ligase | Promega | M1801 | Ligation of DNA fragments. |

| Enzyme | Manufacturer | Product N° | Details |
|---|---|---|---|
| T4 DNA polymerase | Promega | M4211 | Used for the synthesis of DNA in the 5'→ 3' direction and its 3'→5' exonuclease activity (Blunt end creation) |
| Klenow fragment | Thermo Scientific | EP0051 | Used to create blunt ends by 5' overhang filling |
| **Other enzymes** | | | |
| Proteinase K | Qiagen | 1019499 | Digestion of archaeal S-layer to create competent cells |

Note: All enzymes were either used in combination with the provided kit-specific reaction buffer or with buffers recommended by the manufacturer.

### 2.1.7. Size markers

| Marker | Manufacturer | Product N° | Details |
|---|---|---|---|
| **DNA markers** | | | |
| λ/*BstEII* | Thermo Scientific (λ DNA & *BstEII*) | SD0011 (λ DNA), ER0391 (*BstEII*) | Fragment size range: 702 – 8454 bp |
| GeneRuler 1kb DNA ladder | Thermo Scientific | SM0311 | Fragment size range: 250 – 10000 bp |
| **Protein marker** | | | |
| PageRuler™ Prestained Protein Ladder | Thermo Scientific | 26616 | Protein size range: 10 proteins spanning 10 - 180 kDa |

### 2.1.8. Nucleotides used

| Nucleotides | Manufacturer | Product N° |
|---|---|---|
| dNTP Mix | Promega | U1511 |
| Biotin-11-dUTP | GeneON | 110 |

### 2.1.9. Primers used

| Name | Sequence (Restriction sites are underlined) | Restriction site(s) | Internal identification number |
|---|---|---|---|
| 56-5 | CAGCAGGATCCATGAGAGAGAACAATCC | *BamHI* | 331 |
| 56-3 | CAGCGTCTAGACTGCAGTCACTGCTGACCACCGG | *XbaI, PstI* | 333 |
| Δ56-1 | GAATTCTAGACCGTGGAGTGGACCGATC | *XbaI* | 931 |
| Δ56-2 | GTCAGGATCCTGCTCTGGGCCTCTTTGC | *BamHI* | 932 |
| Δ56-3 | GAATAAGCTTCGTCTGTCAGACCTGCG | *HindIII* | 933 |
| Δ56-4 | GTCAGGTACCGAGCGCCATCATGACTCT | *KpnI* | 934 |
| 56-5en | GATACCCGAACAGACGAGC | / | 984 |
| 56-3en | GTCGATACCGCACTGCAGC | / | 985 |
| 56-31en | GCTGGCTGATGGGATCTGTG | / | 990 |
| 44-3en | GACGCCTGCAGAACTACCTT | / | 983 |
| 44-3-Bam | GTTAGGATCCACAGAACGGACGTACGAC | *BamHI* | 914 |
| 43-5-N | GTAGCATATGGCAATCGTCACCA | / | 968 |
| 44-5 | CAGCAGTCTAGACGTTGTGCCAGCCGT | *XbaI* | 294 |
| 44-3 | CAGCAGTCTAGACAAACCACAGAACGGACG | *XbaI* | 292 |
| pKS-5 | GTAGCTCTTGATCCGGCA | / | 606 |
| Nov-6 | GGGATCGCAGAGGAGC | / | 347 |
| Nov-9 | GATGTCGGTCATCGCGG | / | 548 |
| Nov-12 | GCCGGTGAGTACTTAACGC | / | 829 |

### 2.1.10. Antibodies used

| Name | Target protein | Dilution used | Source |
|---|---|---|---|
| **Primary antibodies** | | | |
| α-E | ϕCh1 major capsid protein E | 1:2500 | Klein *et al*., 2000 |
| α-gp34$_{52}$ | ϕCh1 gp34$_{52}$, a tail fiber protein | 1:2500 | Till, 2011 |
| α- M.*Nma*ϕCh1I | ϕCh1 main DNA methyltransferase | 1:2500 | Baranyi *et al*., 2000 |
| **Secondary antibody** | | | |
| ECL™ Anti-Rabbit IgG, HRP-linked whole antibody from donkey | Rabbit Immunoglobulin G | 1:5000 | GE Healthcare UK Limited |

### 2.1.11. General buffers and solutions used

#### 2.1.11.1. DNA gel electrophoresis

**50x TAE**

| | |
|---|---|
| 2 M | Tris / HCl pH 8.2 |
| 1 M | Acetic Acid |
| 0.1 M | EDTA |

**0.8% agarose gel**

Amount of agarose needed melted in 1x TAE

**5x DNA loading dye**

| | |
|---|---|
| 50 mM | Tris / HCl pH 8.2 |
| 0,1 % | SDS |
| 0,05 % | Bromphenol blue |
| 0,05 % | Xylene cyanol |

Autoclave, then add

25 % Sucrose (sterile filtered)

### 2.1.11.2. Polyacrylamide gels and western blots

**30 % Acrylamide solution**

| | |
|---|---|
| 29 % | Acrylamide |
| 1 % | N, N'-methylenebisacrylamide |

**Separating gel buffer**

| | |
|---|---|
| 1.5 M | Tris / HCl pH 8.8 |
| 0.4 % | SDS |

$ddH_20$ ad 250 mL

**Stacking gel buffer**

| | |
|---|---|
| 0.5 M | Tris / HCl pH 6.8 |
| 0.4 % | SDS |

$ddH_2O$ ad 250 mL

**10x SDS Running buffer**

| | |
|---|---|
| 0.25 M | Tris |
| 1.92 M | Glycin |
| 1 % | SDS |

**Coomassie staining solution**

| | |
|---|---|
| 25 % | Methanol |
| 10 % | Acetic acid |
| 0.15 % | Coomassie Brilliant Blue R-250 |

**Coomassie destaining solution**

10 % Acetic acid in $ddH_2O$

**10x TBS**

| | |
|---|---|
| 0.25 M | Tris / HCl pH 8 |
| 1.37 M | NaCl |
| 27 mM | KCl |

**Transblot/Transfer buffer**

| | |
|---|---|
| 48 mM | Tris |
| 39 mM | Glycine |
| 0.037 % | SDS |
| 20 % | Methanol |

**Ponceau-S staining solution**

| | |
|---|---|
| 0.5 % | Ponceau - S |
| 3 % | Trichloroacetic acid |

**Blocking solution**

5 % milk powder in 1x TBS

**100 mL 1 M Sodium phosphate buffer pH 6.8**

| | |
|---|---|
| 1 M $Na_2HPO_4$ | 46.3ml |
| 1 M $NaH_2PO_4$ | 53.7ml |

**2x Lämmli sample buffer**

| | |
|---|---|
| 0.12 mM | Tris / HCl pH 6.8 |
| 4 % | SDS |
| 17.4 % | Glycerol |
| 2 % | β - mercaptoethanol |
| 0.02 % | Bromphenol blue |

**Primary antibody solution (in 1x TBS)**

| | |
|---|---|
| 0.3 % | BSA |
| 0.02 % | $NaN_3$ |
| 1:2500 | Respective serum |

L13 acetone powder (antibody saturation)

**Secondary antibody solution (in 1x TBS)**

| | |
|---|---|
| 1:5000 | Respective secondary antibody |

### 2.1.11.3. Protein purification under denaturing conditions

**Buffer B (Lysis Buffer)**

| | |
|---|---|
| 100 mM | $NaH_2PO_4$ |
| 10 mM | Tris |
| 8 M | Urea |

pH 8, to be adjusted before each use (NaOH)

**Buffer C (Wash Buffer)**

| | |
|---|---|
| 100 mM | $NaH_2PO_4$ |
| 10 mM | Tris |
| 8 M | Urea |

pH 6.3, to be adjusted before each use (HCl)

**Buffer D (Elution Buffer)**

| | |
|---|---|
| 100 mM | $NaH_2PO_4$ |
| 10 mM | Tris |
| 8 M | Urea |

pH 5.9, to be adjusted before each use (HCl)

**Buffer E (Elution Buffer)**

| | |
|---|---|
| 100 mM | $NaH_2PO_4$ |
| 10 mM | Tris |
| 8 M | Urea |

pH 4.5, to be adjusted before each use (HCl)

### 2.1.11.4. Southern blot

**20x SSC**

| | |
|---|---|
| 3 M | NaCl |
| 0.3 M | Na - citrate |

pH 7.2

**50x Denhardt's solution**

| | |
|---|---|
| Ficoll 400 | 1g |
| Polyvinylpyrolidone | 1g |
| BSA | 1g |

dd$H_2O$ ad 100 mL

**Hybridization buffer**

| | |
|---|---|
| 20x SSC | 25 mL |
| 50x Denhardt´s Solution | 10 mL |
| 10 % BSA | 5 mL |
| 1M $Na_2HPO_4$ | 5 mL |
| 20 % SDS | 500 µL |
| 0.5 M EDTA | 200 µL |

### 2.1.11.5. *E. coli* – Competent cells

**MOPS I**

| | |
|---|---|
| 100 mM | MOPS |
| 10 mM | KCl |
| 10 mM | RbCl |

pH 7 (KOH)

**MOPS II**

| | |
|---|---|
| 100 mM | MOPS |
| 70 mM | KCl |
| 10 mM | RbCl |

pH 6.2 (KOH)

**MOPS IIa**

| | |
|---|---|
| 100 mM | MOPS |
| 10 mM | KCl |
| 10 mM | RbCl |
| 15 % | Glycerol |

pH 6.2 (KOH)

### 2.1.11.6. *N. magadii* – Competent cells and transformation reagents

**Buffered high salt spheroplasting solution**

| | |
|---|---|
| 50 mM | Tris / HCl pH 8.0 |
| 2 M | NaCl |
| 27 mM | KCl |

After autoclaving add

15 % Sucrose (sterile filtered)

**Buffered high salt spheroplasting solution (+ glycerol)**

| | |
|---|---|
| 50 mM | Tris / HCl pH 9.5 |
| 2 M | NaCl |
| 27 mM | KCl |
| 15 % | Glycerol |

After autoclaving add

15 % Sucrose (sterile filtered)

**Unbuffered high salt spheroplasting solution**

| | |
|---|---|
| 2 M | NaCl |
| 27 mM | KCl |

After autoclaving add

15 % sucrose (sterile filtered)

**60 % PEG 600 in unbuffered high salt spheroplasting solution**

| | |
|---|---|
| PEG 600 | 60 % |
| UHSSPS | 40 % |

**0.5 M EDTA**

0.5 M EDTA

Autoclave

**Proteinase K**

Commercially available from QIAGEN

### 2.1.11.7. Isolation of ϕCh1 virus particles

**High alkaline salt solution**

| | |
|---|---|
| 4 M | NaCl |
| 50 mM | Tris / HCl pH 9.5 |

**1.1 CsCl solution**

| | |
|---|---|
| 2 M | NaCl |
| 50 mM | Tris / HCl pH 8.5 - 9 |
| 0.6 M | CsCl |

**1.3 CsCl solution**

| | |
|---|---|
| 2 M | NaCl |
| 50 mM | Tris / HCl pH 8.5 - 9 |
| 3.7 M | CsCl |

**1.5 CsCl solution**

| | |
|---|---|
| 2 M | NaCl |
| 50 mM | Tris / HCl pH 8.5 - 9 |
| 4 M | CsCl |

## 2.2. Methods

### 2.2.1 DNA methods

#### 2.2.1.1. Agarose gel electrophoresis

Separation of DNA fragments above a size of 700 base pairs was achieved via the use of a 0.8% agarose gel. The required amount of agarose was dissolved (through melting) in 1x TAE before being poured into the gel tray. Here, depending on the subsequent use of the gel, different well combs have been chosen; bigger well combs were chosen for southern blotting applications, whereas smaller ones were chosen for the separation of DNA fragments in all other laboratory applications.

#### 2.2.1.2. Staining and visualization of DNA

Visualization of the separated DNA fragments was achieved via ethidium bromide (EtBr) staining (10 µg/mL, dissolved in $H_2O$). Ethidium bromide is characterized by a high DNA-binding affinity; hence it is a cancerogenic substance. Subsequent visualization of the separated DNA fragments was achieved via exposition to ultraviolet light in an UV transilluminator.

#### 2.2.1.3. Polymerase chain reaction (PCR)

Two different PCR protocols were being used for this thesis work, the so-called 'preparative' PCR protocol and the 'analytical' PCR protocol. All PCRs in this thesis have been performed using a Thermo Scientific Arktik 5020 thermocycler.

#### 2.2.1.3.1. Preparative PCR

The preparative PCR protocol used for this thesis implied the use of the *Pfu* DNA polymerase, a DNA-dependent DNA polymerase, isolated from *Pyrococcus furiosus*. Its 3' – 5' exonuclease activity, or more commonly called 'proofreading' activity, makes it an essential tool for cloning applications. It is thus the enzyme of choice for the correct amplification of DNA fragments.

#### 2.2.1.3.2. General protocol for a preparative PCR (*Pfu* PCR)

The reaction mixture is prepared in 100 µL batches.

| Component | Volume added (µL) |
|---|---|
| Sterile dd$H_2O$ (PCR-quality $H_2O$) | 67 |
| 10x reaction buffer | 10 |
| 2mM dNTP mix | 10 |
| 5' primer | 5 |
| 3' primer | 5 |
| Template | 1 |
| *Pfu* polymerase (2-3 U/µL) | 2 |
| **Total volume** | 100 |

Standard preparative PCR (*Pfu* PCR) program:

| Step | Time (min) | Temperature (°C) | N° of cycles |
|---|---|---|---|
| 1. Initial denaturation | 5 | 95 | 1 |
| 2. Denaturation | 1 | 95 | 35 |
| 3. Annealing | 1 | $T_m$ * | |
| 4. Extension | 1 min per 500 bp | 72 | |
| 5. Final extension | 2x extension time | 72 | 1 |
| 6. Soaking temperature | / | 4 | / |

* $T_m$ refers to the annealing temperature of the primers used. It was calculated by subtracting 4°C of the primer having the lowest melting temperature. All melting temperatures were calculated via the GeneRunner software from Hastings Software Inc.

#### 2.2.1.3.3. Analytical PCR

The analytical PCR protocol used in this thesis takes advantage of the amplification speed of the *Taq* polymerase (1000 bp/min), another DNA-dependent DNA polymerase isolated from *Thermus aquaticus*. The higher amplification speed in comparison to *Pfu* polymerase (500 bp/min) results through the lack of 3' – 5' exonuclease activity of the *Taq* polymerase. Here, usage was limited to the commercially available *GoTaq*® Green Master Mix, containing *Taq* DNA polymerase as well as all necessary PCR reagents aside from template and primers. Through its amplification speed, it is a very useful tool in order to control the success rates of transformations as well as to confirm the correct construction of different plasmid constructs. Thus, these PCRs are often referred to as 'Test PCR'.

#### 2.2.1.3.4. General protocol for an analytical PCR

The reaction mixture is prepared in 25 µL batches.

| **Component** | **Volume added (µL)** |
|---|---|
| *GoTaq*® Green Master Mix | 12.5 |
| Sterile dd$H_2O$ (PCR-quality $H_2O$) | 8.5 |
| 5' primer | 1.5 |
| 3' primer | 1.5 |
| Template | 1 |
| **Total volume** | 25 |

Standard analytical PCR (Test PCR) protocol

| **Step** | **Time (min)** | **Temperature (°C)** | **N° of cycles** |
|---|---|---|---|
| 1. Initial denaturation | 5 | 95 | 1 |
| 2. Denaturation | 1 | 95°C | 20 |
| 3. Annealing | 1 | $T_m$ * | |
| 4. Extension | 1 min per 1000 bp | 72 | |
| 5. Final extension | 2x extension time | 72 | 1 |
| 6. Soaking temperature | / | 4 | / |

* $T_m$ refers to the annealing temperature of the primers used. It was calculated by subtracting 4°C of the primer having the lowest melting temperature. All melting temperatures were calculated via the GeneRunner software from Hastings Software Inc.

#### 2.2.1.3.5. PCR product quality control

In order to control the quality of the respective PCR products, the PCR products were separated on a 0.8% agarose gel. For preparative PCR products, 5x DNA loading dye needed to be added to the product to be controlled whereas analytical PCR products did not need to be supplemented with 5x DNA loading dye as *GoTaq*® Green Master Mix contains all the loading reagents necessary.

#### 2.2.1.3.6. PCR templates

Most of the PCR templates used resulted from crude extracts of either *E. coli* or *N. magadii*. Most positive control templates were prepared from purified and subsequently diluted plasmid DNA.

*E. coli* PCR template:

5 µL of culture were added to 100 µL sterile $ddH_2O$, the mixture was vortexed and subsequently denatured at 95°C for 10 minutes.

*N. magadii* PCR template:

30 µL of culture were centrifuged using a tabletop centrifuge (3–5 min, 13200 rpm, room temperature) and the supernatant was removed. The pellet was then resuspended (lysed) in 100 µL sterile $ddH_2O$.

### 2.2.1.4. Purification of DNA samples

#### 2.2.1.4.1. Purification of PCR products

PCR products were being purified using the GeneJET PCR Purification Kit (Thermo Scientific). This step was necessary to eliminate all remaining PCR reagents contained in the PCR products such as polymerases, nucleotides, magnesium ions as well as reaction buffer. Purification was achieved according to the manufacturer's protocol and purified DNA was eluted in $ddH_2O$.

#### 2.2.1.4.2. DNA gel elution and fragment purification

Here, gel elution was performed in cases where PCR amplification of a given fragment was impossible due to too many amplification errors. In that case the fragment in question needed to be restricted from the plasmid containing said fragment. Ultimately, the fragment was eluted from a 0.8% agarose gel using an UV bench with UV light set to 70% of maximal intensity in order to keep DNA damage at a minimum. Purification of the eluted fragment was achieved using the QIAquick® Gel Extraction Kit. The purified DNA fragment was ultimately eluted in $ddH_2O$.

### 2.2.1.5. DNA restriction

Restriction of DNA was performed using Thermo Scientific restriction enzymes. Reaction buffers were chosen according to the manufacturer's recommendation, both for single digests as well as for double and triple digests. Although a reaction time of 3 hours at 37°C is recommended by the manufacturer, all restriction reactions were performed overnight at 37°C to make sure that the DNA would be restricted in its entirety. Here, no fast-digest restriction enzymes were used.

### 2.2.1.6. DNA modifications

#### 2.2.1.6.1. Blunt end creation via 3' overhang removal

The T4 DNA polymerase from Promega was used to create blunt ends via the removal of 3' overhangs; this was achieved by following the manufacturer's protocol and making sure that no additional dNTPs were added to the reaction mix as this would have resulted in a 5'-overhang-filling activity of T4 DNA polymerase.

#### 2.2.1.6.2. Blunt end creation via 5' overhang fill-in

In order to create blunt ends at 5' overhangs, Thermo Scientific's Klenow fragment was used as it has no 5' → 3' exonuclease activity. This property guarantees that 5' overhangs are not digested, but filled in instead. In order for this reaction to happen, dNTPs must be added to the reaction mix.
Alternatively, T4 DNA polymerase may be used.

#### 2.2.1.6.3. Ligation of DNA fragments

All ligation reactions (blunt end as well as sticky end) were performed using Promega's T4 DNA ligase. The ligation reaction was left to incubate for 3 hours at room temperature or overnight at 16°C. Although an insert-to-vector ratio of 3:1 is recommended, the ratio was raised to 6:1 as it yielded the best results in this case.

### 2.2.1.7. Transformation of DNA in *E. coli*

#### 2.2.1.7.1. Generation of competent *E. coli* cells

In order to generate competent *E. coli* cells (XL1-Blue, Rosetta) the strain of choice was inoculated at an optical density of 0.1 ($OD_{600}$ = 0.1) in 200 mL LB medium containing the required antibiotics for selection. Incubation of the culture was done at 37°C, shaker set to 165 rpm, until an $OD_{600}$ of 0.6 was reached; the $OD_{600}$ of 0.6 guaranteed that the cell culture had reached the logarithmic growth phase. The cells were harvested via centrifugation (16250 x g, 10 min, 4°C) and the supernatant was removed. Next, the pellet was resuspended in 80 mL MOPS I solution and incubated on ice for 10 min. Subsequently, the cells were pelleted via another centrifugation step (16250 x g, 10 min, 4°C) before being resuspended in 80 mL MOPS II solution and incubated on ice for 30 min. A final centrifugation step was performed (16250 x g, 10 min, 4°C), the supernatant was removed and the pellet was then resuspended in 4 mL of MOPS IIa solution. 100 µL aliquots were prepared in Eppendorf tubes that had previously been put on ice. Storage of the prepared competent *E. coli* aliquots happened at -80°C and the cells were usable for DNA transformation for at least a year.

#### 2.2.1.7.2. Transformation of competent *E. coli* cells

The transformation protocol used was the same for all strains of competent *E. coli* (XL1-Blue, Rosetta).
The competent *E. coli* cell aliquots were thawed on ice for 10 minutes. The ligation product (15 µL) was then added to the cell suspension and the reaction was incubated on ice for 30 minutes. In cases where plasmid DNA (resulting from Miniprep isolation/purification) was being transformed, the concentration of purified plasmid DNA being added to the cell suspension was considerably reduced as successful transformation rates with purified plasmid DNA are much higher than with ligation products. After incubating on ice for 30 minutes, the transformation reaction underwent a heat shock step at 42°C for 2 minutes. The heat shock was then followed by a 30-second cold shock on ice. The rapid transition of high-to-low temperatures is responsible for the uptake of DNA by the cells. Subsequently, 300 µL of LB medium (not containing antibiotics) were added to the transformation reaction and the reaction was incubated at 37°C for 30 minutes. This step is called the 'regeneration step', as the cells recover from stress resulting from the transformation procedure. After regeneration, the cells were plated on

selective LB medium agarose plates and incubated at 37°C overnight. The following day, single colonies could be observed.

#### 2.2.1.7.2. Screening of *E. coli* transformants: Quick-prep

A preliminary screening step used in order to find positive clones is a procedure called quick-prep or quick-apply. Here, single colonies were inoculated in test tubes containing 5 mL LB medium complemented with the required antibiotics for selection. After an overnight incubation step at 37°C, 300 µL of respective overnight culture were pelleted (tabletop centrifuge: 13200 rpm, 3 min, room temperature (RT)) and the supernatant was removed. 30 µL of 5x DNA loading dye were added and the cell pellet was resuspended. After resuspension, 14 µL of Phenol/Chloroform (ratio 1:1) were added and the mixture was vortexed for 20 seconds. Phenol/Chloroform extracts total DNA from the cells and is thus considered a poisonous substance that must be disposed of separately. After vortexing, the mixture was centrifuged (13200 rpm, 5 min, RT) and a pellet of cell debris and proteins became visible. 12 µL of the supernatant (containing chromosomal DNA, plasmid DNA and RNA) were applied onto and separated via a 0.8% agarose gel. Staining and visualization were performed as described under 2.2.1.2.

#### 2.2.1.7.3. Screening of *E. coli* transformants: analytical PCR

Analytical PCR makes use of the *Taq* DNA polymerase which, through its amplification speed, is a very useful tool in order to control the success rates of transformations as well as to confirm the correct construction of different plasmid constructs (see 2.2.1.3.3.). *E. coli* transformants that were deemed putative positive clones after the quick-prep procedure were tested via PCR for the presence of the insert of interest. Clones that yielded a positive PCR signal were either deemed positive clones or were submitted to a final restriction analysis if there were doubts (Unspecificity, fragment size slightly off…). Ultimate confirmation was achieved via the sequencing of a plasmid DNA sample through Microsynth AG.

#### 2.2.1.7.4. Screening of *E. coli* transformants: Test restriction analysis

A very reliable method for screening clones was the test restriction analysis where plasmid DNA of a putative positive clone was isolated and the insert of interest was restricted from said plasmid DNA. This was achieved by using the restriction enzymes that had been used previously for the restriction of the empty vector. In case of a positive clone, the inserted fragment was restricted from the vector plasmid, which could easily be visualized on an agarose gel.

#### 2.2.1.7.5. Plasmid DNA isolation from *E. coli*

*E. coli* plasmid DNA was isolated from a freshly grown overnight culture using either the GeneJET Plasmid Miniprep/Midiprep Kit or the Wizard® Plus SV Minipreps DNA Purification System. Isolation and purification were concluded by following the respective manufacturer's protocol. Elution of plasmid DNA was performed with $ddH_2O$.

### 2.2.1.8. Transformation of *N. magadii*

#### 2.2.1.8.1. Generation of competent *N. magadii* cells

In order to generate competent *N. magadii* cells, three baffled 500 mL Erlenmeyer flasks were prepared, each containing 60 mL $NVM^+$ medium as well as 70 µg/mL Bacitracin. 2, 4 and 6 mL of freshly grown *N. magadii* were added to the three Erlenmeyer flasks respectively and the cultures were incubated at 37°C until one of the cultures reached an $OD_{600}$ situated in between 0.5 and 0.6. The desired volume of the culture having reached said optical density was centrifuged (5000 x g, 15 min, RT) and the supernatant was removed. The pellet was then resuspended in half the volume buffered high salt spheroplasting solution (+ glycerol). The cell suspension was then transferred into a 100 mL Erlenmeyer flask (without baffles!) and proteinase K was added to a final 1:1000 dilution. The suspension was then incubated at 42°C (shaker) until spheroplasts became visible (usually overnight). In order to visualize the cells, a standard Nikon light microscope with a 1000x magnification capacity was used. Subsequently, 1.5 mL aliquots of competent cells were prepared which could be used immediately or stored up to one week at -80°C.

#### 2.2.1.8.2. Transformation of competent *N. magadii* cells

Per transformation reaction, 1.5 mL (one competent cell aliquot) were thawed and centrifuged (10000 rpm, 3 min, RT) and the supernatant was eliminated. The pellet was then carefully resuspended in 150 µL buffered high salt spheroplasting solution (without glycerol). This step was followed by the addition of 15 µL 0.5 M EDTA and a subsequent incubation at room temperature for 10 minutes. After incubation, plasmid DNA was added. One had to ensure that 3-5 µg of DNA were transformed for best results and that said amount of DNA was contained in at most 10 µL of $ddH_2O$ in order to ensure a high enough salt concentration provided by the buffered high salt spheroplasting solution. The reaction mixture was left to incubate for 5 minutes at room temperature before 150 µL 60% PEG-600 (in unbuffered high salt spheroplasting solution) were added, followed by another incubation step of 30 minutes at room temperature. Then, 1 mL of rich medium ($NVM^+$ medium) was added to the reaction and the reaction tube was centrifuged (10000 rpm, 3 min, RT). The supernatant was removed and the cell pellet was then washed with 1 mL of $NVM^+$ medium: $NVM^+$ medium was added and the pellet was carefully detached from the bottom of the tube and the tube was subsequently centrifuged again (10000 rpm, 3 min, RT). The supernatant was removed, 1 mL $NVM^+$ medium was added and the pellet was detached carefully from the bottom of the tube. The transformed and washed competent cells were then incubated at 37°C (shaker) until they had regenerated. The regeneration process usually took between 1-3 days; every day the regeneration process was analyzed via light microscopy and the medium was changed (10000 rpm, 3 min, RT, eliminate supernatant, add 1 mL of $NVM^+$, detach pellet, incubate at 37°C, shaker). During the regeneration process, the cells reformed their S-layer. Once the cells had sufficiently regenerated (>90%), they were plated onto selective $NVM^+$/agar plates. Per transformation, 9-10 plates were plated with 100 µL of the undiluted transformation reaction and an additional 10 plates were plated with a 1:10 dilution of the transformation reaction; the dilution was carried out with rich medium.

The plates were then incubated at 43°C in a tightly sealed plastic bag to avoid desiccation; 2-3 weeks later, colonies became visible.

2.2.1.8.3. Screening of *N. magadii* transformants

Colonies were picked and inoculated in Eppendorf tubes containing 700-800 µL rich medium which were afterwards incubated at 37°C for 2-3 days. In order to guarantee fast growth and to keep the cells in good shape (*N. magadii* is strictly aerobically growing), the Eppendorf tubes were aerated daily in sterile conditions next to the Bunsen burner.
The most straightforward way to test these transformants was via analytical PCR (See 2.2.1.3.3.). Templates were prepared as mentioned under 2.2.1.3.6. After identification of a positive clone, it was inoculated in rich medium containing the appropriate antibiotic for selection.

### 2.2.1.9. Homogenization of *N. magadii*/ϕCh1 deletion mutants

For this thesis, the focus lay on the creation of ϕCh1 deletion mutants which needed to be homogenized as *N. magadii* is a polyploid organism containing up to 50 copies of chromosomal DNA and thus also up to 50 copies of ϕCh1 genome. In order to yield homozygous lysogenic mutant strains, mutant virus particles were isolated in order to infect *N. magadii* L13. Plating of the infected *N. magadii* cells on selective medium plates eventually resulted in single colonies made up of cells only containing the mutant virus, assuming that only one virus particle is infecting one cell.

Lysis of the mutant culture indicated the release of viral particles (both wild-type and mutant particles). Samples were taken and centrifuged; the supernatant contained the released virus particles. A series of supernatant dilutions was set up ($10^{-2}$ – $10^{-8}$) of which 200µL respectively were added to a freshly grown culture of *N. magadii* L13. The L13 cultures containing the viral particles were then incubated for 60 minutes at 37°C, just long enough so that the virus particles may attach to the cell wall of *N. magadii* L13. Subsequently, 100 µL per dilution were plated on rich medium plates containing the appropriate antibiotic for selection of the ϕCh1 mutant. Colonies that were visible after 2-3 weeks thus only contained the mutant virus as this virus carried the antibiotic resistance gene necessary for selection whereas the wild-type virus did not.

This method is rather straightforward and yields homozygous deletion mutants in a way that is more efficient than simple culture passaging.

### 2.2.1.10. ϕCh1 virus particle isolation and dialysis

In order to isolate virus particles, the respective strain was inoculated in rich medium at an $OD_{600}$ = 0.1 and incubated at 37 °C. The optical density was measured daily and after exponential growth, the culture was left to lyse until $OD_{600}$ < 0.4. The culture was then centrifuged (5000 x g, 20 min, RT). PEG-6000 was added to the supernatant to a final concentration of 10%. The mixture was left to stir gently overnight for PEG-6000 to completely dissolve. PEG-6000 coats the virus particles and thus the virus particles could be collected via another centrifugation step (5000 x g, 30 min, RT). The resulting pellet was resuspended in high salt alkaline solution (see 2.1.11.7.). The ϕCh1 virus particles themselves have been isolated via a discontinuous CsCl density gradient followed by a continuous density CsCl gradient. In order to achieve that, ultra-centrifuge tubes were successively filled with 2mL 1.5 CsCl solution, 5 mL 1.3 CsCl solution, 6 mL ϕCh1/high salt alkaline solution and 1 mL 1.1 CsCl solution. The tubes were carefully balanced and subsequently ultra-centrifuged (30000 rpm, 20 h, RT). After centrifugation, the ϕCh1 virus particles were distinguishable as an opaque band which could be harvested with a syringe. Further concentration and purification of the ϕCh1 virus particles was achieved via a subsequent continuous 1.3 CsCl solution centrifugation. In order to do so, the harvested ϕCh1 virus particle suspension was mixed with an equivalent volume of 1.3 CsCl solution and the suspension was transferred into an ultra-centrifuge tube. Again, the tubes were carefully balanced and ultra-centrifuged (30000 rpm, 20 h, RT). The purified and concentrated ϕCh1 virus particles were then harvested with a syringe.

As the final ϕCh1 virus particle suspension still contained CsCl, the resulting suspension was dialyzed two consecutive times against high salt alkaline solution to get rid of all $Cs^+$ ions. In order to determine the concentration of ϕCh1 virus particles in the final dialysis product, a virus titer analysis may be performed.

### 2.2.1.11. Virus titer analysis

Virus titer analysis may be performed to either determine the concentration of ϕCh1 virus particles in a dialyzed ϕCh1 virus particle suspension or to determine the plating efficiency of released mutant viruses. In order to do that, a growth curve analysis was performed and samples were taken daily at the same time. The supernatant of every sample taken was complemented with 10 µL of $CHCl_3$ and appropriate dilution series were prepared ($10^{-2}$, $10^{-4}$, $10^{-6}$, $10^{-8}$ and $10^{-10}$). 100 µL of each dilution and 300 µL of well grown *N. magadii* L13 were added to 5 mL $NVM^+$-soft agar (50 - 55°C). The mixture was vortexed and slowly poured onto $NVM^+$-agar plates. The plates were then incubated at 37°C in tightly sealed plastic bags. After 1-2 weeks, virus plaques became visible and plaque-forming-units per mL (pfu/mL) could be calculated.

### 2.2.1.12. ϕCh1 DNA isolation

100 µL of dialysed virus suspension were mixed with 300 µL $ddH_2O$, resulting in the disruption of the viral particles. 200 µL of Phenol/Chloroform (1:1) were added, followed by a 20-second vortexing step. The suspension was centrifuged (13200 rpm, 5 min, RT) and the top layer was transferred into a new Eppendorf tube. This step was repeated until no white interphase was visible anymore. Then 200 µL of $CHCl_3$ (Chloroform) were added, the suspension was vortexed and subsequently centrifuged. Again, the top layer was transferred into an Eppendorf tube. Twice the volume 96% ethanol was added to the suspension for precipitation of viral DNA. The suspension was then centrifuged (18000 rpm, 30 min, 4°C) and the supernatant was removed. The DNA pellet was washed twice with 70% ethanol and subsequently dried (SpeedVac). The pellet was dissolved in a volume of $ddH_2O$ such that the solution was not viscous. A sample of the eluted DNA was loaded onto a 0.8% agarose gel for control of quality and concentration.

### 2.2.1.13. Southern Blot

Southern blotting is a method used to detect a specific DNA sequence in a given DNA sample and it involves three different steps: DNA fragment separation via agarose gel electrophoresis, a subsequent transfer of the separated DNA fragments to a nylon membrane (GE Healthcare Amersham Hybond™-N) followed by a sequence detection step via probe hybridization. The detection principle behind the southern blotting method involves probes containing biotinylated dUTPs that hybridize to the complementary fragments on the restricted, denatured DNA sample. The hybridized probes containing the biotin-labelled dUTPs are then visualized using a streptavidin-HRP-conjugate-dependent method. Streptavidin having a high affinity for biotin, it binds to the biotinylated dUTPs and the streptavidin-associated horseradish peroxidase (HRP) is then responsible for yielding a chemiluminescent signal once the substrates $H_2O_2$ and luminol are added. The chemiluminescent signal may then be visualized via exposure to X-ray films.

#### 2.2.1.10.1. Probe synthesis

Here, probe synthesis involved a "*GoTaq* Green Master Mix" PCR protocol, enriched with biotinylated dUTPs. A 100 µL PCR batch contained 2.5 µL biotinylated dUTPs and the PCR product was eluted from an agarose gel before being purified using the QIAquick® Gel Extraction Kit. The probes were eluted in 50 µL of $ddH_2O$ and the probe concentration was determined. Afterwards, the probes were ready to use.
Standard probe PCR protocol:

| **Component** | **Final volume** |
|---|---|
| *GoTaq* Green Mastermix | 50 µl |
| 5' primer | 10 µl |
| 3' primer | 10 µl |
| template | 1 µl |
| sterile $ddH_2O$ | 26.5 µl |
| biotinylated dUTPs | 2.5 µl |
| **Total volume** | 100 µl |

#### 2.2.1.10.2. DNA restriction and separation on an agarose gel

The DNA sample to be analyzed was restricted with New England Biolabs High Fidelity restriction enzymes and separated on a 0.8% agarose gel. As already mentioned under 2.2.1.1., for southern blotting applications, bigger combs were used in order to maximize the hybridization surface for the probes. DNA was visualized through ethidium bromide staining and the agarose gel was photographed alongside a ruler in order to identify the fragment sizes where the probes would anneal.

#### 2.2.1.10.3. Blotting of the DNA to a nylon membrane

The nylon membrane (GE Healthcare Amersham Hybond™-N) as well as 6 pieces of Whatman paper and a 4-5 cm big stash of extra-absorbent paper towels were cut to exactly the size of the agarose gel. Before setting up the capillary blot, the DNA had to be denatured as well as neutralized afterwards. Denaturing happened via a 30 minute incubation of the agarose gel in 0.4 M NaOH/ 0.6 M NaCl, followed by a neutralization step where the agarose gel was incubated for 30 minutes in 1.5 M NaCl/ 0.5 M Tris/HCl pH 7.5.

The capillary blot was built up according to the following protocol:

- Empty agarose gel electrophoresis chamber

- Whatman paper was placed so that it reaches into the buffer wells at each side of the chamber

- 3 correctly cut pieces of Whatman paper were put into the middle of said piece of Whatman paper

- The agarose gel was put on top of the 3 pieces of Whatman paper (inverted!)

- A correctly cut piece of nylon membrane was equilibrated in 10x SSC and put on top of the gel

- Another layer of 3 pieces of Whatman paper

- An 8-10 cm stash of extra-absorbent paper towels were put on top of the construct

After having correctly built up the capillary blot, the buffer wells of the electrophoresis chamber were filled with 10x SSC and the plastic lid of the electrophoresis chamber was put on top, compressing the capillary blot construction. A weight was put on top of the lid to make sure that the blotting construct was compressed tightly. The DNA was then left to blot onto the nylon membrane overnight. After transferring the DNA to the nylon membrane overnight, the membrane was incubated in 0.4 M NaOH for 1 minute, followed by incubation in 0.2 M Tris/HCl pH 7.5 for 1 minute as well. Next, the blotted DNA was fixed onto the nylon membrane via UV-crosslinking (standard settings).

#### 2.2.1.10.4. Membrane blocking and hybridization

Before adding the probes to the membrane, the membrane needed to be blocked first in order to prevent unspecific probe binding. Therefore, the membrane was incubated with 12 mL of hybridization buffer (see 2.1.11.4.) complemented with 120 µL of salmon sperm DNA (10 mg/mL) in a specialized hybridization tube; this blocking step took 3 hours at 65°C in a rotary incubator. After the blocking step, the probes were denatured at 95°C for 10 minutes and added to the hybridization tube. The hybridization took place overnight at 65°C in the rotary incubator.

#### 2.2.1.10.5. Washing of the membrane and blot development

After overnight hybridization and before development of the blot, the membrane had to undergo different washing steps (in the hybridization tubes):

Two successive washing steps with 2 x SSC / 0.1 % SDS at room temperature, 5 minutes each and two successive washing steps with 0.1 x SSC / 0.1 % SDS at 65 °C (rotary incubator), 15 minutes each.

Development of the blot was carried out using Thermo Scientific's Chemiluminescent Nucleic Acid Detection Module Kit as well as X-ray films.

### 2.2.2. Protein methods

#### 2.2.2.1. Preparation of crude protein extracts

Here, crude protein extracts were prepared in order to detect the production of proteins of interest via SDS-PAGE and Western Blot analysis. Both *E. coli* and *N. magadii* crude extracts have been prepared in an almost identical fashion. Culture samples were taken as needed and the cells contained in 1.5 mL of culture were harvested via centrifugation. The supernatant was removed (followed by a quick-spin step and additional supernatant removal) and the pellet was resuspended in 5mM sodium phosphate buffer pH 6.8 and 2x Lämmli buffer (see 2.1.11.2.) according to the formula $V_{Na\text{-}P/Lämmli} = OD_{600}$ x 75. *E. coli* crude extracts were resuspended in both buffers and denatured at 95°C immediately afterwards. *N. magadii* crude extracts needed to incubate at 37°C until the solution was not viscous anymore; the viscosity resulted from the high amount of DNA contained in the cell and disappeared throughout incubation as the DNA was degraded. After incubation at 37°C, *N. magadii* crude extracts were denatured at 95°C as well.

#### 2.2.2.2. SDS-PAGE

SDS-PAGE (Sodium dodecyl sulphate polyacrylamide gel electrophoresis) is a method for the separation of proteins according to their size. SDS denatures the protein so that this separation may take place. The gel is composed of two different gels: a 4% PAA stacking gel and a 12% PAA separating gel.

Bio-Rad Mini-Protean equipment was used for the preparation of the gels as well as for the run itself. The gels were cast using 0.75 mm spaced glass plates, resulting in 0.75 mm thick gels. First, the separating gel mixture was prepared and poured in between the glass plates. The mixture was then immediately covered with isopropanol to get rid of air bubbles and to obtain a perfectly horizontal separation line. After polymerization of the separating gel, the isopropanol was removed and the stacking gel mixture was poured on top of the polymerized separating gel until the top of the lower glass plate was reached. A 10-well comb was gently stuck into the stacking gel mixture and the gel was left to polymerize.

| Composition | Separating gel (12%) | Stacking gel (4%) |
|---|---|---|
| Acrylamid solution | 2 mL | 267 µL |
| Separating gel buffer | 1.25 mL | / |
| Stacking gel buffer | / | 0.5 mL |
| $H_2O$ | 1.75 mL | 1.233 mL |
| **Total volume** | 5 mL | 2 mL |
| | **Mix on ice** | **Mix on ice** |
| APS (10%) | 60 µL | 20 µL |
| TEMED | 10 µL | 5 µL |

The gels were clipped into the holding device and introduced into the SDS-PAGE chamber. The space between two gels (or one gel and a buffer dam) was completely filled with 1x SDS running buffer and the well comb was removed. The chamber was then filled with 1x SDS running buffer according to the manufacturer's specifications. Protein samples were loaded onto the gel alongside a 10-180 kDa prestained protein marker.

*E. coli* crude extract samples were subjected to the following running protocol:

- 40 V until the bromphenol blue had reached the lower part of the sample pocket

- 80 V until the bromphenol blue had reached the separating gel

- 100 V until finished

*N. magadii* crude extract samples needed to be separated at a continuous 40 V because of the high salt concentration in the samples. Higher voltage might have caused melting of the gel.

### 2.2.2.3. Coomassie staining

In order to verify total protein concentration in *N. magadii* crude extracts or to check for the presence of an over-expressed protein (*E. coli*), Coomassie staining was applied. After the SDS-PAGE run had finished, the glass plates were separated and the stacking gel was removed. The separating gel containing the separated proteins was then stained for roughly 5-10 minutes in Coomassie staining solution before being destained in destaining solution (see 2.1.11.2.). After sufficient destaining, blue protein bands became visible on a clear background.

### 2.2.2.4. Acetone powder

Acetone powder was used for the saturation of the primary antibodies used for western blotting techniques. Here, only acetone powder synthesized from the cured *N. magadii* L13 strain was used to saturate the antibodies in order to prevent unspecific reactions with host-encoded proteins. In order to prepare the acetone powder, 1 L of *N. magadii* L13 was left to grow in rich medium until the stationary phase was reached. The culture was centrifuged (5000 x g, 20 min, RT) and the resulting pellet was resuspended in 1 mL 0.9 % saline solution per gram wet weight before being incubated on ice for 5 minutes. Per 2 mL cell suspension, 8 mL acetone solution (pre-cooled to –20°C) were added and the solution was mixed thoroughly before being incubated on ice for 30 minutes. A magnetic stirrer was added to the solution and the ice box containing the Erlenmeyer flask was placed onto a magnetic stirring plate so that continuous stirring during the incubation on ice was guaranteed. After incubation the solution was centrifuged (10000 x g, 10 min, 4°C), the supernatant was removed and the pellet was resuspended in fresh acetone (cooled to -20°C) and incubated on ice for 10 minutes. The suspension was centrifuged again (10000 x g, 10 min, 4°C), the supernatant was removed and the pellet was transferred onto a piece of filter paper. The pellet could be broken into smaller pieces for easier drying. Once the pellet was completely dry it was pulverized in a mortar and the resulting acetone powder was stored in a Falcon tube at room temperature.

### 2.2.2.5. Western Blot

The western blotting technique was used to detect and quantify a specific protein in a protein mixture. This was achieved via blotting the proteins onto a nitrocellulose membrane and subsequently exposing the membrane to a specific primary antibody solution directed against the protein of interest. A secondary labeled antibody directed against the primary antibody in combination with a chemiluminescent substrate was used for the detection of the protein of interest.

#### 2.2.2.5.1. Transfer of the proteins (Semi-dry blotting)

An SDS-PAGE gel was prepared and treated as mentioned under 2.2.2.2. Six pieces of Whatman paper were cut to the size of the gel (9 cm x 6 cm) as well as a piece of nitrocellulose membrane (GE Healthcare Amersham™ Protran™ 0.2 µm NC). After the run, the gel was rinsed in transfer buffer during the build-up of the blotting device (Bio Rad Trans-Blot® Turbo™ Transfer System). Three pieces of Whatman paper were imbibed in transfer buffer onto which the transfer-buffer-soaked nitrocellulose membrane was put, followed by the protein gel. The gel was covered with another layer of three pieces of Whatman paper, again imbibed in transfer buffer. The construct was flattened using the rolling device supplied with the blotting device. This was a very important step as it ensured excellent blotting results through the removal of any remaining air bubbles in the transfer construct.

Blotting protocol:

The pre-installed Bio Rad blotting protocol was the same for one or two mini gels (25 V - 1 A - 30 min); only the number of gels per blotting tray had to be chosen (one or two mini-gels).

#### 2.2.2.5.2. Ponceau – S staining

After the blotting procedure, a reversible Ponceau – S staining was applied to the membrane. Ponceau – S stains the transferred proteins and is usually applied to identify and mark the bands of the protein marker. As a pre-stained protein marker was used for this thesis, the Ponceau - S staining served the purpose of a direct control after the semi-dry blotting in order to verify the correct and complete blotting of all proteins onto the nitrocellulose membrane. It is an easily reversible staining procedure, as the membrane can effectively be de-stained using $H_2O$ (tap water).

#### 2.2.2.5.3. Membrane blocking

Before being subjected to the antibody treatment, the membrane containing the transferred proteins needed to be blocked. The blocking step served the purpose of completely saturating the membrane in proteins unrelated to the ones that were being analyzed. In this case this was achieved using a so-called blocking solution (1x TBS containing 5% milk powder) which was poured onto the nitrocellulose membrane. The membrane was subsequently left to block at 4°C overnight whilst gently shaking.

#### 2.2.2.5.4. Antibody solutions

Primary antibody solutions were prepared in 1x TBS. The sera used here were diluted to a final 1:2500 dilution and the solution was complemented to a final concentration of 0.3% BSA and 0.02% $NaN_3$ (see 2.1.10.). Additionally, acetone powder prepared from *N. magadii* L13 was added in order to saturate the antibodies (see 2.2.2.4.). The solution was left to stir overnight at 4°C. Secondary antibody solutions were not re-usable and were thus freshly prepared for every new reaction (see 2.1.10.).

#### 2.2.2.5.5. Antibody reactions

After overnight blocking of the membrane, the blocking solution was disposed of and the membrane was washed with 1x TBS until all remains of the blocking solution were eliminated. Antibody solutions are best prepared previously so that the acetone powder may saturate the antibodies accordingly. 10 – 15 mL of primary antibody solution were pipetted onto the membrane and the membrane was incubated for 1 hour whilst gently shaking. After incubation, the primary antibody solution was collected as it may be re-used and the membrane was washed three times for 5 minutes in 1x TBS (on shaker). 10 mL of freshly prepared secondary antibody solution were poured onto the membrane and the membrane was again incubated for 1 hour whilst gently shaking. The incubation was followed by the disposal of the secondary antibody solution and three subsequent 10-minute washing steps with 1x TBS (on shaker).

#### 2.2.2.5.6. Detection

The horseradish-peroxidase-coupled secondary antibody was detected using the commercially available SuperSignal® West Pico Chemiluminescent Substrate. Horseradish peroxidase oxidizes its substrate luminol using $H_2O_2$ and thus produces a chemiluminescent signal that may be detected using X-ray films. The substrates contained in the detection kit were pipetted onto the membrane in a 1:1 proportion. The reaction was left to incubate for 5 minutes with occasional shaking to make sure the substrate solution covered the membrane in its entirety. The membrane was then transferred into the exposure cassette before being exposed to an X-ray film (GE Healthcare Amersham Hyperfilm™ ECL) in the dark room. Exposure time was chosen according to signal strength and the film was developed using an AGFA Curix 60 X-ray film processor.

### 2.2.2.6. Over-expression, isolation and purification of recombinant proteins in *E. coli*

Here, ϕCh1-derived genes have been over-expressed in *E. coli* (Rosetta) and their gene products were subsequently isolated as well as purified in order to yield positive control samples used during western blotting procedures. The proteins having been isolated for this thesis were the major capsid protein E (encoded by ORF11), the ORF34 gene product $gp34_{52}$ (a tail fiber protein), as well as the ϕCh1 main methyltransferase (M.*Nma*ϕCh1I) encoded by ORF94. All of these open reading frames had previously been cloned into the multiple cloning site of the expression vector pRSET-A. pRSET-A contains the $T_7$ promoter, the strongest known promoter as of now, specific for the $T_7$ polymerase. Over-expression was induced through IPTG, a structural analog of allolactose, and the protein to be synthesized was provided with an N-terminal 6x His-tag. The N-terminal 6x His-tag is very useful as it binds $Ni^{2+}$ ions; thus the over-expressed protein could subsequently be isolated through Ni-NTA affinity chromatography and/or detected via an α-His antibody.

#### 2.2.2.6.1. Overexpression of the desired gene

A freshly grown overnight culture of the *E. coli* strain carrying the expression vector containing the open reading frame encoding for the desired protein was inoculated at an $OD_{600}$ of 0.1. The culture was incubated at 37°C until an $OD_{600}$ of 0.3-0.4 was reached. This guaranteed that all inoculated cells had divided at least once; hence expression was induced in fresh cells. Transcription was induced through the addition of IPTG to a final concentration of 0.5 mM. Samples were taken before as well as 2 hours after induction to check whether the protein of interest was being over-expressed correctly. Crude extracts were prepared from these samples for SDS-PAGE analysis. 2 hours after induction, the culture was centrifuged (5000 x g, 15 min, 4°C), the supernatant was removed and the pellet was frozen overnight at -20°C. This overnight freezing step induced the breaking of the cell walls due to ice crystal formation.

#### 2.2.2.6.2. Protein purification under denaturing conditions

The frozen cell pellet was thawed on ice for 10 minutes and resuspended in lysis buffer (buffer B, see 2.1.11.3.). The cell suspension was transferred into an Erlenmeyer flask, a magnetic stirrer was added and the suspension was left to stir slowly overnight (avoiding foaming) at room temperature. The next day, the cell suspension was controlled via microscope; in case of still intact cells, the suspension was sonicated to completely lyse the cells. The suspension was centrifuged (10000 x g, 20 min, 4°C) and the supernatant was transferred into a new Erlenmeyer flask. 300 µL of Ni-NTA agarose suspension were added to the supernatant, a magnetic stirrer was added and the suspension was left to stir slowly overnight.

The following day, the raw extracts were poured onto a chromatography column and the flow-through was collected. The column was subsequently washed twice with 6 mL of wash buffer (buffer C, see 2.1.11.3.), the flow-through having been collected. Elution of the protein started with elution buffer D (see 2.1.11.3.): 4 times 0.5 mL of elution buffer D was poured onto the column and the fractions were collected separately. A second elution step was achieved through the use of elution buffer E (see 2.1.11.3.): Again, 4 times 0.5 mL of elution buffer E was poured onto the column and the fractions were collected separately. From every fraction a sample was taken, complemented with 2x Lämmli buffer, denatured and analyzed via SDS-PAGE in order to find out in which fraction the protein had been eluted.

2.2.2.6.3. Dialysis

After SDS-PAGE analysis and Coomassie staining, the fractions containing the eluted protein were pooled and dialyzed against 1x PBS in two steps:

- A one-hour step against 1x PBS
- Overnight against fresh 1x PBS

A final check of the dialysis product via SDS-PAGE was performed to control the quality and concentration of the dialyzed protein. The prepared protein was now ready to be used as a positive control for western blotting applications or for antibody production.

## 2.2.3. Cloning strategies

### 2.2.3.1. Cloning strategies for the creation of an *N. magadii* L11-ORF56 deletion mutant

In order to create an *N. magadii* L11-ORF56 deletion mutant, a plasmid was constructed in several steps containing the up- and downstream regions of ORF56 separated by a novobiocin resistance cassette in forward and reverse orientation, respectively (pKSII-Δ56-Nov$^R$-R and pKSII-Δ56-Nov$^R$-F). Transformation of these constructs into *N. magadii* L11 was expected to yield deletion mutants where the originally encoded ORF56 is replaced by the respective novobiocin resistance cassette through homologous recombination. Mutants would then be selected via plating on rich medium plates containing novobiocin.

The up- and downstream regions of ORF56 have been amplified via PCR using a ϕCh1 DNA template and primers Δ56-1/Δ56-2 for the upstream region (582 bp) as well as primers Δ56-3/Δ56-4 for the downstream region (1183 bp). In a first step, the amplified upstream region was cloned into the vector pBlueScript II KS(+). This was achieved via the restriction of both vector and PCR product with *BamHI* and *XbaI*, followed by a ligation step and transformation into *E. coli* XL1-Blue.

In a second step, the amplified downstream region of ORF56 was cloned into pBlueScript II KS(+) already containing the aforementioned upstream region of ORF56. Here, vector and PCR product were restricted with *HindIII* and *KpnI*, ligated and transformed into *E. coli* XL-1 Blue.

These cloning steps resulted in a pBlueScript II KS(+) vector construct containing both the upstream and the downstream region of ORF56 (pKSII-ORF56-1-4).

To finalize the construct, the novobiocin resistance cassette ($Nov^R$) was cloned in between the up- and downstream region of ORF56, both in "forward" as well as in "reverse" orientation. This was achieved via the isolation of $Nov^R$ from pUC19-$Nov^R$ "reverse" and pUC19-$Nov^R$ "forward", respectively. As $Nov^R$ needed to be eluted from a 0.8% agarose gel due to the fact that it could not be amplified via PCR, the $Nov^R$ cassettes were isolated via restriction with *PstI* and *SmaI* and the remaining pUC19 vector was digested with *DraI*. This was a mandatory step as the $Nov^R$ cassette and the vector pUC19 have comparable sizes ($Nov^R$: 2453 bp, pUC19: 2686 bp), thus making them almost indistinguishable on an agarose gel. pKSII-ORF56-1-4 was restricted with *PstI* and *SmaI* and the gel-eluted and purified respective $Nov^R$ cassettes were ligated into the construct and transformed into *E. coli* XL1-Blue, resulting in the constructs pKSII-Δ56-$Nov^R$-R and pKSII-Δ56-$Nov^R$-F.

#### 2.2.3.2 Cloning strategies for the creation of an *N. magadii* L11-ORF44 deletion mutant

In order to create an *N. magadii* L11-ORF44 deletion mutant, plasmids were constructed in several steps containing the up- and downstream regions of ORF44, separated by a novobiocin resistance cassette in forward (pKSII-Δ44-1-4-$Nov^R$-F; Brait, 2016) and reverse (pKSII-Δ44-1-4-$Nov^R$-R; Tschurtschenthaler, 2015) orientation. Transformation of these constructs into *N. magadii* L11 was expected to yield deletion mutants where the originally encoded ORF44 is knocked out and replaced by the respective novobiocin resistance cassette through homologous recombination. Mutants would then be selected via plating on rich medium plates containing novobiocin.

# 3. Results and discussion

## 3.1. ϕCh1 ORF56 – Indications for a regulatory function

### 3.1.1. Effects of ϕCh1 ORF56 on the expression of ϕCh1 protein E, gp34$_{52}$ and M.*Nma*ϕCh1I

#### 3.1.1.1. ϕCh1 ORF56 – Preliminary indications for a putative regulatory function

Through sequence alignment analysis, ϕCh1 ORF56 is predicted to be a putative transcriptional regulator. Bioinformatic analysis suggested putative transcriptional regulation functions for ORF21, ORF55 and ORF56, where ORF56 was interestingly the only open-reading frame not exhibiting a helix-turn-helix DNA-binding motif, such a motif being characteristic of many repressor molecules that can be found in bacteriophages (Schöner, 2013).

Transformation of the construct pRo-5-ORF56 into the wild-type strain *N. magadii* L11 [*N. magadii* L11 (pRo-5-ORF56)] however revealed a clear influence of ORF56 on the lysogenic behavior of ϕCh1 (Schöner, 2013). Other transformation experiments involving ORF21 and ORF55 yielded the over-expressing strains *N. magadii* L11 (pRo-5-ORF21) and *N. magadii* L11 (pRo-5-ORF55), which showed similar growth- and lysis behavior as the wild-type strain *N. magadii* L11 (pRo-5). However, the ORF56-over-expressing strain *N. magadii* L11 (pRo-5-ORF56) showed no significant lysis behavior as can be seen in Figure 9 (Schöner 2013).

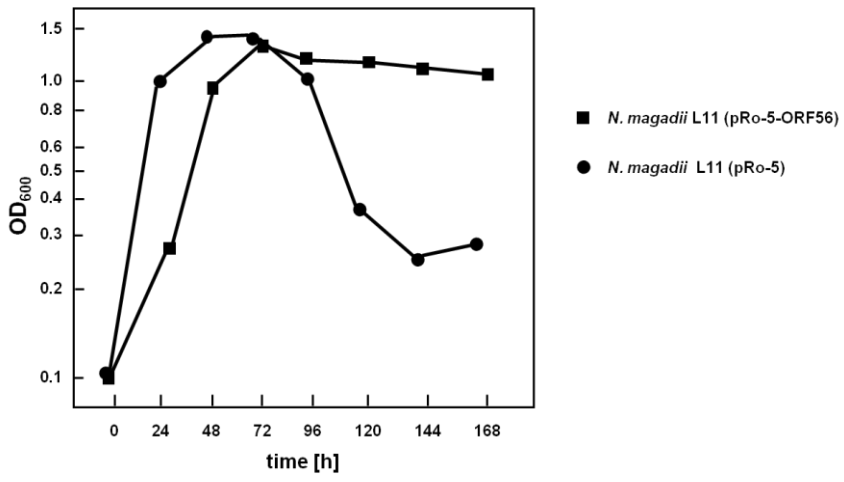


**Figure 9: Growth kinetics of *N. magadii* L11 (pRo-5) versus *N. magadii* L11 (pRo-5-ORF56)**

*N. magadii* L11 (pRo-5) serves as control. Here, growth- and lysis behavior of *N. magadii* L11 (pRo-5-ORF56) has been analyzed. The growth behavior of *N. magadii* L11 and *N. magadii* L11 (pRo-5) is identical (data not shown). For the wild-type, lysis occurs after 2-3 days of incubation. Nearly no lysis could be observed for any of the 4 *N. magadii* L11 (pRo-5-ORF56) clones analyzed.

### 3.1.1.2. Southern Blot

In order to investigate whether *N. magadii* L11 (pRo-5-ORF56) contained ϕCh1 integrated as a provirus, a Southern Blotting analysis was performed. Chromosomal DNA of both *N. magadii* L11 (pRo-5) and *N. magadii* L11 (pRo-5-ORF56) was digested using *Bgl*II and the DNA concentrations were adapted. Hybridization probes were synthesized using a ϕCh1 template, primers Soj-5 and Soj-3 as well as biotinylated dUTPs. Probes were 764 bp in size whereas the DNA fragment where the probes would anneal was 3130 bp in size. The results demonstrated that *N. magadii* L11 (pRo-5-ORF56) contained ϕCh1 integrated as a provirus in the host genome and that the phenotype was not a consequence of a lost provirus (Schöner, 2013).

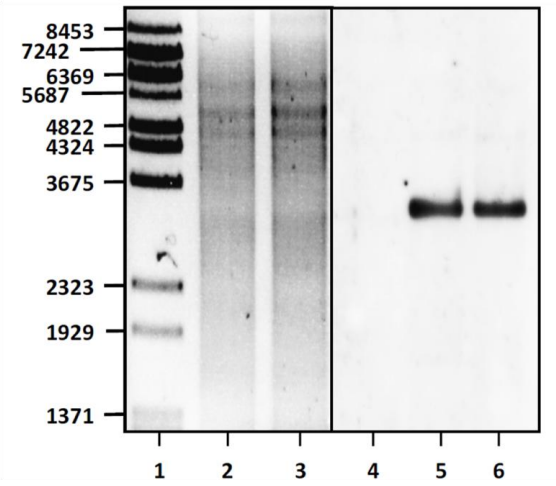


**Figure 10: Southern Blot analysis of *N. magadii* L11 (pRo-5) versus *N. magadii* L11 (pRo-5-ORF56)**

Left panel: Lanes 2 and 3 depict the adjusted amounts of restricted chromosomal DNA from *N. magadii* L11 (pRo-5) (lane 2) and *N. magadii* L11 (pRo-5-ORF56) (lane 3). Right panel: Southern Blotting results for *N. magadii* L11 (lane 5) and *N. magadii* L11 (pRo-5-ORF56) (lane 6). The probes detected the same 3130 bp fragment with a comparable intensity, thus proving an integration of the provirus in the chromosomal DNA of. *N. magadii* L11 (pRo-5-ORF56).

Lea Schöner, 2013

### 3.1.1.3. Virus titer analysis

As ϕCh1 is a lysogenic virus, the virus terminates its life cycle inside the host via lysis of the host organism *N. magadii*, thus resulting in the release of progeny viruses. In order to investigate whether ORF56 has an influence on the release of progeny viruses, a virus titer analysis comparing wild-type *N. magadii* L11 (pRo-5) to *N. magadii* L11 (pRo-5-ORF56) was performed (Figure 11).

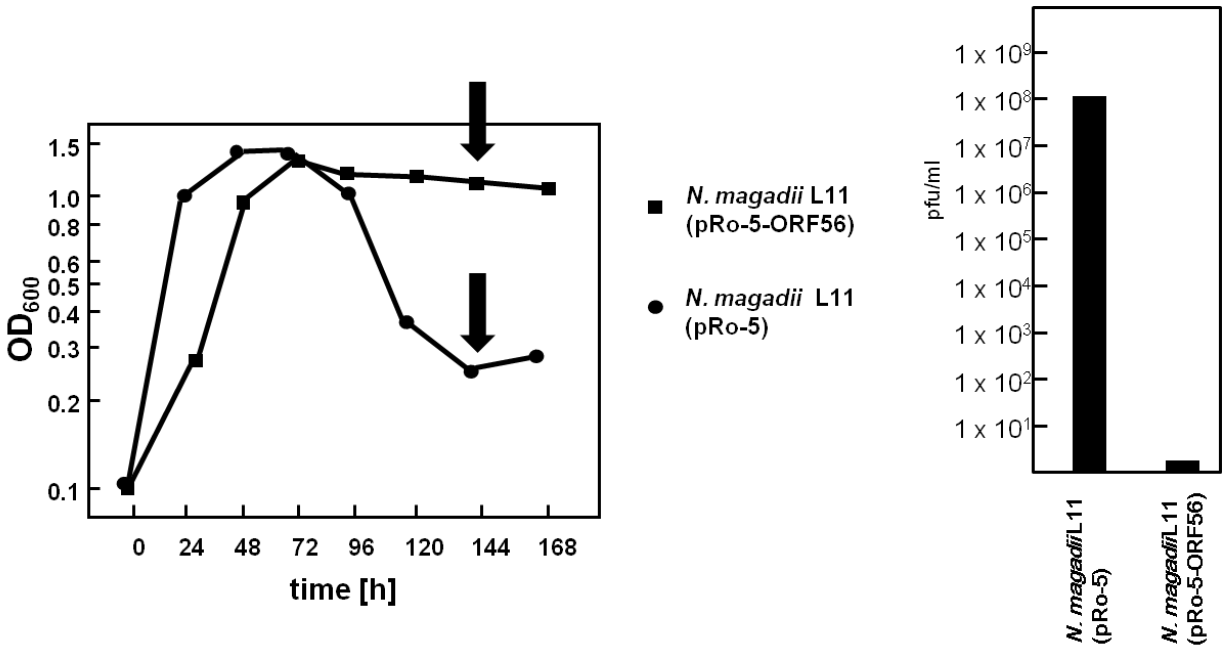


Lea Schöner, 2013

**Figure 11: Virus titer analysis of *N. magadii* L11 (pRo-5) versus *N. magadii* L11 (pRo-5-ORF56)**

Here, supernatant samples containing virus particles were taken upon complete lysis of the strain *N. magadii* L11 (pRo-5). At the same time point, supernatant samples were taken for the strain *N. magadii* L11 (pRo-5-ORF56). The arrows indicate the time point where the samples were taken (day 7 after inoculation). The cured strain *N. magadii* L13 was infected with the two respective supernatant samples for the virus titer analysis. As reflected by the growth curve analysis, a widely reduced viral plaque formation could be observed for the strain *N. magadii* L11 (pRo-5-ORF56). (Lea Schöner, 2013)

Virus titer analysis confirmed the preliminary growth curve experiment results; the ORF56-over-expressing strain *N. magadii* L11 (pRo-5-ORF56) exhibits a widely reduced viral plaque formation, thus a reduced plating efficiency (Schöner, 2013).

### 3.1.1.4. Western Blot

In order to further investigate the over-expression of ORF56 on protein levels, western blotting analyses were performed on the wild-type *N. magadii* L11 (pRo-5) as well as the mutant strain *N. magadii* L11 (pRo-5-ORF56).

To get an idea of the effect of an ORF56 over-expression on protein levels, a preliminary experiment was performed where growth curve analysis was performed with both strains and samples were taken in both cases at a specific time point where lysis was complete for the wild-type strain *N. magadii* L11 (pRo-5). Thereby, a direct comparison of lytic behavior versus reduced lytic behavior of both strains relative to protein expression could be made (Figure 12).

Three different Western Blot analyses were performed for each strain and primary antibodies were chosen in a way that spans all three major parts of the ϕCh1 genome:

- α-E antibodies directed against ϕCh1 major capsid protein E (gpE), a structural component of ϕCh1 encoded by ORF11, ORF11 being situated at the 5' end of the ϕCh1 genome.

- α-gp$34_{52}$ antibodies directed against ϕCh1 tail fiber protein gp$34_{52}$ encoded by ORF34, ORF34 being situated at the 3' end of the genome part encoding for structural- and assembly-related components. The locus of the open-reading frame encoding for gp$34_{52}$ is closest to the DNA replication domain of the ϕCh1 genome, situated towards the middle of the ϕCh1 genome. Therefore these antibodies were chosen as there were no antibodies available as of this date that were directed against proteins encoded by the open-reading frames situated in the DNA replication domain of the ϕCh1 genome.

- α-M.*Nma*ϕCh1I antibodies directed against the main methyltransferase of ϕCh1 encoded by ORF94, ORF94 being situated at the 3' end of the ϕCh1 genome.

All antibody solutions were prepared as mentioned in 'Materials and Methods', section 2.2.2.5.4.

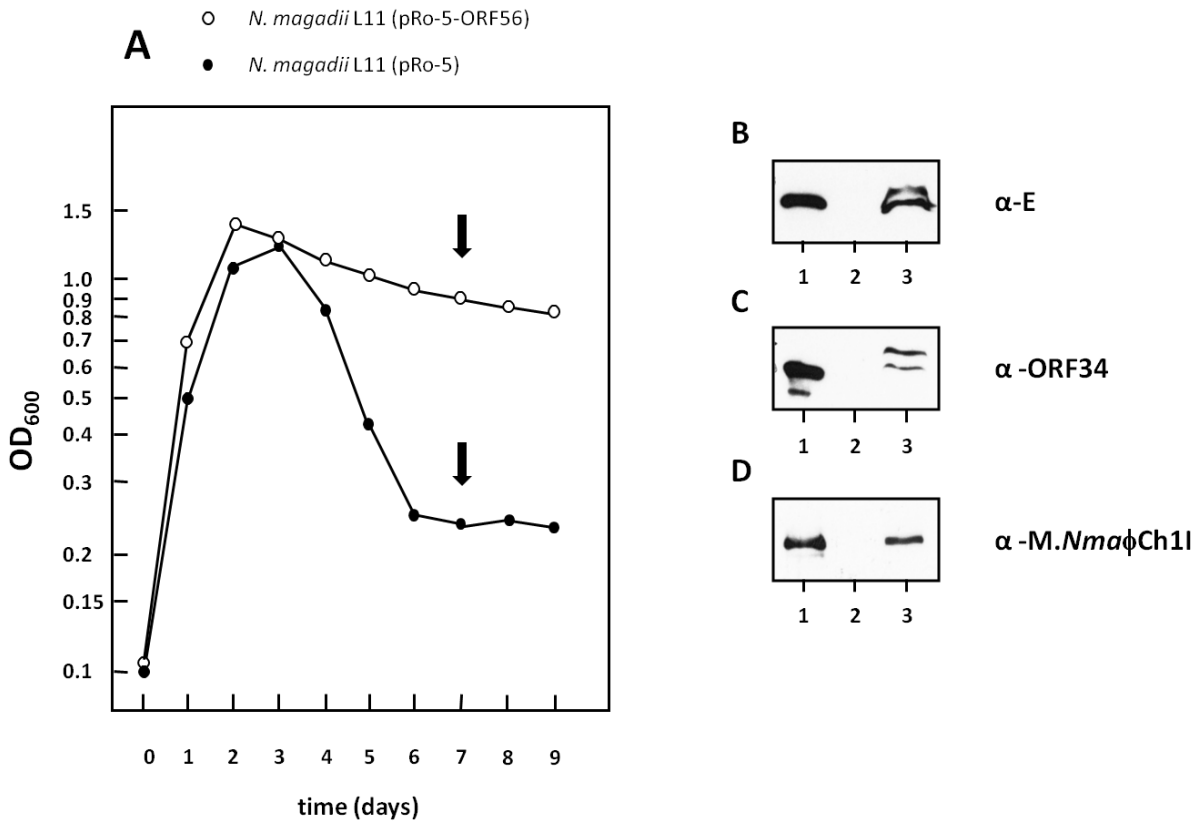


**Figure 12: Growth kinetics and protein expression of *N. magadii* L11 (pRo-5) and *N. magadii* L11 (pRo-5-ORF56)**

**A**: Growth kinetics of *N. magadii* L11 (pRo-5) and *N. magadii* L11 (pRo-5-ORF56). Optical density was measured daily at the same time. The black arrows indicate the time point where the samples were taken. **B, C, D**: Summary of α-E, α-gp34$_{52}$ and α-M.*Nma*ϕCh1I Western Blots with samples taken on day 7. Lane 1: Positive control, lane 2: *N. magadii* L11 (pRo-5-ORF56), lane 3: *N. magadii* L11 (pRo-5). Sample amounts were adapted via a previous Coomassie staining.

When comparing the Western Blotting results summarized in Figure 12, one can see a clear disparity in the expression of proteins E, gp34$_{52}$ and M.*Nma*ϕCh1I between *N. magadii* L11 (pRo-5) and *N. magadii* L11 (pRo-5-ORF56) for samples taken at day 7. These results suggest a regulating effect of an over-expressed ORF56 in the wild-type strain *N. magadii* L11 on the expression of the aforementioned proteins, showcased by an undetectable amount of these virus-related proteins in *N. magadii* L11 (pRo-5-ORF56) when compared to the wild-type strain *N. magadii* L11 (pRo-5).

To verify whether this trend was valid for other time points sampled during the growth of both strains, another Western Blot analysis was subsequently performed with samples taken over the complete time series for both strains. These Western Blotting results are depicted in Figure 13.

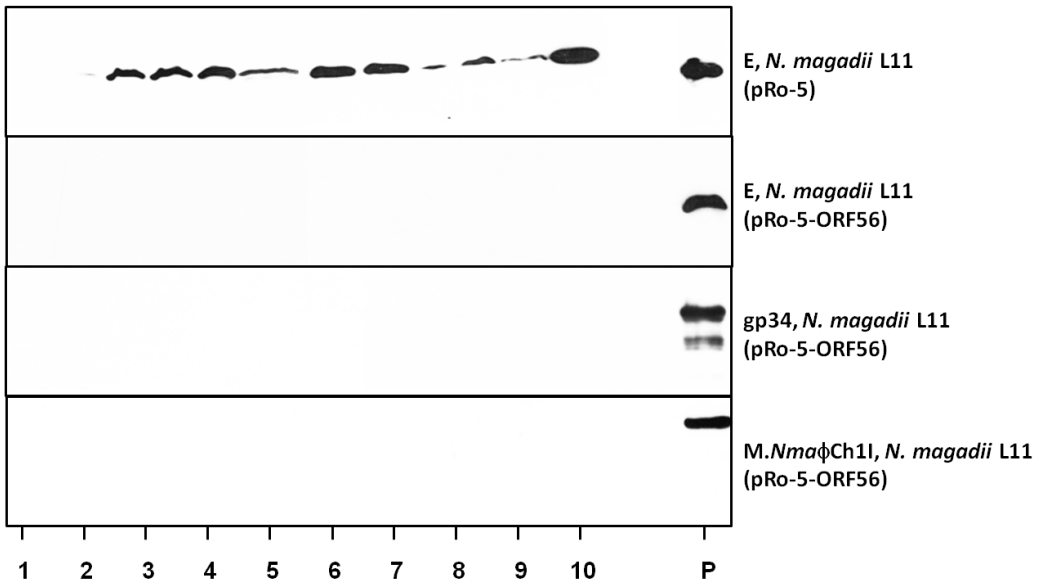


**Figure 13: Western Blotting results for *N. magadii* L11 (pRo-5-ORF56) using α-E, α- gp34$_{52}$ and α-M.NmaϕCh1I antibodies**

Sample amounts were adapted via a previous Coomassie staining step. Amounts of positive control samples were the same for every blot. Here, expression of the three viral proteins gpE, gp34$_{52}$ and M.*Nma*ϕCh1I in *N. magadii* L11 (pRo-5-ORF56) is vastly reduced to the point of undetectability over a period of 10 days when compared to the wild-type strain *N. magadii* L11 (pRo-5). ORF56 over-expression in *N. magadii* L11 seems to have a direct influence on the expression of the three viral proteins gpE, gp34$_{52}$ and M.*Nma*ϕCh1I. The *N. magadii* L11 (pRo-5) α-E Western Blot serves a reference purpose; *N. magadii* L11 (pRo-5) α- gp34$_{52}$ and α- M.*Nma*ϕCh1I Western Blots revealed the same expression pattern as the *N. magadii* L11 (pRo-5) α-E Western Blot.

This Western Blotting series of experiments has previously been performed using α-E and α- gp34$_{52}$ antibodies (Lea Schöner, 2013) with analogous results to the ones obtained here. However, here, additional Western Blots were generated using α-M.*Nma*ϕCh1I antibodies. Through their application, it has been demonstrated that the effect of an over-expressed ORF56 in the wild-type strain *N. magadii* L11 extends to the expression of the main ORF94-encoded ϕCh1 methyltransferase. Therefore one can affirm that an over-expressed ORF56 in the wild-type strain exhibits a repressor function on the expression of three viral proteins encoded by three different ORFs that stretch over the entirety of the ϕCh1 genome. As mentioned before, previous Southern Blotting results demonstrated the presence of ϕCh1 integrated as provirus in the genome of *N. magadii* L11 (pRo-5-ORF56) (Schöner, 2013). Therefore the results obtained through Western Blot analysis are not due to the loss of a ϕCh1 provirus but rather due to a repressing function of the over-expressed ORF56 relative to the synthesis of ϕCh1 gpE, gp34$_{52}$ and M.*Nma*ϕCh1I.

### 3.1.1.5. Discussion

The outline of this study was to analyze three ϕCh1 open-reading frames with putative transcriptional regulation functions, namely ORF21, ORF 55 and ORF56. Main focus relative to a putative transcriptional regulation function lay on ORF21 and ORF55 as bioinformatic analysis had revealed the presence of a helix-turn-helix DNA-binding motif for both open-reading frames, characteristic for repressor molecules in bacteriophages. Over-expression of all three open-reading frames in the cured strain *N. magadii* L13 revealed no significant difference in growth behavior when compared individually as well as when compared to the *N. magadii* L13 control transformed with the empty vector [*N. magadii* L13 (pRo-5)]. A similar trend could be observed when comparing over-expression of the three open-reading frames in the wild-type strain *N. magadii* L11: *N. magadii* L11 (pRo-5-ORF21) and *N. magadii* L11 (pRo-5-ORF55) showed similar growth and lysis behavior as the wild-type strain *N. magadii* L11 (pRo-5) with the exception of the ORF56-over-expressing strain *N. magadii* L11 (pRo-5-ORF56), which showed no significant lysis behavior when compared to the *N. magadii* control as well as when compared to the transformants over-expressing ORF21 and ORF55. More surprisingly, the over-expression of ORF56 in the wild-type strain *N. magadii* L11 shows indications for a putative transcriptional regulation function although it is the only open-reading-frame of the three not exhibiting a typical helix-turn-helix motif, common for repressor molecules found in bacteriophages. Southern Blotting results subsequently showed that the observed phenotype of *N. magadii* L11 (pRo-5-ORF56) was not due to a lost provirus as ϕCh1 was very well integrated into the host genome as provirus (Schöner, 2013).

Virus titer analysis demonstrated that the number of viruses released by *N. magadii* L11 (pRo-5-ORF56) was substantially lower than the number of viruses released by the wild-type, indicating a repressing role of an over-expressed ORF56 when it comes to virus release.

Taken together, these results suggest a regulatory activity of ORF56 having an effect on the life cycle of ϕCh1 itself, rather than on its host *N. magadii*.

Western Blotting results show that an over-expressed ORF56 in the wild-type strain *N. magadii* L11 has a pronounced effect on the expression of three different ϕCh1-encoded proteins, namely the major capsid protein gpE, the tail fiber protein $gp34_{52}$ as well as the virus' main methyltransferase M.*Nma*ϕCh1I. Though no definitive conclusions can be made whether the repressing activity of ORF56 acts on a DNA- or RNA level one can however affirm that, due to a lack in the expression of the proteins analyzed when

compared to the wild-type strain *N. magadii* L11, over-expressed ORF56 has a substantial repressor effect on the expression of the three viral proteins in question. These observations led to the preliminary conclusion that ORF56 exhibits indeed a general repressor activity.

Further research using Western Blotting procedures involving α-gp56 antibodies is necessary to oversee the time kinetics of gp56 expression during the lysogenic life cycle of *N. magadii* L11. This could represent a further step in expanding the conclusions relative to the regulating function of ORF56 in the wild-type strain. Up to this point however, no α-gp56 antibodies are available.

### 3.1.2. Construction of an ORF56 deletion mutant – *N. magadii* L11-ΔORF56

#### 3.1.2.1. Aim and cloning strategy

The aim of this study was to create an *N. magadii* L11-ORF56 deletion mutant in order to follow up on the investigation of the regulating function of ORF56 in *N. magadii* L11. The cloning strategy involved the construction of a plasmid containing both the upstream- as well as the downstream region of ϕCh1 ORF56, flanked by a novobiocin resistance cassette (*gyrB*) in 'forward' and 'reverse' orientation as well as a terminator sequence. Transformation of these constructs should yield ORF56 deletion mutants via homologous recombination. Two different orientations for the resistance marker cassette were chosen to exclude the possibility that a given orientation of the resistance cassette might interfere with the transcription of adjacent open-reading frames. The terminator sequence ascertains that transcription of the novobiocin resistance cassette stops once the cassette is transcribed, further reducing the possibility of unwanted interferences with the transcription of adjacent open-reading frames.

The cloning strategy dedicated to the creation of a ϕCh1 deletion mutant was first applied successfully by Regina Selb in 2010 where an *N. magadii* L11-ΔORF79 deletion mutant was created, representing the first deletion mutant of a haloalkaliphilic virus (Selb, 2010; Selb *et al*. 2017).

### 3.1.2.2. Plasmid constructs pKSII-Δ56-NovR-R and pKSII-Δ56-NovR-F

Plasmid pBlueScript II KS(+) has been used for construction, implying its so-called 'suicide' characteristic when transformed into *N. magadii*; pKSII does not contain an applicable origin of replication for *N. magadii*, thus resulting in cell death if the finalized construct should not be integrated into the host chromosome or the genome of ϕCh1.

The complete cloning strategy for the construction of a ϕCh1 ORF56 deletion mutant can be found in 'Materials and Methods', section 2.2.2.7.1. Figure 14 schematically depicts the finalized constructs that were transformed into *N. magadii* L11.

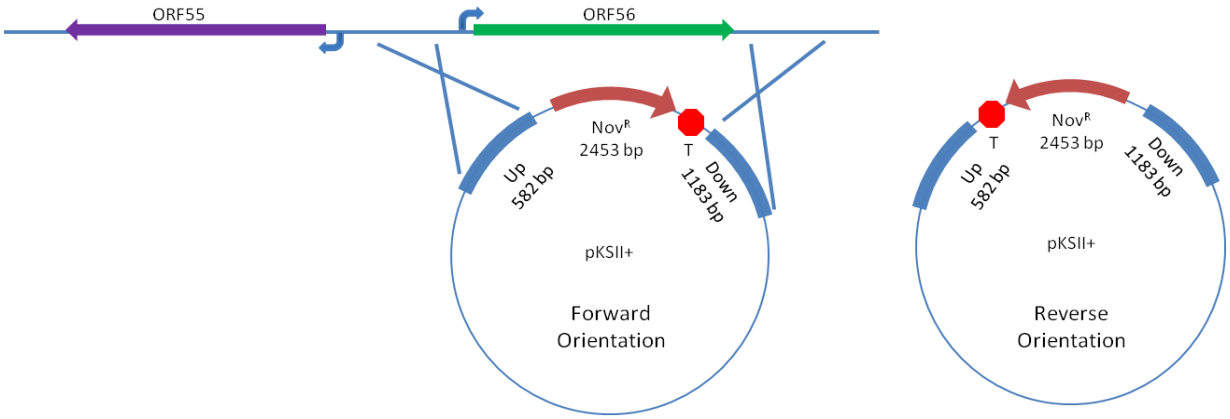


**Figure 14: Schematic representation of constructs pKSII-Δ56-NovR-F and pKSII-Δ56-NovR-R**

A schematic representation of the constructs to be transformed is given here. The blue fragments represent the ORF56 up- and downstream regions which are essential for homologous recombination to take place. The novobiocin resistance cassette is illustrated as a dark red arrow and the terminator sequence is highlighted as a light red dot.

### 3.1.2.3. Transformation in *N. magadii* L11 and possible outcomes

Competent *N. magadii* L11 cells were transformed with the constructs described previously according to the protocol mentioned in 'Materials and Methods', section 2.2.1.8. Transformants were tested via analytical PCR in order to identify clones having undergone a successful homologous recombination event resulting in the deletion of ORF56. However the transformation method used may yield different recombination events, namely two different forms of single cross-over (Figure 15) as well as the expected double cross-over event (Figure 16). Therefore, analytical PCR had to be performed in order to identify mutants having undergone a double cross-over event as for all three recombination events the novobiocin resistance cassette is integrated into the host genome. This entails that all three forms of mutation may thrive on selective medium plates (+ novobiocin) as all three are conferred the novobiocin resistance, thus they cannot be distinguished via simple selection based on novobiocin resistance.

#### 3.1.2.3.1. Single cross-over events

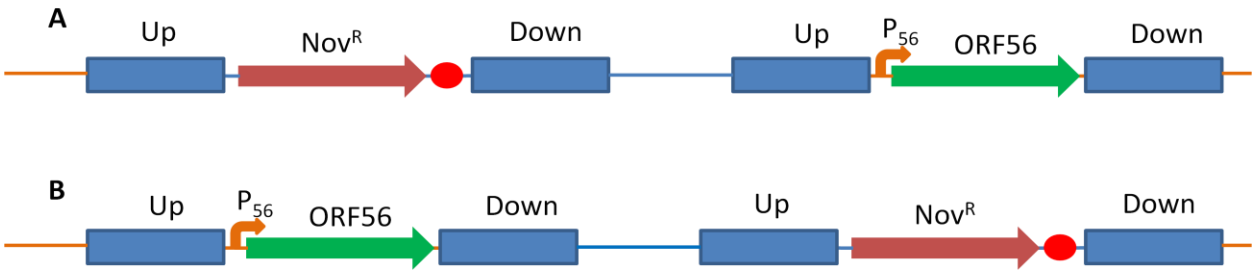


**Figure 15: Possible single cross-over events**

Up- and downstream regions of ORF56 are necessary for homologous recombination to take place. Orange lines represent chromosomal DNA of *N. magadii* L11 whereas blue lines represent plasmid DNA of the constructs pKSII-Δ56-NovR-F. **A** and **B** outline the possible single cross-over events. In both single cross-over events, the complete plasmid DNA is integrated into the host chromosome. **A** depicts the outcome when homologous recombination occurs within the upstream region of ORF56 (5'- cross-over). **B** depicts the outcome when homologous recombination occurs within the downstream region of ORF56 (3'- cross-over).

In the event of a single cross-over, either the up- or downstream region is responsible for a homologous recombination event and the whole plasmid DNA construct is integrated into the chromosome. Figure 15 outlines the two forms of single cross-over that may occur during transformation. In case of a single 5' cross-over event, the whole construct is integrated upstream of ORF56 whereas for a 3' cross-over event, the whole construct is integrated downstream of ORF56. In both cases ORF56 remains present in the genome as no deletion occurs here. As mentioned before, for both single cross-over events the novobiocin resistance cassette is integrated into the host genome, conferring resistance against the antibiotic. These transformants grow in the same fashion on selective medium plates (+novobiocin) as the ORF56-deletion mutants having undergone the double cross-over event. Therefore the three different transformants are indistinguishable on selective medium plates (+novobiocin) and need to be tested via analytical PCR for successful ORF56 deletion.

### 3.1.2.3.2. Double cross-over event

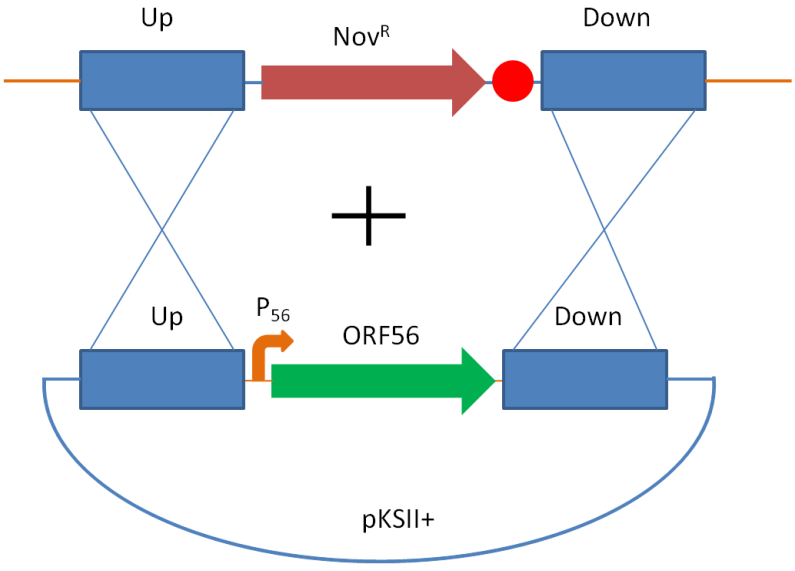


**Figure 16: Double cross-over event**

Here, homologous recombination occurs for the up- and the downstream region of ORF56, resulting in the deletion of ORF56 as well as its promoter $P_{56}$ from the host chromosome and replacement with the novobiocin resistance cassette. Through the homologous recombination, ORF56 and $P_{56}$ are transferred onto the plasmid. Through the absence of a suitable origin of replication on pKSII+, ORF56 is not transcribed and the plasmid is subsequently lost. Analytical PCR must be performed to identify this genotype.

Figure 16 schematically represents the outcome of a successful double cross-over event. Here, ORF56 as well as its promoter are deleted from the chromosome and replaced with a novobiocin resistance cassette through homologous recombination within both the up- and downstream region of ORF56. ORF56 and $P_{56}$ are transferred to the plasmid pKSII+ which is subsequently lost as it lacks a suitable origin of replication.

### 3.1.2.4. Screening transformants for successful homologous recombination

*N. magadii* L11 transformants resulting from the transformation of constructs pKSII-Δ56-NovR-R and pKSII-Δ56-NovR-F were tested via analytical PCR to screen for a double cross-over, preliminarily indicating a successful deletion of ORF56. Primers were chosen as follows: A set of primers binding the sequence of the novobiocin resistance cassette (Nov-9 and Nov-12), a primer annealing upstream of the upstream region of ORF56 (56-5en) as well as primers annealing downstream of the downstream region of ORF56 (56-3en / 56-31en). A schematic overview of the primer binding sites can be found in Figure 17.

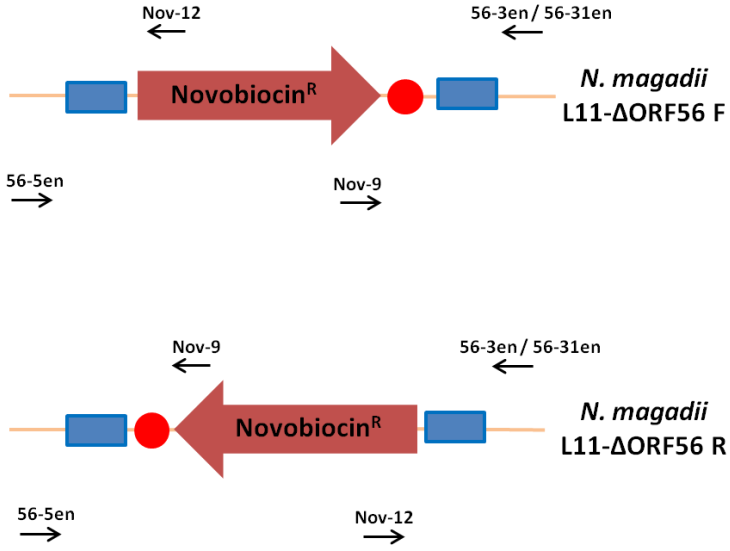


**Figure 17: Schematic overview of primer binding sites in order to screen for a double cross-over**

Depending on the orientation of the novobiocin resistance cassette, different primer combinations had to be used to identify homologous recombination at the upstream- and downstream region. For clones *N. magadii* L11-ΔORF56 F, primers 56-5en and Nov-12 were used to check for successful homologous recombination at the upstream region whereas primers Nov-9 and 56-3en/56-31en were used to check for successful homologous recombination at the downstream region. For clones *N. magadii* L11-ΔORF56 R, primers 56-5en and Nov-9 were used to check for successful homologous recombination at the upstream region whereas primers Nov-12 and 56-3en/56-31en were used to check for successful homologous recombination at the downstream region.

A typical picture of the analytical PCRs performed in order to identify *N. magadii* L11-ΔORF56 F is represented in Figure 18. Analysis relative to the identification of *N. magadii* L11-ΔORF56 F revealed that homologous recombination only occurred in some rare cases at the downstream region using primers Nov-9 and 56-3en. No signal relative to homologous recombination at the upstream region could be observed for any transformant tested. Any observed signal qualified as an unspecific signal.

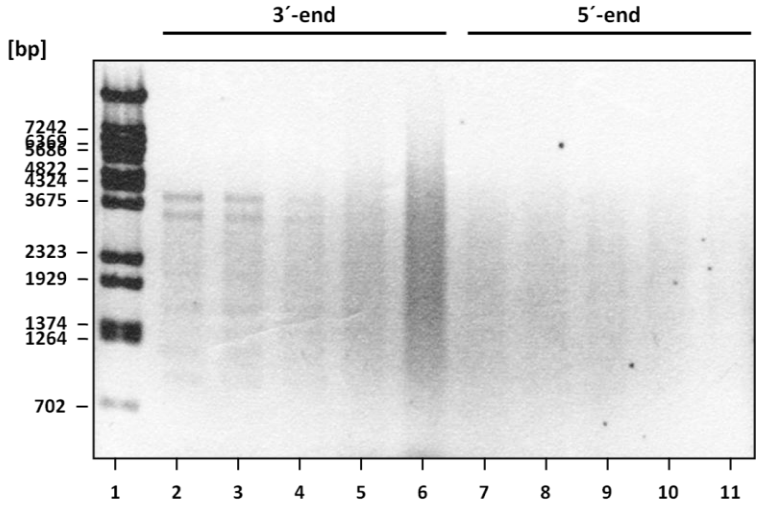


**Figure 18: A typical agarose gel picture resulting from a screening of transformants in order to identify *N. magadii* L11-ΔORF56 F**

Homologous recombination at the upstream region (5‘- end) was tested using primers 56-5en and Nov-12. No positive signal indicating a successful homologous recombination at the upstream region could be identified for any of the transformants tested. Homologous recombination at the downstream region (3‘- end) was tested using primers Nov-9 and 56-3en. The signals obtained for lanes 2, 3 and 4 were unspecific and the expected 2000 bp fragment was not present. Only on some rare occasions a PCR product the size of 2000 bp, indicating a successful homologous recombination at the downstream region, could be observed. No such case could however be documented for any of the screenings relative to homologous recombination at the upstream region.

Analysis relative to the identification of *N. magadii* L11-ΔORF56 R revealed that generally, homologous recombination occurred at the upstream region of ORF56 but no case could be observed where homologous recombination occurred at the downstream region of ORF56, neither by itself nor in combination with homologous recombination at the upstream region of ORF56 (data not shown). Again, the bands observed were qualified as being unspecific as their sizes were completely different to the expected PCR fragment size.

To summarize, transformation of construct pKSII-Δ56-NovR-R in *N. magadii* L11 yielded mutants where homologous recombination occurred exclusively at the upstream region of ORF56 whereas transformation of construct pKSII-Δ56-NovR-F in *N. magadii* L11 yielded mutants where homologous recombination occurred exclusively at the downstream region of ORF56 (data not shown). The type of homologous recombination observed seemed to be entirely dependent on the orientation of the novobiocin resistance cassette contained in the transformed construct. In both cases, homologous recombination only took place at either the up- or downstream region of ORF56, resulting in the complete integration of the respective plasmid constructs into the chromosome of *N. magadii* L11 and thus not in the deletion of ϕCh1 ORF56.

These observations remained consistent for a total of 532 transformants analyzed. It was therefore preliminarily concluded that, with the used method, no deletion mutants of ORF56 could be created in *N. magadii* L11.

### 3.1.2.5. Discussion

Previously, it has been demonstrated that an over-expressed ϕCh1 ORF56 in the wild-type strain *N. magadii* L11 exhibited a repressor function characterized by a reduced lysis behavior of the strain *N. magadii* L11 (pRo-5-ORF56) as well as the absence of detectable amounts of viral proteins gpE, $gp34_{52}$ and main methyltransferase M.*Nma*ϕCh1I when compared to the wild-type strain *N. magadii* L11, preliminary indicating an important impact of ORF56 on the life cycle of ϕCh1. In order to further investigate the described repressor function of ORF56, deletion mutants of this open-reading frame were to be created. The method used in order to create these ORF56 deletion mutants in *N. magadii* L11 was first successfully applied in 2010 (Selb, 2010). Using the homologous recombination method described, three different ϕCh1 deletion mutants have so far been created successfully: *N. magadii* L11-ΔORF79*,* an ORF79 deletion mutant (Selb 2010), *N. magadii* L11-ΔORF34*,* an ORF34 deletion mutant (Till, 2011 & Dimmel 2013) and *N. magadii* L11-ΔORF44, an ORF44 deletion mutant (this thesis). It has however been shown that, using the same method, it proved itself as being impossible to yield ORF56 deletion mutants in order to create the strain *N. magadii* L11-ΔORF56. Transformation of the constructs pKSII-Δ56-NovR-R and pKSII-Δ56-NovR-F in *N. magadii* L11 yielded mutants where homologous recombination only occurred at either the upstream region of ORF56 (pKSII-Δ56-NovR-R) or at the downstream region of

ORF56 (pKSII-Δ56-NovR-F), in both cases leading to the integration of the whole construct into the genome of *N. magadii* L11 rather than a deletion of ORF56 through simultaneous homologous recombination at the up- and downstream regions of ORF56.

The exact mechanism underlying this observation is unknown but a hypothesis as to why ORF56 could not be deleted can be made based on its locus in the genome of ϕCh1. ORF56 is a putative transcriptional regulator exhibiting a repressor function, its locus being in the centre of the DNA replication domain of ϕCh1 composed of 15 different open-reading frames (ORF46 – ORF60). This entails that out of 98 different open-reading frames that make up the genome of ϕCh1, only 15 are responsible for the replication of viral DNA which represents a small proportion of genome responsible for a major task in assuring the completion of the life cycle of ϕCh1. Based on this fact, it is most likely that the repressing function of ORF56 is a crucial step in the precise replication of viral DNA, so crucial in fact that it seems essential for the correct sequence of events leading to the synthesis of new viral particles. Thereby one can hypothesize that, although up to 50 copies of ORF56 are present in the genome of *N. magadii* L11, its impact in said sequence of events in the life cycle of ϕCh1 seems to be so tremendous that a deletion of ORF56 using a standard homologous recombination method is not possible without seriously compromising viral stability.

## 3.2. Construction and characterization of a ϕCh1 ORF44 deletion mutant

### 3.2.1. ORF43/ORF44 – A putative toxin-antitoxin system

Previous studies relative to the regulation of gene expression in virus ϕH infecting *H. salinarum* have shown that different fragments of an immunity-conferring construct pϕHL conferred immunity against ϕH infection to *H. salinarum* when cloned individually, however the immunity-conferring efficiencies of these individual constructs were different from the ones observed for a strain having been transformed with the entire pϕHL construct (Gropp *et al*., 1992). Especially the transcripts T9 and T10 (encoding two ORFs of 54 bp and 131 bp, respectively) acted co-operatively with the ϕH repressor (Stolt and Zillig 1993). Since a high degree of sequence similarity has been found between these two ORFs and ϕCh1 ORF43/44 (90% and 94%, respectively), these ORFs seemed good candidates for an investigation relative to the regulation of gene expression in ϕCh1 alongside ORF48/49 (Iro *et al*., 2007). The observation that promoter sequences could only be found upstream of ORF43 ($p_{43}$) as well as the fact that start- and stop codons of ORF43 and ORF44 overlap suggest that ORF43 and ORF44 are co-transcribed as well as co-translated (Klein *et al*., 2002), thus forming an operon together. Additional sequence analysis of both ORFs revealed a similarity to the so-called VapBC toxin-antitoxin system where ORF43 would code for the inhibitor VapB and ORF44 would code for the nuclease VapC as its sequence contains a PIN-like domain (Hofbauer, 2015). VapBC (Virulence-associated proteins) toxin-antitoxin systems are characterized by two genes whose start- and stop codons overlap, organizing them in an operon. The unstable VapB antitoxin (here: putatively ORF43) builds a complex with the stable toxin VapC (here: putatively ORF44) and the complex auto-regulates its own expression. Upon degradation of the inhibitor, the toxin becomes active (Arcus *et al*., 2011).

A preliminary binding site for ϕCh1 gp43/44 has been found in the sequence of ORF48 encoding for the repressor protein Rep. Plasmid constructs containing the intergenic region between ORF48 and ORF49, a mutated ORF48 start codon, the *bgaH* gene under the control of the ORF49 promoter as well as ORF43/44 cloned downstream of the *bgaH* gene (pMI-2Δ/43-44), were transformed into *H. volcanii* (Iro *et al*., 2007). A substantial rise in BgaH activity has been demonstrated for this construct when compared to the same construct not containing the ORF43/44 operon (pMI-2Δ) (Iro *et al*. 2007). An analogous trend was observed for a construct only containing ORF43 (pMI-2Δ/43); here BgaH activity was similar to the activity observed for pMI-2Δ/43-44 (Iro *et al*., 2007). No detectable BgaH activity was observed for

pMI-2Δ/44 however, a construct only containing ORF44 (Iro *et al*., 2007). A summary of the results obtained by Iro *et al*. can be seen in Figure 19. In the case of a non-mutated start codon of ORF48, BgaH activity dropped significantly. Taken together these results indicate that ORF43/44 exhibits an enhancing effect on *bgaH* expression with an enhancing activity of ORF43 on the intergenic region and a putative repressing activity of ORF44, all in the presence of the ORF48 coding sequence. The putative repressing- or degrading activity of ORF44 would then be further evidence for the ORF43/44 toxin-antitoxin hypothesis.

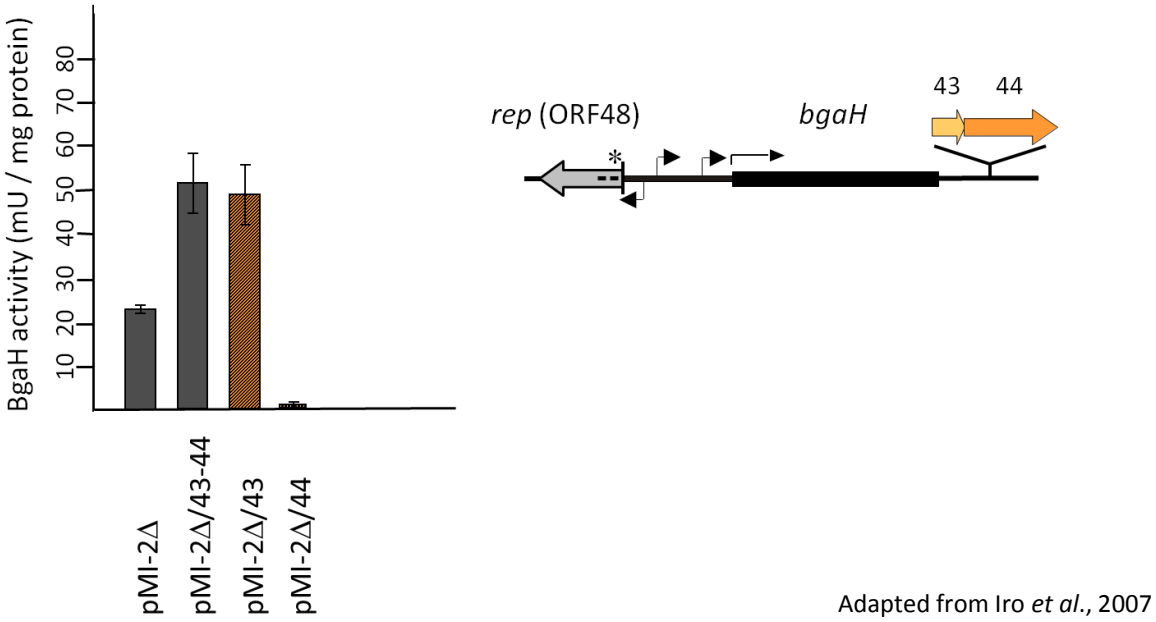


Adapted from Iro *et al*., 2007

**Figure 19: The influence of ORF43/44 on BgaH activity in presence of the ORF48 (*rep*) sequence with a mutated start codon**

Here, a plasmid construct labelled pMI-2Δ containing ORF48 with a mutated start codon, the intergenic region of ORF48 and ORF49 as well as the *bgaH* gene (replacing ORF49) under control of the ORF49 promoter was constructed and transformed in *H. volcanii*. pMI-2Δ gives rise to BgaH activity because of promoter activity in the intergenic region. The enhancing effect of ORF43 as well as ORF43/44 on the BgaH activity in presence of the coding sequence of ORF48 is clearly visible. ORF44 alone exhibits a repressing activity in the presence of the ORF48 coding sequence. (Iro *et al*., 2007)

A first series of experiments relative to the characterization of ϕCh1 ORF44 in its native host *N. magadii* showed a similar trend: Cloning ORF43 and ORF43/44 under the control of the constitutive promoter $p_{43}$ in the cured strain *N. magadii* L13, not containing ϕCh1 integrated as a provirus, showed no difference in reporter gene expression when compared to the wild-type (Hofbauer, 2015). However, transformation of ORF44 under the control of $p_{43}$ in *N. magadii* L13 revealed a 48 hour delay in reporter gene expression and subsequent densitometry analysis revealed a 48-hour repressing activity of gp44 when it comes to reporter gene expression as well as, more importantly, a truncated reporter gene product (Hofbauer, 2015).

The aim of this study therefore was to further investigate the influence of ORF44 in regulating ϕCh1 gene expression in the native host *N. magadii* through the deletion of ORF44 itself in order to get more insight on a potential repressing and/or toxin role of ORF44.

### 3.2.2. Construction of an ORF44 deletion mutant – *N. magadii* L11-ΔORF44

#### 3.2.2.1. Aim and cloning strategy

The aim of this study was to create a wild-type *N. magadii* L11-ORF44 deletion mutant in order to investigate the function of ORF44 in *N. magadii* L11. The cloning strategy involved the construction of a plasmid containing both the upstream- as well as the downstream region of ϕCh1 ORF44, flanked by a novobiocin resistance cassette (*gyrB*) in 'forward' and 'reverse' orientation as well as a terminator sequence. Transformation of these constructs should yield ORF44 deletion mutants via homologous recombination. Two different orientations for the resistance marker cassette were chosen to exclude the possibility that a given orientation of the resistance cassette might interfere with the transcription of adjacent open-reading frames. The terminator sequence ascertains that transcription of the novobiocin resistance cassette stops once the cassette is transcribed, further reducing the possibility of unwanted interferences with the transcription of adjacent open-reading frames.

### 3.2.2.2. Plasmid constructs pKSII-Δ44-NovR-R and pKSII-Δ44-NovR-F

Plasmid pBlueScript II KS(+) has been used for construction, implying its so-called 'suicide' characteristic when transformed into *N. magadii*; pKSII does not contain an applicable origin of replication for *N. magadii*, thus resulting in cell death if the finalized construct should not be integrated into the host chromosome. The complete cloning strategy for the creation of a ϕCh1 ORF44 deletion mutant can be found in the 'Materials and Methods' part of this thesis, section 2.2.2.7.3. Figure 20 schematically depicts the finalized constructs that were transformed into *N. magadii* L11.

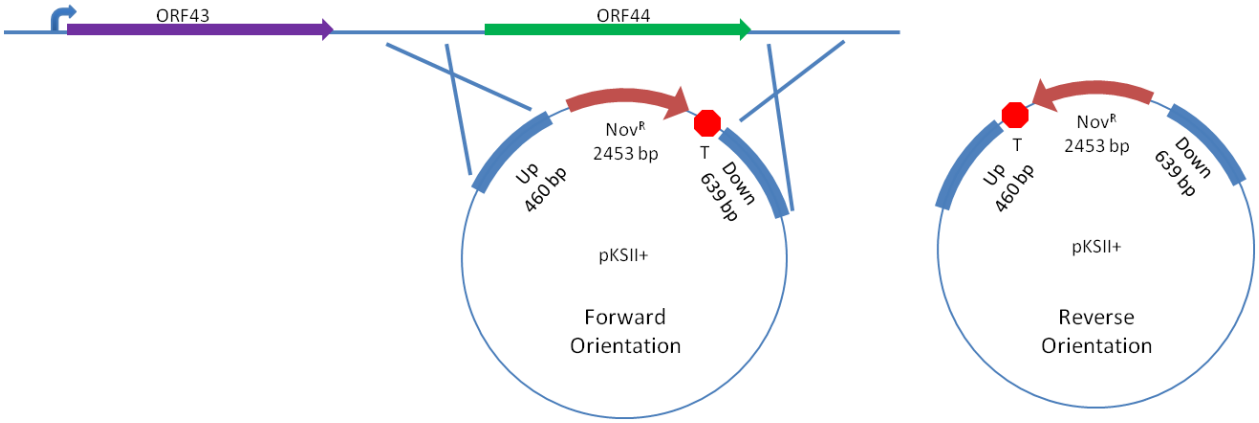


**Figure 20: Schematic representation of constructs pKSII-Δ44-NovR-F and pKSII-Δ44-NovR-R**

A schematic representation of the finished constructs to be transformed is given here. The blue fragments represent the ORF44 up- and downstream regions which are essential for homologous recombination to take place. The novobiocin resistance cassette is illustrated as a red arrow and the terminator sequence is highlighted as a light red dot. The dark blue arrow represents promoter $p_{43}$.

### 3.2.2.3. Transformation in *N. magadii* L11 and possible outcomes

Competent *N. magadii* L11 cells were transformed with the constructs described previously according to the protocol mentioned in 'Materials and Methods', section 2.2.1.8. Transformants were tested via analytical PCR in order to identify clones having undergone a successful homologous recombination event resulting in the deletion of ORF44. As mentioned under section 3.1.2.3., the transformation method used may yield different recombination events, namely two different forms of single cross-over (Figure 21) as well as the expected double cross-over event (Figure 22). Only transformants having undergone a successful double cross-over event were considered to be putative ORF44 deletion mutants and were thus analyzed further.

#### 3.2.2.3.1. Single cross-over events

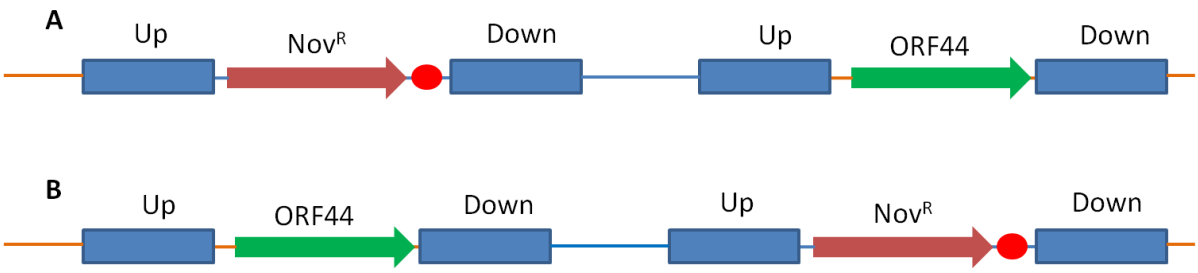


**Figure 21: Possible single cross-over events**

Up- and downstream regions of ORF44 are necessary for homologous recombination to take place. Orange lines represent chromosomal DNA of *N. magadii* L11 whereas blue lines represent plasmid DNA of the constructs pKSII-Δ44-NovR-F and pKSII-Δ44-NovR-R. **A** and **B** outline the possible single cross-over events. In both single cross-over events, the complete plasmid DNA is integrated into the host chromosome. **A** depicts the outcome when homologous recombination occurs within the upstream region of ORF44 (5'- cross-over). **B** depicts the outcome when homologous recombination occurs within the downstream region of ORF44 (3'- cross-over).

As mentioned under section 3.1.2.3.1., in the event of a single cross-over, either the up- or downstream region is responsible for a homologous recombination event and the whole plasmid DNA construct is integrated into the chromosome. Figure 21 outlines the two forms of single cross-over that may occur during transformation. In case of a single 5' cross-over event, the whole construct is integrated upstream of ORF44 whereas for a 3' cross-over event, the whole construct is integrated downstream of ORF44. In both cases ORF44 remains present in the genome as no deletion occurs here. As mentioned before, for both single cross-over events the novobiocin resistance cassette is integrated into the host genome, conferring resistance against the antibiotic. These transformants grow in the same fashion on selective medium plates (+novobiocin) as the ORF44-deletion mutants having undergone the double cross-over event. Therefore the three different transformants are indistinguishable on selective medium plates (+novobiocin) and need to be tested via analytical PCR for successful ORF44 deletion.

### 3.2.2.3.2. Double cross-over event

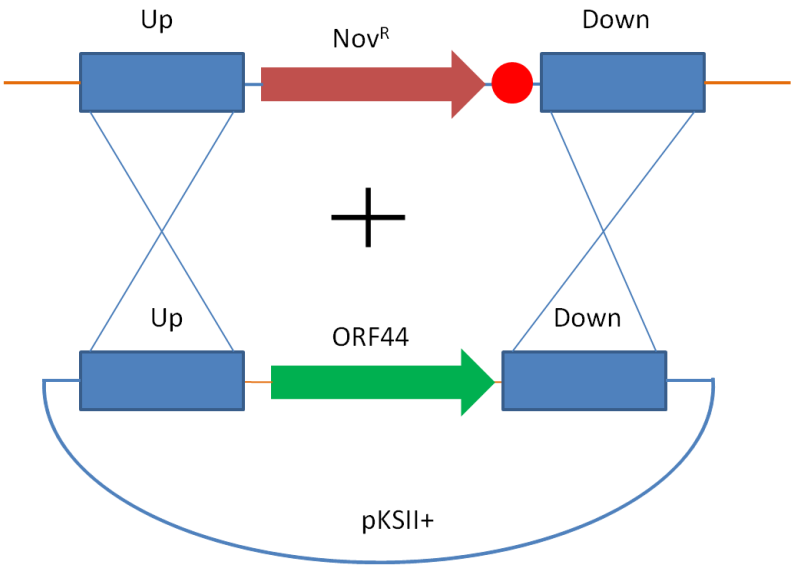


**Figure 22: Double cross-over event**

In this case, homologous recombination occurs for the up- and the downstream region of ORF44, resulting in the deletion of ORF44 from the host chromosome and replacement with the novobiocin resistance cassette. Through the homologous recombination, ORF44 is transferred onto the plasmid. Through the absence of a suitable origin of replication on pKSII+, ORF44 is not transcribed and the plasmid is subsequently lost. Analytical PCR must be performed to identify this genotype.

Figure 22 schematically represents the outcome of a successful double cross-over event. Here, ORF44 is deleted from the chromosome and replaced with a novobiocin resistance cassette through homologous recombination within both the up- and downstream region of ORF44. ORF44 is transferred to the plasmid pKSII+ which is subsequently lost as it lacks a suitable origin of replication.

### 3.2.2.4. Screening transformants for successful homologous recombination

*N. magadii* L11 transformants resulting from the transformation of constructs pKSII-Δ44-NovR-R and pKSII-Δ44-NovR-F were tested via analytical PCR to screen for a double cross-over, preliminarily indicating a successful deletion of ORF44. Primers were chosen as follows: A set of primers binding the sequence of the novobiocin resistance cassette (Nov-9 and Nov-12), a primer annealing upstream of the upstream region of ORF44 (44-5) as well as a primer annealing downstream of the downstream region of ORF44 (44-3en). A schematic overview of the primer binding sites can be found in Figure 23.

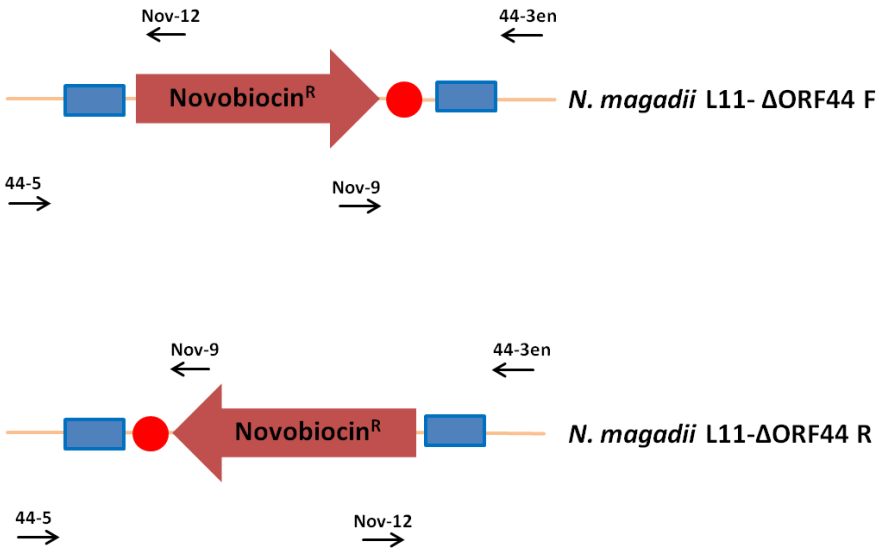


**Figure 23: Schematic overview of primer binding sites in order to screen for a double cross-over**

Depending on the orientation of the novobiocin resistance cassette, different primer combinations had to be used to identify homologous recombination at the upstream- and downstream region. For clones *N. magadii* L11-ΔORF44 F, primers 44-5 and Nov-12 were used to check for successful homologous recombination at the upstream region whereas primers Nov-9 and 44-3en were used to check for successful homologous recombination at the downstream region. For clones *N. magadii* L11-ΔORF44 R, primers 44-5 and Nov-9 were used to check for successful homologous recombination at the upstream region whereas primers Nov-12 and 44-3en were used to check for successful homologous recombination at the downstream region.

Using the sets of primers designed to identify homologous recombination with the novobiocin resistance cassette integrated in "reverse" orientation described above, a preliminarily positive ORF44 deletion mutant could be identified. The analytic PCR screening with the respective primers revealed PCR products for both primer combinations matching the expected fragment sizes relative to a homologous recombination event at both the up- and downstream region: 880 bp for homologous recombination at the upstream region and 700 bp for homologous recombination at the downstream region (data not shown). Only in this particular case where a PCR product is obtained for both analytic PCRs, the indication of a double cross-over event is given. Wild-type *N. magadii* L11 template was used as negative control (data not shown).

### 3.2.2.5. Homogenization of *N. magadii* L11-ΔORF44 R

Homogenization was a necessary step in order to create homozygous *N. magadii* L11-ΔORF44 R mutants. As *N. magadii* L11 contains up to 50 copies of chromosomal DNA and thus also up to 50 copies of ϕCh1 DNA, the preliminary *N. magadii* L11-ΔORF44 R mutants needed to be homogenized so that every existing copy of ORF44 would effectively be deleted. The method of choice in order to homogenize *N. magadii* L11-ΔORF44 R consisted in an hour-long incubation of a dilution series of culture supernatant containing the mutant virus with *N. magadii* L13 and subsequent plating on rich medium plates complemented with novobiocin. Using this method, homozygous *N. magadii* L11-ΔORF44 R mutants were created in a way that is much faster and more efficient than the passaging method. An overview of the applied procedure can be seen in Figure 24. A detailed description of the method used can be found under 'Materials and Methods', section 2.2.1.9.

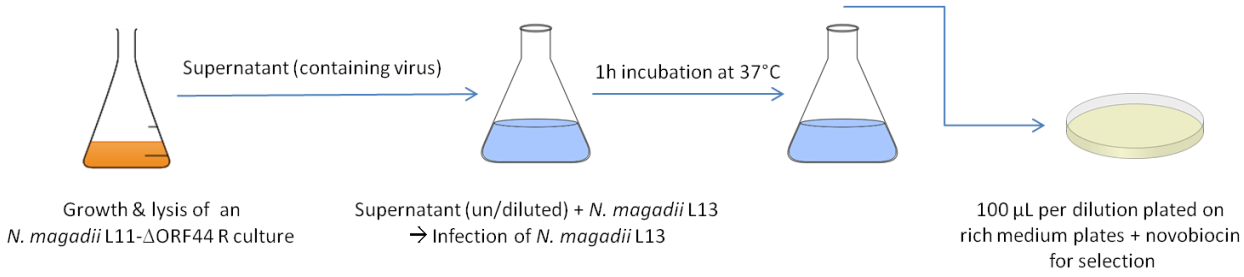


**Figure 24: Homogenization of *N. magadii* L11-ΔORF44 R**

*N. magadii* L11-ΔORF44 R was grown in rich medium (without novobiocin) until complete lysis of the culture. After centrifugation, the culture supernatant containing the mutant virus was collected and a dilution series was prepared with rich medium. The dilution series was then incubated with freshly grown *N. magadii* L13 for 1 hour at 37°C so that the viruses may bind to their receptor on the cell wall of *N. magadii* L13**.** Afterwards, 100 µL per dilution were plated on rich medium plates containing novobiocin. This method yielded homozygous *N. magadii* L11-ΔORF44 R mutants in a way that is faster and more efficient than passaging.

In order to summarize, an *N. magadii* L11-ΔORF44 R culture was incubated in rich medium without novobiocin until complete lysis of the culture occurred. Serial dilutions were established with the resulting culture supernatant that were then used to infect a freshly grown culture of *N. magadii* L13. The infected cells were then plated on rich medium agar containing novobiocin. Single colonies were incubated at 37 °C and subsequently tested for the deletion of ORF44. This was achieved with the same primers used for the testing of correct homologous recombination at the upstream and downstream regions of ORF44 (see Figure 23). Another PCR reaction was prepared using primers 44-5 and 44-3 which anneal at the 5'-end respectively the 3'-end of ORF44. This 50-cycle PCR was set up to ensure that every copy of ORF44 would eventually have been deleted through the homogenization method used. The procedures used here ultimately resulted in the identification of three different, putatively homozygous ORF44 deletion mutants, namely clones 4, 7 and 8. Figure 25 summarizes the results obtained and indicates the putative homozygous deletion of ORF44 for all three clones analyzed.

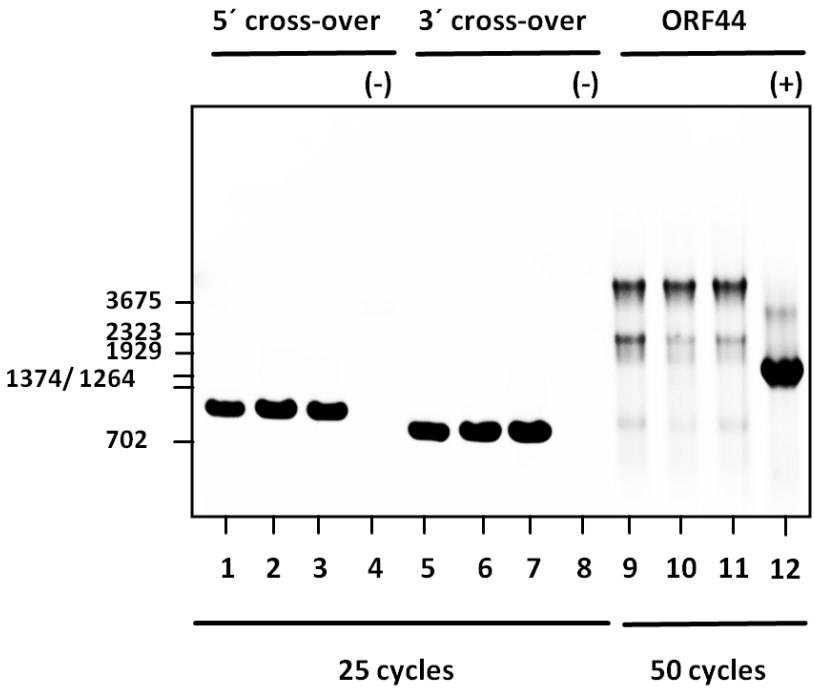


**Figure 25: Verification of the mutant strain *N. magadii* L11-ΔORF44 R after homogenization. Lanes 1, 5 and 9: clone 4. Lanes 2, 6 and 10: clone 7. Lanes 3, 7 and 11: clone 8. Lanes 4, 8 and 12: wild-type *N. magadii* L11.**

In order to verify the correct integration of the novobiocin resistance cassette as well as the correct deletion of every copy of ORF44 after the homogenization step, analytic PCRs were repeated with the same primers used before (see Figure 23). Lanes 1, 2 and 3 illustrate the correct homologous recombination at the upstream region of ORF44 using primers 44-5 and Nov-9, yielding the expected 880 bp PCR fragment for each analyzed clone. Lanes 5, 6 and 7 illustrate the correct homologous recombination at the downstream region of ORF44 using primers Nov-12 and 44-3, yielding the expected 700bp PCR fragment for each analyzed clone. Lanes 4 and 8 represent the respective wild-type negative control. Lanes 9, 10 and 11 show that, even after 50 cycles, wild-type ORF44 could not be detected using primers 44-5 and 44-3, thus indicating a successful deletion of every copy of ORF44. Lane 12 serves as a wild-type positive control, using the same primers 44-5 and 44-3. Size markers (in bp) are given on the left.

### 3.2.2.6. Confirmation of the homozygous *N. magadii L11*-ΔORF44 R mutants - Southern Blot

Taking into account the possibility of erroneous PCR results, no definitive conclusions could be made relative to the total deletion of ORF44 based on PCR analysis alone. Therefore, another approach was used in order to undoubtedly confirm the generation of a homozygous *N. magadii* L11-ΔORF44 R mutant, namely a Southern Blot analysis. In order to do so, virus particles and subsequently viral DNA of both wild-type ϕCh1 as well as ϕCh1-ΔORF44 R clones 4, 7 and 8 were isolated (see 'Materials and Methods' sections 2.2.1.10 and 2.2.1.12) and restricted using *PstI*. The restricted fragments were

separated on a 0.8% agarose gel and the respective DNA concentrations were adapted. The exact protocol for the synthesis of the biotinylated probes as well as for the blotting procedure can be found in 'Materials and Methods' section 2.2.1.13. The synthesis of the upstream region (5' probe) of ORF44 was achieved using primers Δ44-1 and Δ44-2, resulting in a PCR fragment of 480 bp and synthesis of the downstream region (3' probe) of ORF44 was achieved using primers Δ44-3 and Δ44-4, here resulting in a PCR fragment of 659 bp. In both cases, ϕCh1 DNA was used as template and biotinylated dUTPs were added to the reaction for labeling purposes. The probe hybridization scheme can be seen in Figure 26.

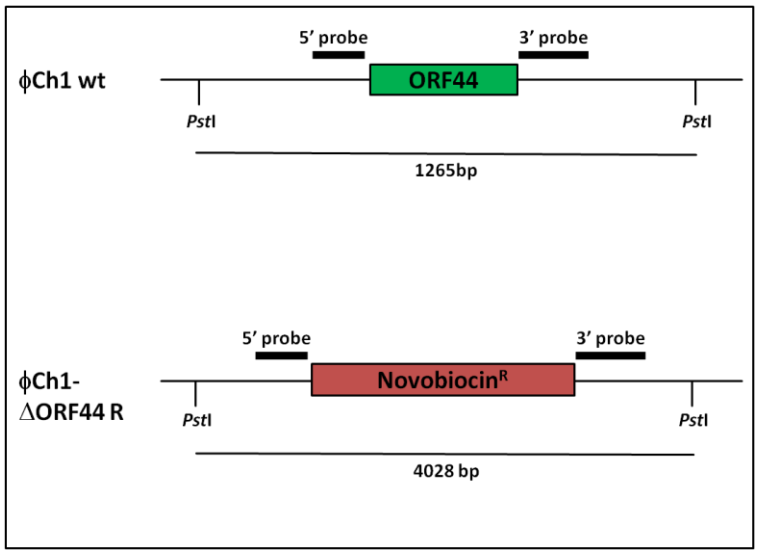


**Figure 26: Probe hybridization scheme**

Wild-type and mutant ϕCh1 DNA was restricted with *PstI*, resulting in one larger fragment of interest for ϕCh1-ΔORF44 R as the novobiocin resistance cassette is substantially larger than ORF44 and a smaller fragment of interest for the ϕCh1 wild-type. Both ORF44 as well as the novobiocin resistance cassette do not contain a supplementary *PstI* restriction site. In the case of ϕCh1 wt, the biotinylated 5' and 3' probes thus detect the same 1265 bp fragment. As the much larger novobiocin resistance cassette replaces ORF44 in ϕCh1-ΔORF44 R and as up- and downstream regions are present, both biotinylated probes detect the same, larger 4028 bp fragment here.

The results of the southern blotting analysis are depicted in Figure 27. Here, one can see that different results have been obtained for the three putative homozygous ϕCh1-ΔORF44 R clones analyzed. Due to the presence of the expected 4028 bp fragment for both biotinylated probes, ϕCh1-ΔORF44 R clones 7 and 8 have undoubtedly been confirmed as being homozygous ORF44 deletion mutants where ORF44 has been replaced by a novobiocin resistance cassette in "reverse" orientation. In the case of ϕCh1-ΔORF44 R clone 4, the southern blotting procedure demonstrated that this was not the case here; clone 4 does not represent a homozygous ORF44 deletion mutant where ORF44 has been replaced by a novobiocin resistance cassette in "reverse" orientation.

These results underline the importance of generally confirming the generation of homozygous ϕCh1 deletion mutants in *N. magadii* via Southern Blot; verification via analytical PCR only represents a

preliminary process of elimination. As can be seen in Figure 25 (section 3.2.2.5.), the analytical PCR testing of clone 4 exhibited the exact same results as for clones 7 and 8 in any of the tests performed. However, only an ultimate evaluation via Southern Blot was able to identify clone 4 as a mutant of other origin. As the aim of this study resided in the construction as well as the characterization of homozygous *N. magadii* L11-ΔORF44 R mutants, clone 4 was discarded from the study and the subsequent experiments were only performed on the homozygous *N. magadii* L11-ΔORF44 R clones 7 and 8.

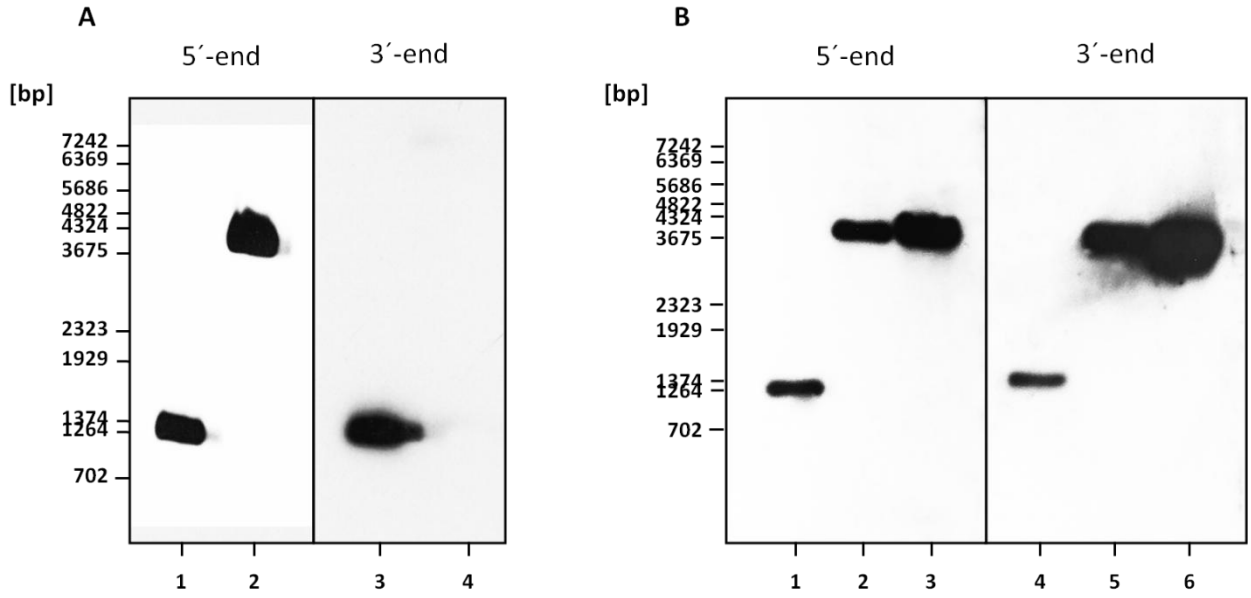


**Figure 27: Southern Blot analysis for *N. magadii* L11-ΔORF44 R clones 4, 7 and 8**

**A** Lanes 1, 3: L11 wt; Lanes 2, 4: L11-ΔORF44 R clone 4. Here, the Southern Blotting results for *N. magadii* L11-ΔORF44 R clone 4 are illustrated. For the wild-type control *N. magadii* L11, the 5‘- and 3‘ probes hybridized with the expected 1265 bp fragment, indicating the presence of ORF44. In the case of *N. magadii* L11-ΔORF44 R clone 4, the 5‘ probe hybridized with a fragment of the expected 4028 bp length, yet no signal relative to the hybridization of the 3‘ probe could be detected. **B** Lanes 1, 4: L11 wt; Lanes 2, 5: L11-ΔORF44 R clone 7 Lanes 3, 6: L11-ΔORF44 R clone 8. Here, the Southern Blotting results for *N. magadii* L11-ΔORF44 R clones 7 and 8 are illustrated. Again, the wild-type control *N. magadii* L11 signals show that the 5‘- and 3‘ probes hybridized with the expected 1265 bp fragment. For both clones 7 and 8, the 5‘- as well as the 3‘ probes hybridized with the expected 4028 bp fragment, thereby proving the successful deletion of ORF44 and its replacement with the novobiocin resistance cassette in „reverse“ orientation.

After their expected genotype was confirmed through Southern Blotting, the homozygous ORF44 deletion mutants *N. magadii* L11-ΔORF44 R clones 7 and 8 were considered two biological replicates; all subsequent experiments were carried out with both strains.

### 3.2.3. Characterization of *N. magadii* L11-ΔORF44 R

#### 3.2.3.1. Growth kinetics analysis

In order to investigate the effect of an ORF44 deletion on the phenotype of *N. magadii* L11, a preliminary growth curve analysis was performed where growth- and lysis behavior of the wild-type strain *N. magadii* L11 was compared to the growth- and lysis behavior of *N. magadii* L11-ΔORF44 R clone 7, *N. magadii* L11-ΔORF44 R clone 8 as well as the cured strain *N. magadii* L13. The results are compiled in Figure 28. Data shown for *N. magadii* L11-ΔORF44 R represents the average growth kinetics of clones 7 and 8.

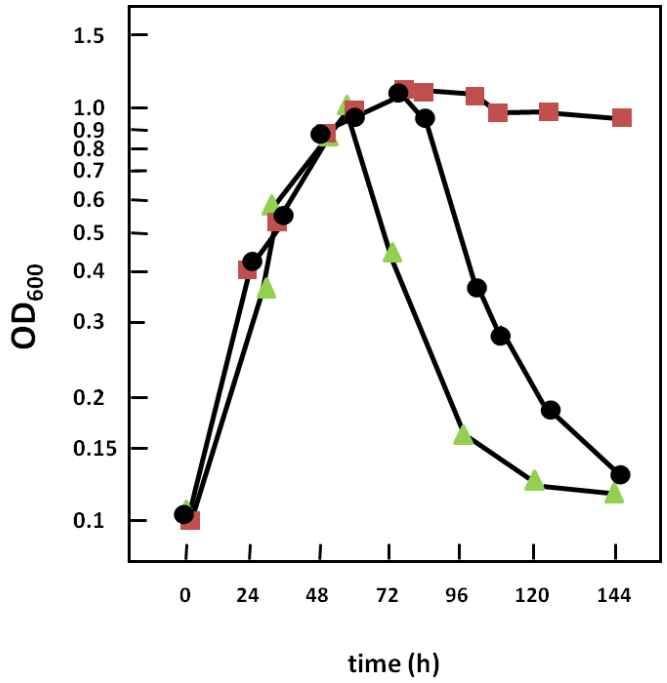


**Figure 28: Growth kinetics analysis of *N. magadii* L11-ΔORF44 R**

The red squares represent growth kinetics of *N. magadii* L13 and the black circles show growth kinetics of *N. magadii* L11. Both strains exhibit the expected growth- and lysis behaviour. *N. magadii* L11-ΔORF44 R (green triangles) behaves almost identical to *N. magadii* L11/*N. magadii* L13 in the logarithmic growth phase but the onset of lysis occurs 24 hours earlier in the case of *N. magadii* L11-ΔORF44 R .

Figure 28 clearly outlines the different growth kinetics of *N. magadii* L11 when compared to *N. magadii* L11-ΔORF44 R. The initial growth behavior is comparable between the strains, whereas the differences occur with respect to the lytic behavior of the respective strains. In the case of *N. magadii* L11-ΔORF44 R, lysis occurs 24 hours earlier than for the wild-type strain *N. magadii* L11; this is a preliminary indication

for a regulating effect of ORF44 strictly relative to the onset of lysis as lysis itself is neither reduced nor accelerated.

### 3.2.3.2. Virus titer analysis and Western Blots

In order to investigate the number of viruses released at given time points during a growth kinetics analysis and in order to visualize the phenotype of *N. magadii* L11-ΔORF44 on protein levels, the time course experiment previously described was repeated. Here, culture samples were now taken and the respective supernatants were stored separately. Crude protein extracts were prepared from the culture samples as mentioned under 'Materials and Methods', section 2.2.2.1.

#### 3.2.3.2.1. Virus titer analysis

Phage titer analysis was performed as mentioned under 'Materials and Methods', section 2.2.1.11. Virus titer results are visualized in Figure 29.

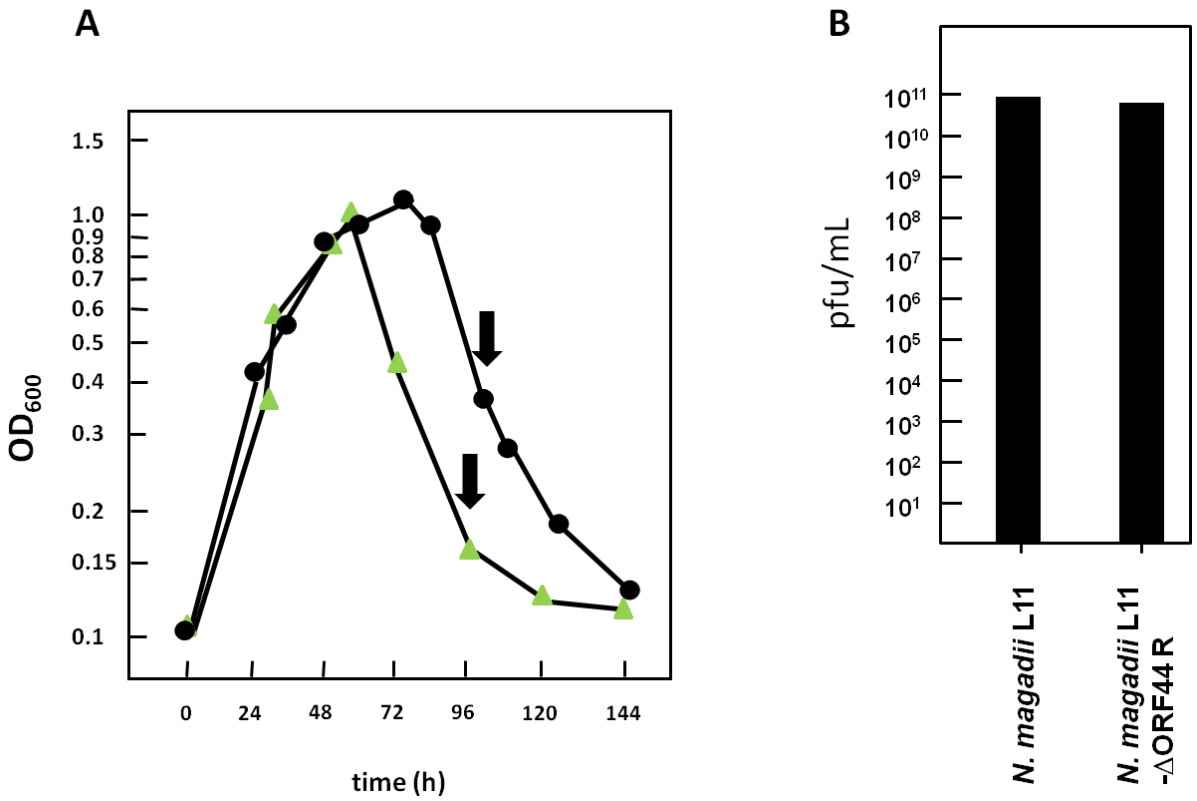


**Figure 29: Virus titer analysis of *N. magadii* L11 versus *N. magadii* L11- ΔORF44 R**

**A** The black circles represent *N. magadii* L11, the green triangles represent *N. magadii* L11-ΔORF44 R. Here, supernatant samples containing virus particles were taken at the time points indicated by the black arrows. The cured strain *N. magadii* L13 was infected with the two respective supernatant samples for the virus titer analysis. **B** Virus titer analysis showed that there is no significant difference in viral plaque formation during lysis when comparing wild-type to *N. magadii* L11-ΔORF44 R. Although the onset of lysis occurs 24 hours earlier in the case of *N. magadii* L11-ΔORF44 R, no significant difference in the amount of virus particles released could be observed between wild-type and mutant strain.

Figure 29 B illustrates virus particle release of *N. magadii* L11 versus *N. magadii* L11-ΔORF44 R at the time points indicated by the black arrows in Figure 29 A. Figure 29 B suggests no significant difference in the amount of virus particles released at the chosen time points of virus particle supernatant sampling. This is a supplementary indication for the fact that, although lysis occurs 24 hours earlier in the case of *N. magadii* L11-ΔORF44 R when compared to the wild-type, its lysis kinetics remain identical to the ones observed for the wild-type. This confirms the hypothesis, resulting from the growth curve analysis, that ORF44 seems to exclusively influence the onset of lysis rather than lysis itself.

3.2.3.2.2. Influence of ϕCh1 ORF44 on the expression of ϕCh1 protein E, $gp34_{52}$ and M.*Nma*ϕCh1I – Western Blots

Western Blotting analysis was performed in order to investigate the possible role of ϕCh1 ORF44 in altering ϕCh1 gene expression and thus the expression of proteins E, $gp34_{52}$ and the main ϕCh1 methyltransferase (M.*Nma*ϕCh1I). As mentioned under 3.1.1.4., the antibodies used were chosen in a way that spans the whole genome of ϕCh1. At the time of the study, no α-gp44 antibodies were available. The Western Blots and all related procedures were performed as mentioned in 'Materials and Methods', section 2.2.2. An overview of the Western Blotting results can be found in Figure 30 B. It has been shown that, although the onset of lysis occurs 24 hours earlier in the case of *N. magadii* L11-ΔORF44 R when compared to the wild-type *N. magadii* L11, the detectability kinetics of protein E remain almost identical: Protein E is detectable after 48 hours following inoculation in both cases. A similar trend has been observed for α-$gp34_{52}$ Western Blots as well as α-M.*Nma*ϕCh1I Western Blots (data not shown). Based on the results obtained, a disparity between onset of lysis and the detectability of the three major proteins tested could be observed when comparing *N. magadii* L11 to *N. magadii* L11-ΔORF44 R. This observation led to the designing of the so-called "Outgrowth" experiments where protein detectability kinetics as well as growth kinetics were monitored based on the moment of re-inoculation of the respective cultures; the moment of re-inoculation revolving around the point of onset of lysis. A first series was designed where re-inoculation was performed closely after the onset of lysis and a second series where re-inoculation happened closely before the onset of lysis.

### 3.2.3.3. Outgrowth experiments

Growth kinetics analysis of *N. magadii* L11-ΔORF44 R has shown that ORF44 exhibits an influence on the onset of lysis when compared to the wild-type strain *N. magadii* L11; the onset of lysis occurs 24 hours earlier in the case of *N. magadii* L11-ΔORF44 R. Figures 30 A and B illustrate that, although lysis occurs 24 hours earlier for *N. magadii* L11-ΔORF44 R, the detection of major capsid protein E (gpE) arises at the same time point in the growth kinetics analysis for both the wild-type as well as the mutant strain (after 48 hours). In order to investigate how the difference in the onset of lysis alongside the time-wise identical initial detectability of major capsid protein E (same trend for $gp34_{52}$ and M.*Nma*ϕCh1I; data not shown) would act on growth behavior and protein expression upon re-inoculation, a series of outgrowth experiments was performed with *N. magadii* L11 and *N. magadii* L11-ΔORF44 R alongside the corresponding Western Blots.

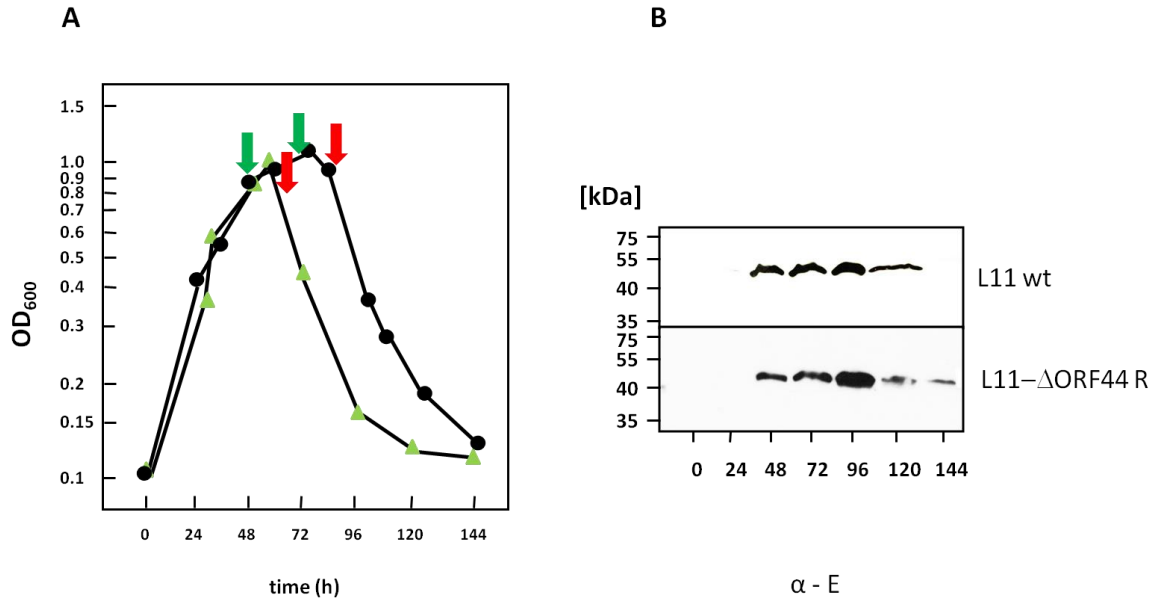


**Figure 30: The early onset of lysis in *N. magadii* L11-ΔORF44 R does not affect the initial detectability of major capsid protein E when compared to the wild-type *N. magadii* L11**

**A**: The black circles represent *N. magadii* L11 and the green triangles represent *N. magadii* L11-ΔORF44 R. Lysis occurs 24 h earlier in the case of *N. magadii* L11-ΔORF44 R in contrast to the wild-type *N. magadii* L11. The arrows represent the time points of re-inoculation for the subsequent outgrowth experiments: The green arrows indicate the time points before onset lysis and the red ones the time points after onset of lysis. **B**: Although the onset of lysis occurs 24 hours earlier in the case of *N. magadii* L11-ΔORF44 R when compared to *N. magadii* L11, the detectability kinetics of the major capsid protein E however remain identical: Protein E is detectable after 48 hours in both cases. The α-E Western Blot serves a reference purpose here; α- $gp34_{52}$ and α-M.*Nma*ϕCh1I Western Blots revealed the same expression pattern as the α-E Western Blot (data not shown).

3.2.3.3.1. Outgrowth experiment – After onset of lysis

A first series of experiments was performed in which a culture of *N. magadii* L11 and *N. magadii* L11-ΔORF44 R were grown until closely after the onset of lysis had occurred before being re-inoculated to an $OD_{600}$ of 0.1-0.15. The time points of re-inoculation can be seen in Figure 30 A and are labeled with red arrows. The re-inoculated cultures were grown until occurrence of lysis. Growth curve analysis was performed as depicted in Figure 31. Samples were taken at the same time points and crude extracts were prepared. α-E, α-gp34$_{52}$ and α-M.*Nma*ϕCh1I Western Blot analyses were performed with all samples.

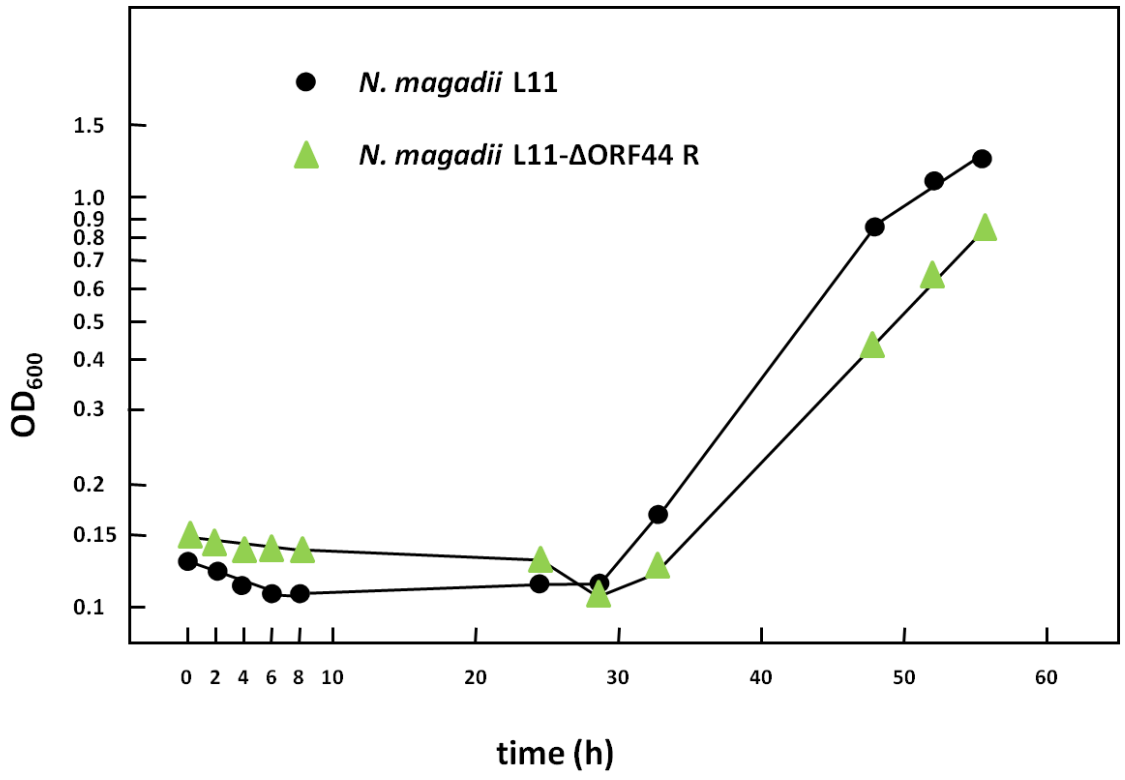


**Figure 31: Outgrowth curve analysis of *N. magadii* L11 and *N. magadii* L11-ΔORF44 R following re-inoculation after the onset of lysis**

Here, the respective pre-cultures were grown until closely after the onset of lysis before being re-inoculated (Figure 30 A, red arrows). The resulting growth curve can be seen above. Growth-wise, both *N. magadii* L11 and *N. magadii* L11-ΔORF44 R behave almost identically; a 28-hour lag phase can be observed in both cases before the re-emergence of growth. The optical density was measured at a wavelength of 600 nm ($OD_{600}$).

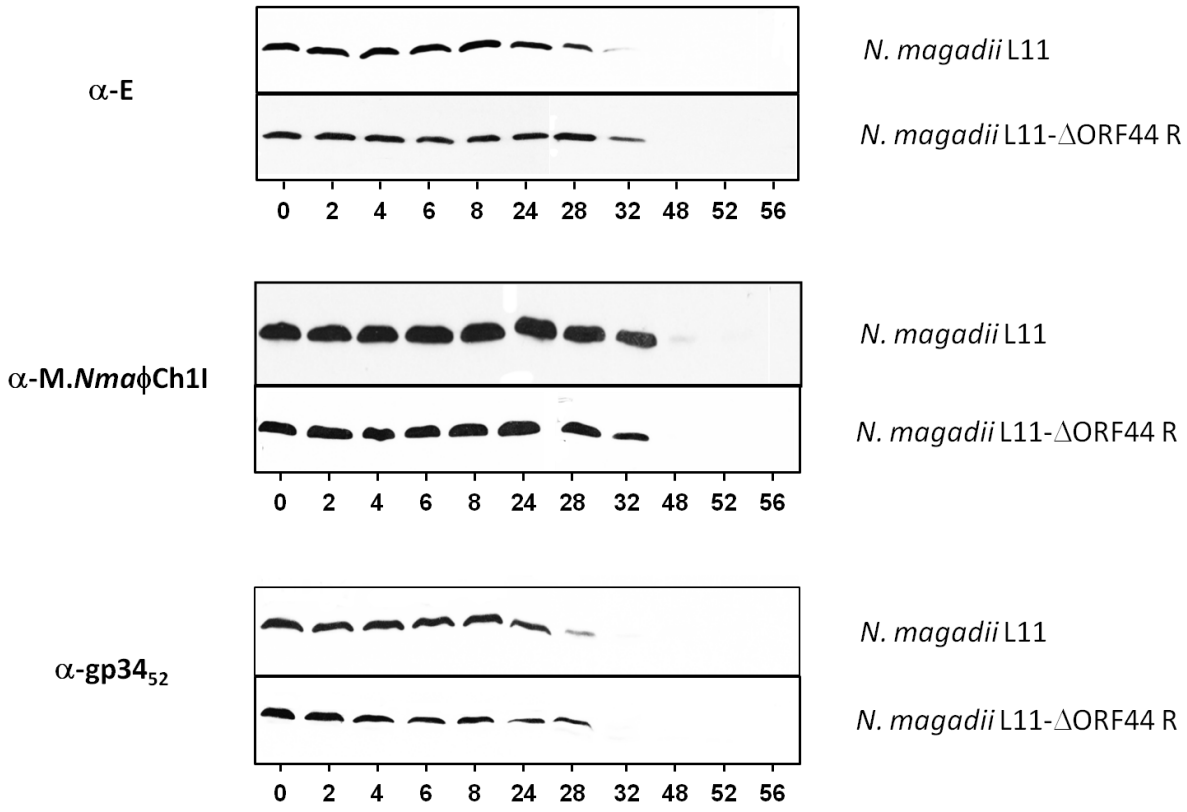


**Figure 32: Western Blot analysis of *N. magadii* L11 and *N. magadii* L11-ΔORF44 R crude extracts following re-inoculation after the onset of lysis**

Samples of the different cultures were taken 0, 2, 4, 6, 8, 24, 28, 32, 48, 52, and 56 h after inoculation (see Figure 31) and crude extracts were prepared. Aliquots were separated on a 12% SDS-PAGE, transferred to a nitrocellulose membrane and incubated with antibodies as indicated on the left. The different strains are indicated on the right. Comparing *N. magadii* L11 to *N. magadii* L11-ΔORF44 R, Western Blot analysis using α-E, α- gp34$_{52}$ and α-M.*Nma*ϕCh1I antibodies shows no significant differences in protein expression during the first 56 hours after re-inoculation. In both cases all three proteins are detectable during the 28-hour lag phase observable in the growth curve before becoming undetectable during exponential growth phase (see Figure 31).

Figure 32 illustrates the Western blotting results of *N. magadii* L11 and *N. magadii* L11-ΔORF44 R following re-inoculation after the onset of lysis. No significant changes in the expression of the three proteins in question could be observed over a period of 56 hours following the re-inoculation. This observation is in accordance with the hypothesis that ORF44 does not influence lysis itself since a re-inoculation after the onset of lysis with subsequent outgrowth of both *N. magadii* L11 and *N. magadii* L11-ΔORF44 R reveals no significant difference in the protein expression pattern of both strains following the first 56 hours after re-inoculation.

3.2.3.3.2. Outgrowth experiment – Before onset of lysis

Subsequently, another series of experiments was performed in which a culture of *N. magadii* L11 and *N. magadii* L11-ΔORF44 R were grown until closely before the onset of lysis before being re-inoculated to an $OD_{600}$ of 0.1- 0.15. The time points of re-inoculation can be seen in Figure 30 A and are labeled with green arrows. The re-inoculated cultures were grown until occurrence of lysis. Growth curve analysis was performed and samples were taken as depicted in Figure 33. Again, α-E, α-gp34$_{52}$ and α-M.*Nma*ϕCh1I Western Blot analyses were performed with all samples.

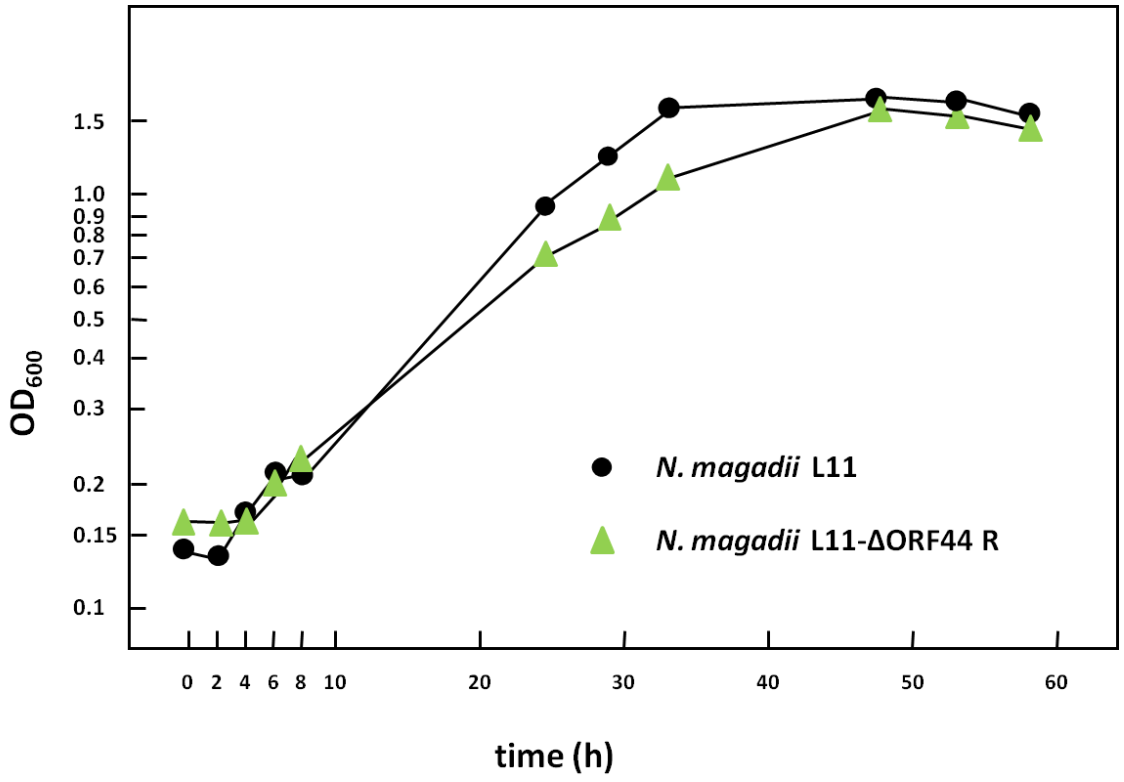


**Figure 33: Outgrowth curve analysis of *N. magadii* L11 and *N. magadii* L11-ΔORF44 R following re-inoculation before the onset of lysis**

Here, the respective pre-cultures were grown until closely before the onset of lysis before being re-inoculated (Figure 30, green arrows). The resulting growth curve can be seen above. In this case, the lag phase lasts about 2 hours before the re-occurrence of growth. Growth wise, *N. magadii* L11 and *N. magadii* L11-ΔORF44 R again exhibit the same trend. The optical density was measured at a wavelength of 600 nm ($OD_{600}$).

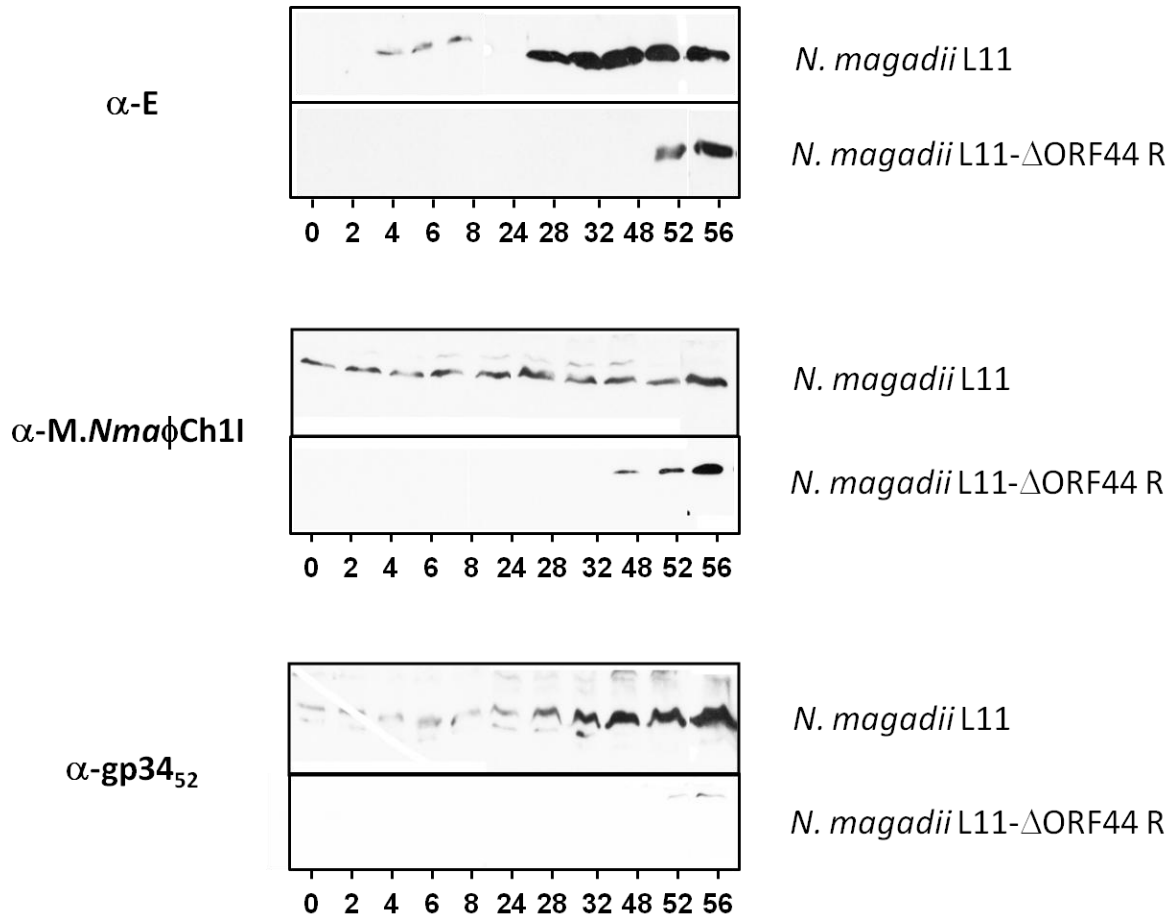


**Figure 34: Western Blot analysis of *N. magadii* L11 and *N. magadii* L11-ΔORF44 R crude extracts following re-inoculation before the onset of lysis**

Samples of the different cultures were taken 0, 2, 4, 6, 8, 24, 28, 32, 48, 52, and 56 h after inoculation (see Figure 33) and crude extracts were prepared. Aliquots were separated on a 12% SDS-PAGE, transferred to a nitrocellulose membrane and incubated with antibodies as indicated on the left. The different strains are indicated on the right. Comparing *N. magadii* L11 to *N. magadii* L11-ΔORF44 R, Western Blot analysis using α-E, α-gp34$_{52}$ and α-M.*Nma*φCh1I antibodies shows a significantly different expression pattern of all three proteins following re-inoculation. In the case of *N. magadii* L11, protein E is detectable after 4 hours following re-inoculation before being intensely detectable after 28 hours. M.*Nma*φCh1I is detectable directly after re-inoculation with a rise in amount after 56 hours. gp34$_{52}$ is detectable directly after re-inoculation with a substantial rise in quantity after 32 hours. In the case of *N. magadii* L11-ΔORF44 R, the expression pattern of the three proteins is substantially altered compared to the wild-type. Both protein E and gp34$_{52}$ are detectable 52 hours after re-inoculation whereas M.*Nma*φCh1I is re-detectable after 48 hours following re-inoculation. During the whole of the exponential growth phase, none of the proteins is detectable in the case of *N. magadii* L11-ΔORF44 R, whereas for the wild-type they are.

Figure 34 illustrates the Western blotting results of *N. magadii* L11 and *N. magadii* L11-ΔORF44 R following re-inoculation before the onset of lysis. Although no major differences in the protein expression pattern could be observed between *N. magadii* L11 and *N. magadii* L11-ΔORF44 R in the case of re-inoculation after the onset of lysis, considerable differences in the protein expression pattern were noticeable upon re-inoculation before the onset of lysis. In the case of *N. magadii* L11, protein E became slightly detectable 4 hours following re-inoculation before undergoing a substantial rise in abundance after 28 hours following re-inoculation. The signals relative to $gp34_{52}$ and M.*Nma*ϕCh1I showcased a comparable pattern; both were detectable immediately following re-inoculation with M.*Nma*ϕCh1I exhibiting similar quantities throughout the time series. $Gp34_{52}$ showcased a substantial rise in detectable quantities after 32 hours. For *N. magadii* L11-ΔORF44 R, the detection patterns were completely different compared to the wild-type ones: Protein E as well as $gp34_{52}$ became detectable 52 hours following re-inoculation whereas M.*Nma*ϕCh1I became re-detectable 48 hours following re-inoculation. All three proteins remained undetectable during the 2-hour lag phase before re-occurrence of growth as well as the entire exponential growth phase (See Figure 33). This observation was in complete contrast to the wild-type where all three proteins remained detectable during the exponential growth phase. $Gp34_{52}$ and M.*Nma*ϕCh1I were also detectable during the 2-hour lag phase in the case of *N. magadii* L11 whereas protein E was not.

### 3.2.4. Discussion

The outline of this study was set to characterize ϕCh1 ORF44, a 395 bp open-reading frame situated upstream of the ϕCh1 DNA replication domain (Klein *et al*., 2002). Previous studies identified ORF43 and ORF44 as being good candidates for an investigation relative to the regulation of gene expression in ϕCh1 (Iro *et al*., 2007). Experiments conducted by Iro *et al*. identified ORF43/44 (ORF43) as having an enhancing effect on the intergenic region between ORF48 and ORF49 by potentially binding directly or indirectly to 5' repeats within the ORF48 (*rep*) sequence and thereby enhancing transcription of ORF49 (Iro *et al*., 2007): Evidence was given for a potential role of ORF49 in activating the lytic life cycle of ϕCh1 (Iro *et al*., 2007).

These previous experiments with regard to the characterization of ϕCh1 ORF44 (and ORF43) were exclusively performed in *H. volcanii*, the model organism for halophilic *Archaea*, as no suitable

transformation system for the native ϕCh1 host *N. magadii* was available at the time of publication of said results.

Christoph Hofbauer was the first to perform experiments relative to ϕCh1 ORF44 characterization in its native host *N. magadii*. He demonstrated that upon transformation of ORF44 under the control of the constitutive promoter $p_{43}$ in the cured strain *N. magadii* L13, a 48-hour delay in reporter gene expression could be observed: densitometry analysis revealed a 48-hour repressing activity of gp44 when it comes to reporter gene expression (Hofbauer, 2015). In addition, he was able to show that the reporter protein was truncated (Hofbauer, 2015). This trend was not observable for both ORF43 as well as ORF43/44 under the control of $p_{43}$ (Hofbauer, 2015). However, these previous experiments were so far only carried out in a virus-free background as these experiments were performed in the cured strain *N. magadii* L13.

In order to follow up on the characterization of ϕCh1 ORF44, a first goal of this study was to create a ϕCh1 ORF44 deletion mutant in its native host *N. magadii* as this would represent a first step in characterizing the function of ORF44 in its native host alongside a virus-encompassing background. This project led to the creation of the third ever deletion mutant in ϕCh1, the previous ones being *N. magadii* L11-ΔORF79*,* an ORF79 deletion mutant (Selb, 2010) and *N. magadii* L11-ΔORF34*,* an ORF34 deletion mutant (Till, 2011 & Dimmel, 2013). The creation of the strain *N. magadii* L11-ΔORF44 R was achieved using the homologous recombination method first successfully applied by Regina Selb in 2010 for the creation of the ORF79 deletion mutant *N. magadii* L11-ΔORF79.

One potentially positive mutant had been identified that was suited for the subsequent homogenization step. As up to 50 copies of archaeal and thus viral genome may be present per cell, homogenization is a mandatory step in the creation of homozygous ϕCh1 deletion mutants. The method of choice used involved the infection of the cured strain *N. magadii* L13 with culture supernatant of a lysed culture, containing mutant virus particles. As ORF44 was deleted and replaced with a novobiocin resistance cassette, subsequent selection through selective medium plates (+ novobiocin) enabled the creation of homozygous ORF44 deletion mutants. A subsequent analysis via analytical PCR and Southern Blot of three homogenized mutants revealed that only two of them actually yielded positive results in both analytical PCR as well as Southern blot analysis; therefore the third mutant was ultimately discarded from the study. Consequently, the generation of homozygous ϕCh1 deletion mutants should always comprise analytical PCR analysis followed by southern blotting hybridization.

A first step in characterizing the newly created mutant strain *N. magadii* L11-ΔORF44 R was through growth curve analysis. Here, it has been shown that ORF44 clearly influences the onset of lysis as the onset of lysis occurred 24 hours earlier in the case of *N. magadii* L11-ΔORF44 R when compared to the wild-type *N. magadii* L11. However, lysis kinetics did not seem to be influenced.

Virus titer experiments also determined that there was no significant difference in the amount of viral particles released during lysis when comparing both strains. This further suggests a unique influence of ORF44 on the onset of lysis rather than lysis kinetics.

Western Blot analysis has shown that, although the onset of lysis occurred 24 hours earlier in the case of *N. magadii* L11-ΔORF44 R when compared to *N. magadii* L11, the detectability kinetics of the major capsid protein E remained almost identical; for both strains, protein E was detectable 48 hours after inoculation.

As the identical detectability kinetics of major capsid protein E contradicted the observed difference relative to the onset of lysis when compared to the wild-type, outgrowth experiments were subsequently performed on both *N. magadii* L11 and *N. magadii* L11-ΔORF44 R to monitor growth kinetics as well as the production of the two major viral proteins gpE and $gp34_{52}$ as well as the main methyltransferase M.*Nma*ϕCh1I.

Two distinct series of outgrowth experiments were performed: A first series where cultures of *N. magadii* L11 and *N. magadii* L11-ΔORF44 R were grown until closely after the onset of lysis before being re-inoculated to an $OD_{600}$ of 0.1-0.15 and a second series where both strains were re-inoculated to an $OD_{600}$ of 0.1-0.15 closely before the onset of lysis. Outgrowth behavior was monitored through growth curve analysis and Western Blot analysis against the three proteins mentioned above.

Re-inoculation after the onset of lysis resulted in a 28-hour lag phase before the re-occurrence of growth for both *N. magadii* L11 and *N. magadii* L11-ΔORF44 R. During the whole 28-hour lag phase, all of the three proteins analyzed remained detectable; gpE and M.*Nma*ϕCh1I remained detectable for 32 hours whereas $gp34_{52}$ remained detectable for 28 hours. The lag phase occurred because lysis of the pre-culture had already set on. Many assembled virus particles were present in the host cells: ϕCh1 virus particles finished their life cycle upon re-inoculation. It is conceivable that there was equilibrium between growing and lysing cells, leading to the lag phase where the proteins were detectable. This is further confirmed by the fact that all three proteins analyzed represent gene products of late genes in the ϕCh1 life cycle. Lysis occurred following 72 hours after re-inoculation for both the wild-type as well

as the mutant strain. Most importantly, no significant difference in either growth or protein expression was observable between wild-type and the mutant strain, further strengthening the hypothesis that the influence of ORF44 relative to lysis is purely limited to the moment of onset rather than to lysis itself.

Re-inoculation before the onset of lysis only resulted in a 2-hour lag phase before growth re-occurred; this was the case for both *N. magadii* L11 and *N. magadii* L11-ΔORF44 R. The subsequent outgrowth curve revealed the same trend for both strains; again, no significant difference in growth behavior was observable for both strains. On protein levels however, substantial differences in expression kinetics could be observed:

In the case of the wild-type *N. magadii* L11, $gp34_{52}$ and M.*Nma*ϕCh1I were detectable throughout the whole time series. An increase in expression could be observed in the case of $ORF34_{52}$, starting from 28 hours after re-inoculation. Expression of ORF94, encoding M.*Nma*ϕCh1I, rose at 56 hours and expression of ORF11, encoding protein E, arose after 4 hours following re-inoculation, followed by a substantial rise in its expression after 28 hours until 56 hours.

The expression kinetics of the three late-gene-encoded proteins gpE, $gp34_{52}$ and M.*Nma*ϕCh1I however differ considerably for *N. magadii* L11-ΔORF44 R, compared to the wild-type: M.*Nma*ϕCh1I is detectable only after 48 hours following re-inoculation whereas gpE and $gp34_{52}$ become detectable after 52 hours. Here, in the case of *N. magadii* L11-ΔORF44 R, all proteins were detectable by the onset of lysis. Lysis itself occurred between 48 and 52 hours following re-inoculation for both wild-type as well as mutant strain. The protein kinetics present another argument in favour of an influence of gp44 strictly limited to the moment of onset of lysis: re-inoculation before the onset of lysis led to a completely different protein expression pattern in the case of *N. magadii* L11-ΔORF44 R.

In order to summarize we can say that the construction and characterization of a ϕCh1 ORF44 deletion mutant in the native host *N. magadii* has given some insight relative to the function of gp44. It has been shown that gp44 influences the moment of onset of lysis as lysis occurs 24 hours earlier in a wild-type strain lacking ORF44. The resulting hypothesis that gp44 only influences the onset of lysis and not lysis kinetics has been confirmed through the performed experiments. Growth curve analysis has shown that the lytic behavior of *N. magadii* L11-ΔORF44 R is comparable to the wild-type as well as the amount of virus particles released during lysis, altogether indicating that the influence of gp44 does not extend to lysis kinetics. The subsequent outgrowth experiments have shown that only after re-inoculation of an *N. magadii* L11-ΔORF44 R culture closely before lysis, a difference in the expression of the late-gene

encoded proteins gpE, $gp34_{52}$ and M.*Nma*ϕCh1I could be observed in comparison to the wild-type strain *N. magadii* L11. This again is another indication for an influence of gp44 limited to the moment of onset of lysis.

A number of hypotheses can be made in order to preliminarily explain the observed phenotype for a strain lacking ORF44, with respect to the hypotheses postulated by Iro *et al*. that "*The 5'-part of the rep gene positively interferes with the transcription from the ORF49 promoter by allowing binding of gp43/44 which in turn enhances transcription of ORF49 by a still unresolved mechanism.*" (Iro *et al*., 2007) and that ORF49 has probably an involvement in activating the lytic life cycle of ϕCh1 (Iro *et al*., 2007).

A first hypothesis can be made taking into account the differences between wild-type and *N. magadii* L11-ΔORF44 R in protein expression, observable in the case of the outgrowth experiment where re-inoculation was performed before the onset of lysis. Here, the wild-type strain expresses gpE, $gp34_{52}$ and M.*Nma*ϕCh1I during the exponential growth phase whereas *N. magadii* L11-ΔORF44 R does not. In that particular case, the absence of ORF44 hinders the expression of late genes. This would suggest a contradictory "activator" effect of ORF44 relative to the expression of the three proteins tested for. As evidence exists that suggests a repressor function of ORF44, it would be more conceivable to suggest a repressor-repressing activity of ORF44: Absence of ORF44 activates the repressing function of a third molecule, resulting in the repression of gpE, $gp34_{52}$ and M.*Nma*ϕCh1I expression strictly during the exponential growth phase after re-inoculation from a culture closely before lysis. In 2007, Iro *et. al* postulated that the possibility might exist that gp43/44 interact with the 5'-part of *rep* either directly or through an additional protein. The results obtained through the outgrowth experiments may be a first step in confirming the additional protein hypothesis.

A second hypothesis relative to the function of gp44 can be made by taking into account the potential toxin-antitoxin system that the ORF43/44 operon might be. In *N. magadii* L11-ΔORF44 R, the potential toxin-encoding gene ORF44 is deleted which results in a strain not expressing the potential toxin. The antitoxin encoded by ORF43 however is still present and exhibits its enhancing effect on *rep* and thus still indirectly enhances transcription of ORF49 which is probably involved in the progression to the lytic cycle. As ORF44 is deleted, no hypothetical control of gp43 interaction with the *rep* coding sequence can be exhibited by gp44 thus leading to a premature transcription of ORF49 resulting in an earlier onset of lysis of *N. magadii* L11-ΔORF44 R compared to *N. magadii* L11.

A third hypothesis can be generated based on the previous one: The deletion of ORF44 results in an excessive presence of gp43 which would normally be regulated through a putative interaction with gp44. Consequently, the copy number of free gp43 in the strain *N. magadii* L11-ΔORF44 R would be higher than the one in the wild-type strain. The resulting excess of gp43 in strain *N. magadii* L11-ΔORF44 R would then lead to a deregulation of its interaction with the 5'-part of *rep*, thereby leading to a deregulation of ORF49 transcription followed by an earlier onset of lysis.

A few last observations worth noting are for once the fact that grown cultures of *N. magadii* L11-ΔORF44 R spontaneously lyse after a few days of standing motionless and not being incubated at 37°C/42°C as well as the fact that passaging an *N. magadii* L11-ΔORF44 R culture for three to four passages led to a growth behavior strongly reminiscent of the cured strain *N. magadii* L13: No lysis at all could be observed for *N. magadii* L11-ΔORF44 R after three to four passages when compared to *N. magadii* L11 (data not shown). The reasons behind this observation are being investigated as of now.

# 4. References


**Albers S.-V., Meyer B. H.** The archaeal cell envelope. *Nat Rev Microbiol* **9,** 414–26 (2011).

**Andrei A.-Ş., Banciu H., Oren A.** Living with salt: metabolic and phylogenetic diversity of *Archaea* inhabiting saline ecosystems. *FEMS Microbiol Lett.* **330**: 1-9 (2012).

**Arcus V., McKenzie J., Robson J., Cook G.** The PIN-domain ribonucleases and the prokaryotic VapBC toxin–antitoxin array. *Protein Eng Des Sel.* **24**: 33-40 (2011).

**Baranyi U., Klein R., Lubitz W., Kruger D. H., Witte A**. The archaeal halophilic virus-encoded Dam-like methyltransferase M. phiCh1-I methylates adenine residues and complements dam mutants in the low salt environment of *Escherichia coli*. *Mol. Microbiol*. 35, 1168–1179 (2000).

**Barns S. M., Delwiche C. F., Palmer J. D., Pace N. R.** Perspectives on archaeal diversity, thermophily and monophyly from environmental rRNA sequences. *Proc Natl Acad Sci.* **93,** 9188–9193 (1996).

**Brochier-Armanet C., Forterre P., Gribaldo S.** Phylogeny and evolution of the *Archaea*: one hundred genomes later. *Current Opinion in Microbiology* **14:** 274-281 (2011).

**Brock T. D., Brock K. M., Belly R. T., Weiss R. L.** *Sulfolobus*: a new genus of sulfur-oxidizing bacteria living at low pH and high temperature. *Arch Microbiol* **84**: 54-68 (1972).

**Charlebois R., Lam W., Cline S., Doolittle F.** Characterization of pHV2 from *Halobacterium volcanii* and its use in demonstrating transformation of an archaebacterium. *Proc Natl Acad Sci USA.* **84**: 8530-8534 (1987).

**Chatton É.** Titres et Travaux scientifiques (1906-1937). Imprimerie Sottano, Sète, 59 p (1937).

**Cline S., Doolittle F**. Efficient transfection of the archaebacterium *Halobacterium halobium*. *J Bacteriol.* **169**: 1341-1344 (1987).

**Daines D., Wu M., Yuan S.** VapC-1 of Nontypeable *Haemophilus influenzae* Is a Ribonuclease. *J Bacteriol.* **189**: 5041-5048 (2007).

**Dyall-Smith M., Tang S. L., Bath C.** Haloarchaeal viruses: How diverse are they? *Res Microbiol.* **154**: 309-313 (2003).

**Fendrihan S., Legat A., Pfaffenhuemer M., Gruber C., Weidler G., Gerbl F., Stan-Lotter H.** Extremely halophilic *Archaea* and the issue of long-term microbial survival. *Rev Environ Sci Biotechnol.* **5**: 203-218 (2006).

**Grant, W. D., Larsen, H.** Group III. Extremely halophilic archaebacteria, Order *Halobacteriales* ord. nov. In *Bergey's Manual of Systematic Bacteriology*, vol. 3, pp. 2216-2233. Edited by J. T. Staley, M. P. Bryant, N. Pfennig and J. G. Holt. Baltimore, MD: Williams & Wilkins (1989).

**Gropp, F., Grampp, B., Stolt, P., Palm, P., Zillig, W.** The immunity-conferring plasmid pϕHL from the *Halobacterium salinarium* phage ϕH: Nucleotide sequence and transcription. *Virology* **190**: 45–54 (1992).

**Haeckel, E.** Generelle morphologie der organismen. Allgemeine grundzüge der organischen formen-wissenschaft, mechanisch begründet durch die von Charles Darwin reformirte descendenztheorie. *Berlin, G. Reimer* (1866).

**Haider F.** Characterization of the DNA methyltransferase M.NmaϕCh1I and further characterization of a transformation system of haloalkaliphilic *Archaea*. Master thesis (2009).

**Hofbauer C.** The function of gp34 and its regulation by ORF79 of ϕCh1 as well as the influence of other regulation elements. Master thesis (2015).

**Holmes M. L., Dyall-Smith M. L.** Mutations in DNA Gyrase Result in Novobiocin Resistance in Halophilic Archaebacteria. *Journal of Bacteriology* **173:** 642-648 (1991).

**Horikoshi K.** Alkaliphiles: some applications of their products for biotechnology. *Microbiol Mol Biol Rev.* **63**: 735-750 (1999).

**Horikoshi, K.** *Extremophiles Handbook*. (Springer, 2011).

**Huber H., Hohn M. J., Rachel R., Fuchs T., Wimmer V. C., Stetter K. O.** A new phylum of *Archaea* represented by a nanosized hyperthermophilic symbiont. *Nature* **417:** 63-67 (2002).

**Iro, M.** Charaterization of the regulatory region of the virus ϕCh1 infecting *Natrialba magadii*. Dissertation (2006).

**Iro M., Klein R., Galos B., Baranyi U., Rössler N., Witte A.** The lysogenic region of virus ϕCh1: identification of a repressor-operator system and determination of its activity in halophilic *Archaea*. *Extremophiles* **11:** 383-396 (2007).

**Jarrell K. F., Walters A. D., Bochiwal C., Borgia J. M., Dickinson T., Chong J. P.** Processing in *Natrialba magadii* during Virus Maturation. *Virology* **276:** 376-387 (2000).

**Klein R., Greineder B., Baranyi U., Witte A.** The Structural Protein E of the Archaeal Virus ϕCh1: Evidence for Processing in *Natrialba magadii* during Virus Maturation. *Virology* **276**: 376-387 (2000)

**Klein R., Baranyi U., Rössler N., Greineder B., Scholz H., Witte A.** *Natrialba magadii* virus ϕCh1: first complete nucleotide sequence and functional organization of a virus infecting a haloalkaliphilic archaeon. *Molecular Microbiology* **45:** 851-863 (2002).

**Lam W. L., Doolittle W. F.** Mevinolin-resistant Mutations Ientify a Promoter and the Gene for a Eukaryote-like 3-Hydroxy-3-methylglutaryl-coenzyme A Reductase in the Archaebacterium *Haloferax volcanii*. T*he Journal of Biological Chemistry* **267:** 829-5834 (1992).

**Linnaeus, C**. Systema naturae, sive Regna tria naturae. Systematice proposita per Classes, Ordines, Genera, & Species. *Lugduni Batavorum, Apud Theodorum Haak* (1735).

**Ma Y., Galinski E. A., Grant W. D., Oren A., Ventosa A.** Halophiles 2010: Life in saline environments. *Appl Environ Microbiol.* **76,** 6971–81 (2010).

**Matsumi R., Atomi H., Driessen A. J. M., van der Oost J.** Isoprenoid biosynthesis in *Archaea* - biochemical and evolutionary implications. *Res Microbiol.* **162,** 39–52 (2011).

**Mayrhofer-Iro M., Ladurner A., Meissner C., Derntl C., Reiter M., Haider F., Dimmel K., Rössler N., Klein R., Baranyi U., Scholz H., Witte A.** Utilization of Virus ϕCh1 Elements to establish a shuttle vector system for Halo(alkali)philic *Archaea* via Transformation of *Natrialba magadii*. *Applied and Environmental Microbiology* **79:** 2741-2748 (2013).

**Oren A.** Bioenergetic Aspects of Halophilism. **63** (1999).

**Oren A.** Molecular ecology of extremely halophilic *Archaea* and *Bacteria*. *FEMS Microbiology Ecology* **39:** 1-7 (2002).

**Pabo C., Sauer R.** Protein-DNA recognition. *Annu Rev Biochem.* **53**: 293-321 (1984).

**Ptashne M.** Specific Binding of the λ Phage Repressor to λ DNA. *Nature*. **214** (5085): 232–234 (1967).

**Ptashne M.** A Genetic Switch - Phage Lambda Revisited. *3rd Edition, Cold Spring Harbor Laboratory Press* (2004).

**Robson J., McKenzie J.L., Cursons R., Cook G.M., Arcus V.L.** The *vapBC* Operon from *Mycobacterium smegmatis* Is An Autoregulated Toxin–Antitoxin Module That Controls Growth via Inhibition of Translation. *J Mol Biol.* **390**: 353-367 (2009)

**Schnabel H., Zillig W.** Circular structure of the genome of phage ϕH in a lysogenic *Halobacterium halobium*. *Mol Gen Genet.* **193**: 422-426 (1984).

**Schöner L.** Construction of different mutants of *Natrialba magadii* and the influence of different ϕCh1 ORFs on *Natrialba magadii*. Master thesis (2013).

**Seegers L., Sonnenberg R., Yamamoto R.** Molecular analysis of the *Alcolapia* flock from lakes Natron and Magadi, Tanzania and Kenya (Teleostei: Clichidae), and implications for their systematics and evolution. *Ichthyol Explor Freshwat*. **10**: 175-199 (1999).

**Selb R.** Construction of mutants of *Natrialba magadii* and ϕCh1. Master thesis (2010)

**Selb R., Derntl C., Klein R., Alte B., Hofbauer C., Kaufmann M., Beraha J., Schöner L., and Witte A.** The viral gene ORF79 encodes a repressor regulating induction of the lytic life cycle in the haloalkaliphilic virus ϕCh1. *J Virol* doi:*10.1128/JVI.00206-17* (2017).

**Shahmohammadi H. R., Asgarani E., Terato H., Saito T., Ohyama Y., Gekko K., Yamamoto O., Ide H**. Protective roles of bacterioruberin and intracellular KCl in the resistance of *Halobacterium salinarum* against DNA-damaging agents. *J Radiat Res* 39251–262 (1998).

**Stolt P., Zillig W.** Antisense RNA mediates transcriptional processing in an archaebacterium, indicating a novel kind of RNase activity. *Molecular Microbiology* **7** (6): 875-882 (1993).

**Stolt P., Zillig W.** Transcription of the halophage ϕH repressor gene is abolished by transcription from an inversely oriented lytic promoter. *FEBS Lett.* **344**: 125-128 (1994).

**Till P.**, Deletion of the tail fibre protein of ϕCh1 and further characterization of the inversion within its gene locus. Master thesis (2011).

**Tindall B. J., Ross H. N. M., Grant W. D.** *Natronobacterium gen. nov*. and *Natronococcus gen. nov*., Two New Genera of Haloalkaliphilic Archaebacteria. *Systematic and Applied Microbiology* **5:** 41-57 (1984).

**Torsvik T., Dundas I. D.** Bacteriophage of *Halobacterium salinarium*. ***Nature* 248**: 680-1 (1974).

**Van de Vossenberg, J. L., Driessen, A. J., Grant, W. D., Konings, W. N.** Lipid membranes from halophilic and alkali-halophilic *Archaea* have a low $H^+$ and $Na^+$ permeability at high salt concentration. *Extremophiles* 253–257 (1999).

**Van de Vossenberg J. L., Driessen a J., Konings W. N.** The essence of being extremophilic: the role of the unique archaeal membrane lipids. *Extremophiles* **2,** 163–70 (1998).

**Whittaker R.** New concepts of kingdoms or organisms. Evolutionary relations are better represented by new classifications than by the traditional two kingdoms. *Science*, **163**: 150-194 (1969).

**Woese C. R., Fox G. E.** Phylogenetic structure of the prokaryotic domain: The primary kingdoms. *Proc Natl Acad Sci.* **74:** 5088-5090 (1977).

**Woese C. R., Kandler O., Wheelis M. L.** Towards a natural system of organisms: Proposal for the domains *Archaea*, *Bacteria*, and *Eucarya*. *Proc Natl Acad Sci.* **87:** 4576-4579 (1990).

**Witte A., Baranyi U., Klein R., Sulzner M., Luo C., Wanner G., Krüger D. H., Lubitz W.** Characterization of *Natronobacterium magadii* phage ϕCh1, a unique archaeal phage containing DNA and RNA. *Molecular Microbiology* **23:** 603-616 (1997).

**Yanisch-Perron C., Vieira J., Messing J.** Improved M13 phage cloning vectors and host strains: nucleotide sequences of the M13mp18 and pUC19 vectors. *Gene* **33**: 103-19 (1985).

**Zhou M., Xiang H., Sun C., Tan H.** Construction of a novel shuttle vector based on an RCR-plasmid from a haloalkaliphilic archaeon and transformation into other haloarchaea. *Biotechnol Lett.* **26:** 1107-13 (2004).

# 5. List of figures

# 6. Abstract

Transcriptional regulation in the virus ϕCh1 infecting the haloalkaliphilic archaeon *Natrialba magadii* represents an important field of research in order to fully understand the regulation of the viral life cycle. Ultimately understanding transcriptional regulation in ϕCh1 represents a major achievement with regard to the development of genetic manipulation tools suitable for use in its host *N. magadii*. In order to gain insight relative to viral transcriptional regulation, this thesis discusses the potential role of two distinct ϕCh1 open-reading frames in regulating the transcription of viral genes and thus the progression of the viral life cycle: ϕCh1 ORF56 and ORF44.

Previous work involving over-expression of ORF56 in the wild-type strain *N. magadii* L11 suggested a putative transcriptional regulator function of ORF56 and presented evidence for a potential repressor activity, demonstrated by a reduced lysis behaviour and an alteration in the expression of certain major viral proteins. A first part of this thesis therefore aims at following up on the characterization of ORF56 by investigating additional potential alterating effects of an over-expressed ORF56 on protein expression. It has been shown that the repressor effect of ORF56 extends to a third, late gene-encoded protein: The ORF94-encoded main ϕCh1 methyltransferase M.*Nma*ϕCh1I.

The second part of this work aims at further characterizing the transcriptional regulator function of ORF56 through the creation of an ORF56 deletion mutant via homologous recombination. It was however impossible to yield strain *N. magadii* L11-ΔORF56 through the standard homologous recombination method used, probably because of the fact that the impact of ORF56 in regulating the viral life cycle is so tremendous that a deletion of ORF56 would result in virus particles not able to lysogenize *N. magadii*.

A third part of this work aims at characterizing ϕCh1 ORF44, a putative repressor. Previous studies have shown that ORF43/44 represents an operon and that ORF44 shows similarities to a PIN-like domain which would confer a nuclease function to gp44, thus potentially making it the VapC toxin of a VapBC TA system, with ORF43 representing the putative VapB antitoxin part. Additional evidence gathered demonstrated a repressor activity of gp44 with a potential role of ORF43/44 in regulating the progression of the lytic life cycle of ϕCh1. In order to characterize ϕCh1 ORF44 in a virus-encompassing background, the ORF44 deletion mutant *N. magadii* L11-ΔORF44 was created. Its subsequent characterization led to new insights with regard to the repressor function exhibited by gp44. Here, it

could be demonstrated that a delay in gene expression is detectable for cultures having been inoculated from a fresh culture growth-wise situated directly before the onset of lysis.

# 7. Zusammenfassung

Die Regulation der Transkription von Virus ϕCh1, welches das haloalkaliphile Archaeon *Natrialba magadii* infiziert, ist ein wichtiges Forschungsfeld im Bezug auf das Verständnis der Regulation des viralen Lebenszyklus. Das vollständige Verständnis dieser transkriptionellen Regulation würde einen wichtigen Schritt in Richtung Entwicklung von geeigneten genetischen Werkzeugen, welche im Wirt *N. magadii* anwendbar sind, darstellen. Um weitere Einblicke in die virale Transkriptionsregulation zu erhalten, befasst sich diese Arbeit mit der potentiellen Rolle zweier verschiedener offener Leserahmen von ϕCh1 bezüglich der Regulation der Transkription viraler Gene: ϕCh1 ORF56 und ORF44. Die gesammelten Erkenntnisse sollten Aufschlüsse bezüglich deren Einfluss auf den viralen Lebenszyklus geben.
Bisherige Arbeiten, welche die Überexpression von ORF56 im Wildtyp *N. magadii* L11 nutzten, schlugen eine mögliche transkriptionelle Regulationsfunktion für ORF56 vor und brachten Beweise für eine potentielle Repressorfunktion hervor. Diese Schlussfolgerungen spiegelten sich durch ein reduziertes Lysierverhalten und eine Änderung im Expressionsmuster bestimmter viraler Proteine wider. Ein erster Teil dieser Arbeit beschäftigt sich daher mit der Weiterführung der Charakterisierung von ORF56 bezüglich seines Einflusses auf das Expressionsmuster der Hauptmethyltransferase M.*Nma*ϕCh1I von ϕCh1. Es wurde dahingehend bewiesen dass ORF56 einen zusätzlichen Einfluss auf das Expressionsmuster von M.*Nma*ϕCh1I hat.

Der zweite Teil dieser Arbeit befasst sich mit der weiterführenden Charakterisierung der transkriptionellen Regulationsfunktion von ORF56 durch das Herstellen eines ORF56 Deletionsmutanten in *N. magadii* L11. Es stellte sich allerdings heraus dass es unmöglich ist den Stamm *N. magadii* L11-ΔORF56 durch die herkömmliche homologe-Rekombinationsmethode herzustellen. Ein Grund hierfür ist der warscheinlich enorme Einfluss von ORF56 auf das erfolgreiche Abschliessen des viralen Lebenszyklus: Ein Deletieren von ORF56 würde wahrscheinlich zu lytischen viralen Nachkommen führen.

Der abschliessende Teil dieser Arbeit befasst sich mit der Charakterisierung von ϕCh1 ORF44, einem potentiellen Repressor. Bisherige Arbeiten haben gezeigt dass ORF43/44 ein Operon zusammen bilden und dass ORF44 eine PIN-Domäne besitzt welche auf eine Nukleasefunktion des Genproduktes gp44 schliessen lässt. Zusammen genommen weisen diese Beobachtungen auf die Möglichkeit hin dass das

ORF43/44 Operon ein VapBC TA System bilden könnte, in welchem ORF43 das VapB Antitoxin und ORF44 das VapC Toxin bilden würden. Weitere Indizien wiesen auf eine Repressorfunktion von gp44 hin, zusätzlich zu einer potentiellen Rolle von ORF43/44 in der Regulierung des Wechsels von lysogenischem zu lytischem Lebenszyklus des Virus. Um ϕCh1 ORF44 mit einem Virus-beinhaltendem Hintergrund zu charakterisieren, wurde der ORF44 Deletionsmutant *N. magadii* L11-ΔORF44 hergestellt. Die darauffolgende Charakterisierung des Mutanten lieferte neue Erkenntnisse bezüglich der Repressorfunktion von gp44: *N. magadii* Zellen, die eine Deletion von ORF44 besitzen, zeigen ein verändertes Expressionsmuster von Genen in frisch inokulierten Kulturen, wenn diese Zellen aus einer wachsenden Kultur entnommen wurden die kurz vor der Lyse stand.